

2024

Morphology of the lateral ventricles of the brain using high-resolution MRI

<https://hdl.handle.net/2144/51397>

"Downloaded from OpenBU. Boston University's institutional repository."

BOSTON UNIVERSITY

ARAM V. CHOBANIAN & EDWARD AVEDISIAN SCHOOL OF MEDICINE

Thesis

**MORPHOLOGY OF THE LATERAL VENTRICLES OF THE BRAIN USING
HIGH-RESOLUTION MRI**

by

KAYLA LAVERY

B.S., University of Central Florida, 2021

Submitted in partial fulfillment of the
requirements for the degree of
Master of Science

2024

Approved by

First Reader

Richard J. Rushmore, Ph.D.
Associate Professor of Anatomy & Neurobiology

Second Reader

Linda M. Afifi, Ph.D.
Assistant Professor of Anatomy & Neurobiology

DEDICATION

I would like to dedicate this work to my mother, Ellen Bartlett, and fiancé, Gabriel Hernandez – better known as my, “*twin pillars, without whom I could not stand.*” – Rory

Gilmore

ACKNOWLEDGMENTS

To my mother, fiancé, family, and friends... your continued love and support have allowed me to take chances on myself that have offered me opportunities that I never thought would be possible. Having two people believe in me so wholeheartedly has provided me with the strength to succeed and go after my dreams.

To Dr. Rushmore... you have provided me with a wealth of knowledge and continued support throughout my time as a graduate student at BU. You have been kind, compassionate, patient, encouraging, and a delight to work with. You have provided the support I needed to feel confident in myself and my work and strive for greatness.

To Dr. Afifi... you have been not only a great educator, but someone who was able to provide words of wisdom in times of need. You are someone who people can rely on and it is greatly appreciated.

To Savannah Walker... my dear friend. I appreciate your continued support throughout this program. From dissection buddies to roommates, you have continued to be someone I could rely on, and I am so thankful for you.

To Florina Tynyanova in the ILL Department... you went out of your way to try to find the articles and books I needed to complete my thesis work. Not only did you work extremely hard to fulfill my multiple requests, but you were always kind.

To my cohort: Savannah, Grace, and Aris, and my lab mates: Roach, Aris, Daren, Maggie, Murtala, Sri, Laura, and Blandine... these are individuals that I will feel bonded to eternally. Thank you for the continued support and many laughs.

**MORPHOLOGY OF THE LATERAL VENTRICLES OF THE BRAIN USING
HIGH-RESOLUTION MRI**

KAYLA LAVERY

ABSTRACT

The lateral ventricles are crucial neuroanatomical structures with significant clinical relevance in various pathologies. Despite extensive work, there is still disagreement about the basic anatomical features of the lateral ventricle in terms of left-right asymmetry, the influence of sex, and the presence of anatomical variations. These disagreements are likely to be a result of studies performed using poorly characterized subject populations and using low-resolution data. To address this gap in knowledge, this study measured lateral ventricular morphology using 174 high-resolution MRI scans from the Human Connectome Project (HCP), focusing on a diverse population of well-characterized healthy, young individuals. We found significant left-right differences in ventricular dimensions, with the left ventricle consistently larger than the right across all subdivisions, including the anterior horn, body, and atrium to the end of the posterior horn. Sex emerged as a crucial determinant, with males exhibiting larger ventricles overall, and significant differences were observed in various subdivisions between sexes. Unexpectedly, we found that the compression of the anterior horn and the disconnection and isolation of the posterior horn were frequently identified in a large and broadly represented proportion of healthy adult subjects, challenging traditional notions of ventricular anatomy. Moreover, our investigation into handedness and age yielded nuanced insights, highlighting the intricate interplay between demographic factors and ventricular

morphology. Our results provide valuable insights into normal lateral ventricular anatomy, facilitating the interpretation of radiological images and aiding in the recognition of pathological deviations. Addressing these considerations in future research has the potential to deepen our understanding of ventricular morphology and its clinical implications, thereby potentially advancing our knowledge of brain structure and function.

TABLE OF CONTENTS

DEDICATION	iv
ACKNOWLEDGMENTS	v
ABSTRACT	vi
TABLE OF CONTENTS.....	viii
LIST OF TABLES	xii
LIST OF FIGURES	xiii
LIST OF ABBREVIATIONS	xvi
INTRODUCTION	1
Overview	1
History	1
Anatomy.....	3
Borders and Subdivisions.....	5
Contents.....	8
Embryology.....	9
Background and Summary of Anatomical Research of the Lateral Ventricles	11
Morphometric Measurements of the Lateral Ventricles	12
Sex Differences and Ventricular Asymmetry	13
Handedness and Ventricular Asymmetry.....	13
Ventricular Size and Asymmetry in Aging	14
Morphometric Studies of Lateral Ventricle Subdivisions	15
Anterior (Frontal) Horn (AH/FH).....	15

Body (Central Part).....	16
Posterior (Occipital) Horn (PH/OH).....	17
Summary of Existing Studies	19
Variations	19
Coarctation And Coaptation.....	20
Clinical Variations	22
Purpose of This Study.....	25
METHODS	27
Experimental Subjects	27
Data Collection.....	27
3D Slicer.....	27
Magnetic Resonance Imaging (MRI) Analysis.....	29
Anatomical Definitions	29
Compression Incidence	31
Compression Severity	31
Statistical Analysis	37
RESULTS	38
Ventricle: Overall / General.....	38
Length	38
Sex Differences.....	42
Age.....	44
Handedness.....	46

Anterior (Frontal) Horn	48
Length	48
Sex Differences.....	50
Age.....	52
Handedness.....	53
AH Variations	55
Definition	55
Left / Right Difference.....	55
Sex Difference	63
Age.....	67
Handedness.....	69
Body (Central) Part.....	72
Length	72
Sex Differences.....	74
Age.....	76
Handedness.....	78
Atrium + Posterior (Occipital) Horn	79
Length	79
Sex Differences.....	81
Age.....	83
Handedness.....	84
PH Variations	86

Definition	86
Left / Right Difference.....	89
Sex Differences.....	92
Age.....	95
Handedness.....	97
DISCUSSION	99
Overall Findings	99
Asymmetry	99
Sex, Age, And Handedness	101
Variations in Ventricular Confluence	104
Limitations and Future Studies.....	106
Conclusion.....	108
BIBLIOGRAPHY	109
CURRICULUM VITAE.....	120

LIST OF TABLES

Table 1: Length of Anterior (Frontal) Horn (AH/FH).....	16
Table 2: Length of Anterior (Frontal) Horn (AH/FH) + Body (Central Part)	17
Table 3. Length of Body (Central Part) of the Lateral Ventricle	17
Table 4: Length of Posterior (Occipital) Horn (PH/OH).....	18
Table 5: Length of Frontal to Occipital Pole (Longitudinal Dimension)	19
Table 6: Length of Lateral Ventricle	19
Table 7. Demographic Characteristics of Participants	38

LIST OF FIGURES

Figure 1. Lateral view perspective of a segmented ventricle.....	3
Figure 2. Superior view of a segmented lateral ventricle.	4
Figure 3. Visualization of MRI dataset in 3D Slicer.	28
Figure 4. MRI Displaying Opening of Anterior Horn.....	29
Figure 5. The coronal section immediately prior to the border between the frontal horn and the body.	30
Figure 6. MRI image of the foramen of Monro in two sequential sections.....	30
Figure 7. Example of Anterior Horn Compression Severity.	32
Figure 8. MRI imaging showing the transition from the body (left) to the atrium (right).	33
Figure 9. End of the Posterior Horn.	34
Figure 10. Posterior Horn Shapes.....	35
Figure 11. MRI Visualization of Posterior Horn Continuity.	36
Figure 12. Length of the Right and Left Lateral Ventricles.	40
Figure 13. Comparison of Right and Left LV of Size by Case.....	41
Figure 14. Length of the Right and Left Lateral Ventricle by Sex.	43
Figure 15. Length of the Right and Left Lateral Ventricles by Age.	44
Figure 16. Length of the Right and Left Lateral Ventricles by Age per Case.....	45
Figure 17. Length of the Right and Left Lateral Ventricles by Handedness.	47
Figure 18. Length of the Right and Left Anterior Horn.	49
Figure 19. Length of the Right and Left Anterior Horn by Sex.....	51
Figure 20. Length of the Right and Left Anterior Horn by Age.....	52

Figure 21. Length of the Right and Left Anterior Horn by Handedness.....	54
Figure 22. Anterior Horn Compression Incidence.....	57
Figure 23. Asymmetrical and Symmetrical Compression Incidence of the Anterior Horn.	60
Figure 24. Right and Left Lateral Anterior Horn Compression Severity.....	61
Figure 25. Right / Left Combined Compression Severity of the Anterior Horn.....	62
Figure 26. Right and Left Anterior Horn Compression by Sex.....	64
Figure 27. Right and Left Anterior Horn Compression Severity by Sex.....	66
Figure 28. Right and Left Anterior Horn Compression by Age.....	67
Figure 29. Right and Left Anterior Horn Compression Severity by Age.....	68
Figure 30. Anterior Horn Compression Incidence by Handedness.....	70
Figure 31. Right / Left Anterior Horn Compression Severity by Handedness.....	70
Figure 32. Length of the Right and Left Body.....	73
Figure 33. Length of the Right and Left Body by Sex.....	75
Figure 34. Length of the Right and Left Body by Age.....	77
Figure 35. Length of the Right and Left Body by Handedness.....	78
Figure 36. Length of the Right and Left Atrium to the End of the Posterior Horn.....	80
Figure 37. Length of the Right and Left Atrium to the End of the Posterior Horn by Sex.	82
Figure 38. Length of the Right and Left Atrium to the End of the Posterior Horn by Age.	83

Figure 39. Length of the Right and Left Atrium to the End of the Posterior Horn by Handedness.....	85
Figure 40. Right Posterior Horn Shape Progression.	87
Figure 41. Left Posterior Horn Shape Progression.....	88
Figure 42. Right and Left Posterior Horn Continuity Incidence.....	91
Figure 43. Right and Left Posterior Horn Continuity by Sex.	92
Figure 44. Right / Left Posterior Horn Continuity by Sex.....	93
Figure 45. Right / Left Posterior Horn Continuity by Sex.....	94
Figure 46. Right and Left Posterior Horn Continuity by Age.	95
Figure 47. Right / Left Posterior Horn Continuity by Age.	96
Figure 48. Right and Left Posterior Horn Continuity by Handedness.	97
Figure 49. Right / Left Posterior Horn Continuity by Handedness.....	98

LIST OF ABBREVIATIONS

3D	Three Dimensional
AD	Alzheimer's Disease
AH	Anterior Horn
ANOVA	Analysis of Variance
ASD	Autism Spectrum Disorder
BD.....	Bipolar Disorder
CC.....	Continuous Continuous
CD.....	Continuous Discontinuous
CI.....	Confidence Interval
CSF	Cerebrospinal Fluid
CT	Computerized Tomography
CTE.....	Chronic Traumatic Encephalopathy
DC.....	Discontinuous Continuous
DD	Discontinuous Discontinuous
DH	Descending Horn
EI	Evan's Index
eTIV.....	Estimated Total Intracranial Volume
FH.....	Frontal Horn
HCP	Human Connectome Project
HD	Huntington's Disease
HSD	Honest Significant Difference

IH.....	Inferior Horn
LV.....	Lateral Ventricle
LVs.....	Lateral Ventricles
MC.....	Mild Compression
mm.....	Millimeter
MRI.....	Magnetic Resonance Imaging
MS.....	Multiple Sclerosis
NC.....	No Compression
OH.....	Occipital Horn
PD.....	Parkinson's Disease
PH.....	Posterior Horn
SC.....	Severe Compression
SCZ.....	Schizophrenia
SD.....	Standard Deviation
T1W.....	T1 Weight
TBIs.....	Traumatic Brain Injuries
TBV.....	Total Brain Volume
TH.....	Temporal Horn
TIDS.....	Transverse Inner Diameter of the Skull

INTRODUCTION

Overview

The size of the lateral ventricles has significant clinical relevance as biomarkers for various pathologies. However, our understanding of these conditions is complicated by variations in normal anatomy that warrant deeper exploration. Conducting a comprehensive anatomical study of the lateral ventricular variations will not only broaden our understanding of normal anatomical diversity but also highlight the importance of lateral ventricle size and variations in the development of diseases.

History

The lateral ventricles of the brain were among the first brain regions of interest (Galen, Vesalius) to philosophers and physicians. Initial diagrams and drawings of the brain illustrated the ventricular shape and periventricular brain structures in detail, whereas the overlying cerebral cortex was not a structure of concern (see Finger, 2004; Gross, 1999). During the Renaissance, the conception of “cellulae” (or ventricles) underwent an evolution. Initially, the ventricles were thought to comprise four “small stomachs” that were involved in the production of thoughts, feelings, and emotions. Later conceptualizations included 3-5 discrete parts depending on the illustration, but it was not until Leonardo da Vinci injected wax into ox’s ventricular system that an accurate depiction of the anatomy of the ventricles was produced (Mortazavi et al., 2014).

The ventricular system was initially conceived to house humors, behavior and illness, animal spirit and/or air (Clarke and O’Malley, 1968; Mortazavi et al., 2014; Scelsi,

2020). In 1764, Domenico Felice Antonio Contugno discovered the clear, watery fluid known as cerebrospinal fluid (CSF) within the ventricles and discovered the connection between the ventricles and the subarachnoid space, a finding confirmed by Francois Magendie in 1825 in humans and mammals (Clarke and O'Malley, 1968; Mortazavi et al., 2014; Scelsi, 2020).

Since these early studies, the anatomy of the ventricular system in general, and the lateral ventricles (LV) in particular has been examined in cadaveric specimens, through the use of pneumoencephalography, roentgenological, and microscopy. More recently computerized tomography (CT) and magnetic resonance imaging (MRI) have been able to identify the anatomy of the ventricular structure in vivo and at higher resolution than previous techniques. Together, these reports have characterized the anatomical changes that occur in the lateral ventricles in health and disease.

Even though the lateral ventricles have been studied for over 300 years, much of the information about structural variations have been derived from cadavers, older individuals, or in pathological conditions. By contrast, limited results have been obtained about the variability and variations of the anatomy of the lateral ventricle structure in vivo and in the normal adult human. Moreover, the studies that have been performed typically study a small number of individuals and thereby may not have sufficient power to capture the range of variability and variation in the adult human lateral ventricles. In the current project, we investigated structural variations in the lateral ventricle of normal adult human brains.

Anatomy

The ventricular system is centered in the middle of the brain and is defined as four CSF-filled cavities. There are two lateral ventricles each associated with a cerebral hemisphere, a third ventricle between the left and right diencephalons, and a fourth ventricle between the brainstem and cerebellum. Each lateral ventricle is a confluent space comprising an anterior (frontal) horn, a body (central) portion, an atrium, a posterior (occipital) horn, and an inferior (descending or temporal) horn. These different subdivisions of the lateral ventricles are associated with a different lobe of the brain.

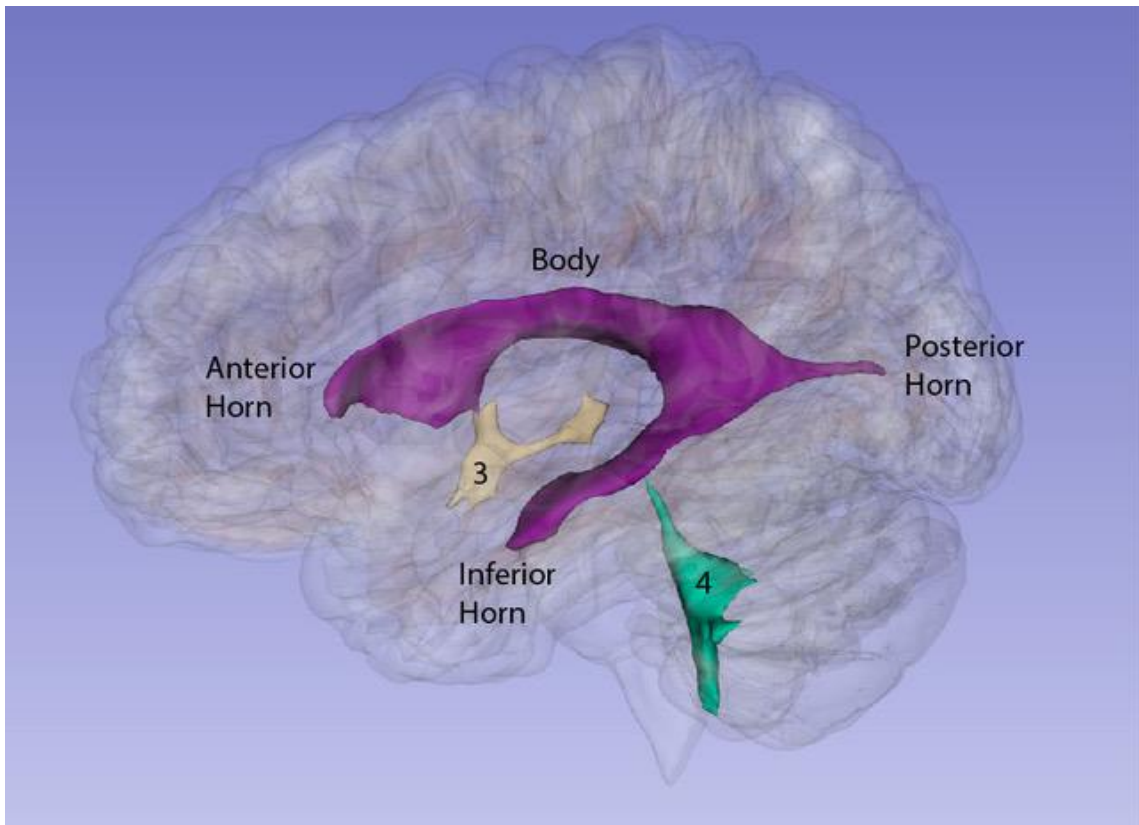


Figure 1. Lateral view perspective of a segmented ventricle. Visualization of the lateral ventricle (purple) subdivisions: Anterior Horn, Body, Atrium (not depicted), Posterior Horn, and Inferior Horn, alongside the third (3; yellow) and fourth (4; green) ventricles.

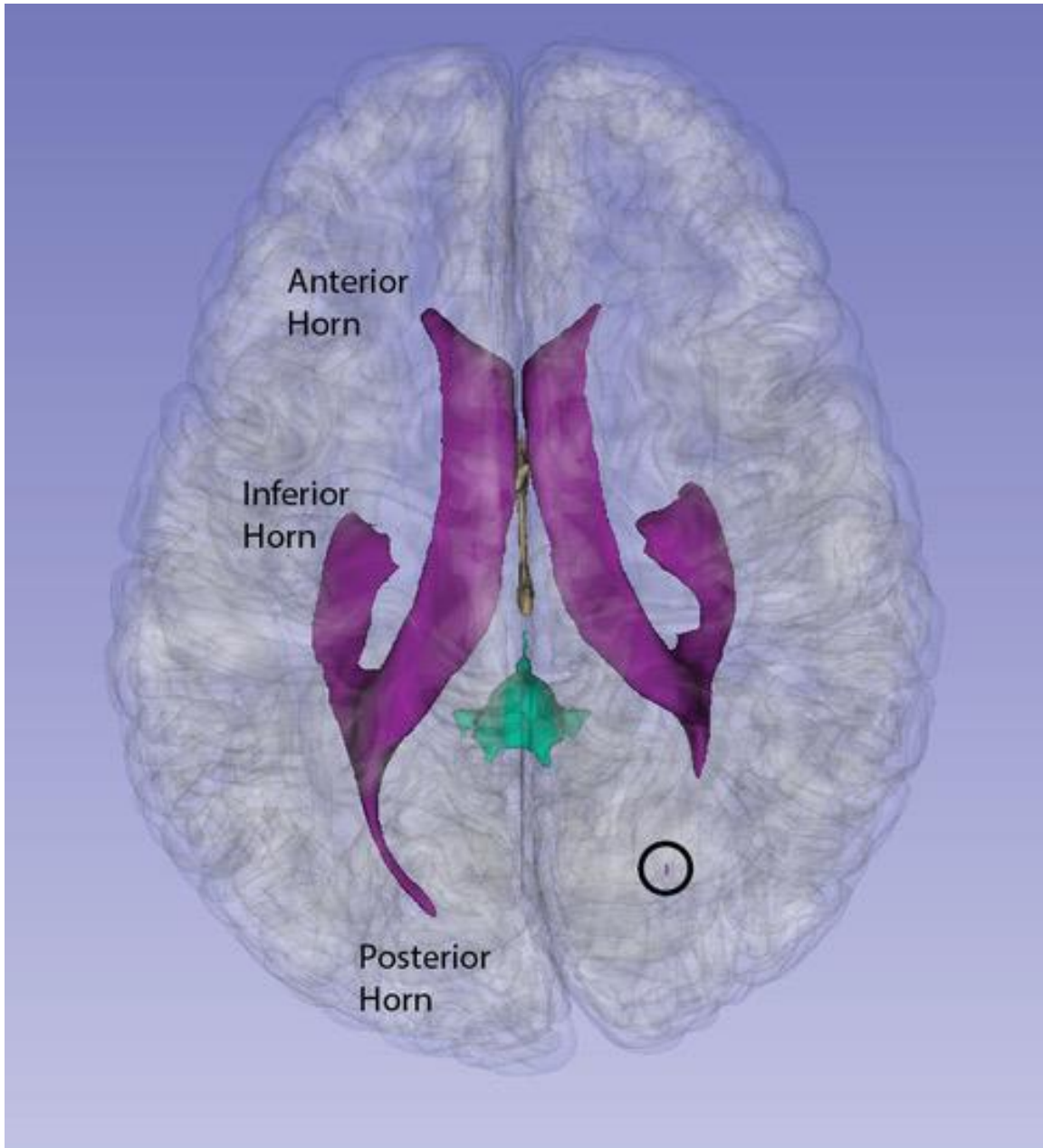


Figure 2. Superior view of a segmented lateral ventricle. Visualization of the left and right lateral ventricles and their subdivisions: Anterior Horn, Body (not depicted), Atrium (not depicted), Posterior Horn, and Inferior Horn. The right-side displays a discontinuous posterior horn that appears disconnected from the rest of the ventricle (circled in black).

Borders and Subdivisions

The divisions between the subdivisions of the lateral ventricle have been evaluated based on multiple sources (Mortazavi et al., 2014; Stratchko, 2016; Trimarchi, 2012; C. L. Scelsi, 2020; Chaddad-Neto, 2022; Morris JA et al., 2022). Specific anatomical structures, landmarks and conventions are used to delineate the borders between the lateral ventricle subdivisions. Some borders are generally agreed on, but some differences persist, as discussed below.

Anterior (Frontal) Horn (AH/FH)

The anterior horn of the lateral ventricle is deep to the frontal lobe of the cerebral cortex. The blind anterior end is delimited by the genu of the corpus callosum, thereby forming the anterior wall of the AH. The roof of the AH is the body of the corpus callosum and the floor is the rostrum of the corpus callosum. The posterior border of the AH is the interventricular foramen of Monro. The medial wall of the AH is the septum pellucidum which separates the left and right AH/FHs. The inferomedial wall border is the columns of the fornix near the foramen of Monro. The forceps minor of the corpus callosum and the head of the caudate nucleus constitute the lateral wall.

Body (Central Part)

The body of the lateral ventricle projects posteriorly from the foramen of Monro to the level of the splenium of the corpus callosum, where it expands as the atrium. The roof of the lateral ventricular body is the corpus callosum, and the floor is the thalamus and the fornix. The superomedial wall is formed by the septum pellucidum and the inferomedial wall is formed by the body of the fornix. The lateral wall is formed superiorly by the caudate nucleus and inferiorly by the thalamus.

Atrium

The body, the posterior horn, and the temporal horn join in a dilated region of the ventricle posterior to the thalamus. The roof of the atrium consists of the body, splenium, and tapetum of the corpus callosum while the collateral trigone makes up the floor. The medial wall is formed by the calcar avis, an indentation produced by the calcarine sulcus and comprised by the intervening white matter. The lateral wall is made up of the curved posterior end of the caudate nucleus, and tapetum of the corpus callosum which continues down from the roof and continues laterally. The anterior limit is the pulvinar of the thalamus medially, the crura of the fornix laterally, and the choroidal fissure inferiorly. The posterior limit is the callosal bulb (the impression made by the splenium of the corpus callosum), the calcar avis, and fibers of the tapetum of the corpus callosum (Feres Chaddad Neto, 2022).

Posterior (Occipital) Horn (PH/OH)

The posterior horn is located posteriorly to the atrium and comprises the portion of the ventricle that tapers from the dilated atrium to end blindly in the occipital lobe. Throughout, the posterior horn is bounded by cerebral white matter. Unlike other ventricular regions, the border between the atrium and the posterior horn is indistinct.

Inferior (descending or temporal) horn (IH/DH/TH)

The inferior horn extends anteroinferiorly from the atrium through the temporal lobe and terminates within the temporal pole adjacent to the amygdala. The roof of the temporal horn consists of the tail of the caudate nucleus, thalamus, and the tapetum of the corpus callosum. A small portion of the roof, specifically on the medial side, is formed by the stria terminalis. The medial floor is formed by the hippocampus. The lateral floor is formed by the collateral eminence which is formed by an impression of the cerebral white matter by the collateral sulcus of the cerebral cortex. The medial wall is formed by a small cleft between the fornix fimbria and the thalamus. The choroidal fissure runs along the medial wall and is composed of the fimbria of the hippocampus where the choroid plexus overlays. The lateral wall is composed of the tapetum which runs inferiorly and separates the wall from the optic radiation. In some instances, the collateral fissure may form a protuberance on the lateral wall.

*Contents***Choroid Plexus**

The choroid plexus is a highly vascular structure that creates CSF and is present inside the body, atrium, and temporal horns of the lateral ventricle. At any given time, the lateral ventricle holds 150 mL of CSF in an average adult and the CSF production ranges anywhere between 400-600 mL per day (Stratchko et al., 2016).

Lining / Ependymal cells

The ventricles are lined with a glial cell known as an ependymal cell, of which there are three different types: E1, E2, and E3. These cells line the ventricular surface in a single layer of ciliated columnar cells. The multinucleated E1 ependymal cells are the predominant type that line the lateral ventricles. E1 cells are polarized and contain cilia on their apical surface. The cilia are motile and beat CSF in the direction of the interventricular foramen of Monro. E2 ependymal cells are also ciliated, while the E3 cells are unciliated. Together, E2 and E3 play a role in both the recognition of CSF metabolites and regulation of progenitor cell activity (Mirzadeh, 2017), and contribute to the generation of newborn neurons in periventricular regions such as the median eminence (Deng, 2023). Coordinated cilia beating of the ependymal cells allows for CSF to move through the lateral ventricles. Ependymal cells mediate selective passage of substances between the brain tissue and CSF (Silverberg et al., 2001; Igarashi et al., 2014).

Embryology

Upon conception, the embryo begins folding and undergoing rapid changes induced by an array of genes and hormones that lead to the closure of the neural tube around the fourth week of gestation (Scelsi, 2020). During the fifth week of gestation, the forebrain, also known as the prosencephalon, gives rise to the telencephalon and the diencephalon. The telencephalon leads to the development of the two cerebral hemispheres. At the initial stages, the telencephalon produces two evaginations. Each is a fluid-filled chamber lined with epithelium. The epithelial lining will become of the cells, nuclei and cortex of the telencephalon, and each chamber will become the lateral ventricles. The corpus striatum is found in the medial basal portion of the cerebral hemispheres, and it undergoes rapid growth that leads to changes in the shape of the developing lateral ventricle. This dramatic change leads to the early development of foramen of Monro, the connection between the lateral ventricle and the midline third ventricle. This foramen narrows within the sixth week of gestation as the choroidal fissure forms. During the eighth week, the continued growth of telencephalic neural structures causes the lateral ventricle to adopt a C-shaped appearance. The ependyma are derived from radial glial cells around embryonic day fourteen and sixteen (Deng, 2023). At around 32 days of development, the choroid plexus fills the majority of the lateral ventricle. By the end of the first trimester, a large proportion of the cerebral hemisphere is occupied by the fast-expanding lateral ventricles, while the parenchymal growth remains minimal. At the twenty-first week of gestation, during the second trimester, the parenchymal growth accelerates, allowing the distinct development of the frontal, temporal, and occipital horns. At the thirty-first week, or the beginning of

the third trimester, the anatomy of the lateral ventricle is similar to that of the adult (Mortazavi et al., 2014; Scelsi, 2020; Huff, 2023).

During the sixth and seventh month of fetal life, the posterior horn of the lateral ventricle is larger than any other time during an individual's life. As development continues, the calcarine and parieto-occipital fissures grow, and the production of CSF begins to encroach on the posterior horn space. Postnatally, the cerebellum rapidly expands and pushes into the occipital lobe so much so that the pressure is reflected on the PH of the LVs (Curran, 1909).

Several studies focusing on prenatal and infant subjects have evaluated the size of the lateral ventricles. A study using ultrasound examined 66 infants without intracranial pathology and found that in 41 infants, the right and left lateral ventricle bodies were of equal size. In 21 subjects, however, the left lateral ventricle body was larger than the right (Horbar, 1983). Another study used MRI in 84 participants between 14 and 35 weeks found that up to 24 gestational weeks, there were no significant difference between the right and left lateral ventricles. However, after 24 gestational weeks, there was a significant difference between the left and right LV with the left LV having a larger volume (Li Z et al., 2019).

Background and Summary of Anatomical Research of the Lateral Ventricles

The anatomy of the lateral ventricles has been studied largely in cadaveric specimens, through the use of pneumoencephalography, and more recently using computerized tomography (CT) and magnetic resonance imaging (MRI).

Despite the long history of anatomical investigation of the lateral ventricles, little systematic information has been obtained on several normal anatomical variations of the lateral ventricles. Studies on age, size, shape, sex difference, handedness, and asymmetry have been completed with mixed results.

The most common measurements of the lateral ventricle are related to morphology and include length and volume. In addition, several morphometric indices (Cella media index, Evan's index, Huckman's index, bicaudate index, bifrontal index, cella media index, third ventricular index, and ventricular index) have been developed as secondary measures. The Evan's index is defined as the largest bifrontal diameter, determined by a line that connects the two front corners of the AH divided by the largest inner skull diameter. Huckman's index combines the smallest LV width and the largest bifrontal diameter. The bicaudate index is the smallest width of the LV divided by the second horizontal plane minus the smallest width of the LV. The bifrontal index is the largest bifrontal diameter divided by the diameter of the bifrontal distance. The Cella media index is defined as the combined width of the cella media divided by the smallest inner skull diameter. The third ventricle ratio (or index) is the largest distance between the third ventricle's lateral margins divided by the distance between the cortical surfaces (left to right). The ventricular index is the smallest width of the LV divided by the largest bifrontal diameter.

Morphometric Measurements of the Lateral Ventricles

The ventricles constitute 2% of the total brain volume (TBV) and the LV contribute to 82% of the total ventricular system (Patnaik et al., 2016), and have an average measurement of 20.1 cubic centimeters (or 20,100 mm³; Apostolova LG et al., 2012). Recent studies using automated and manual (FreeSurfer or 3D Slicer) approaches to determining volume of the left and right consistently show that on average the left lateral ventricle is larger than the right lateral ventricle (van Erp TGM et al., 2016; Guadalupe T et al., 2017; Rushmore et al., 2022), with the left LV measuring 7.62 ± 3.94 cm³ and the right LV measuring 6.88 ± 3.17 cm³ (Rushmore et al., 2022). The variation between subjects is considerable (46-51%) and makes it difficult to conclude that the ventricles are reliably larger on one side than the other in a specific individual. Thus, multiple studies have concluded that the left ventricle is larger (Harvey RW, 1911; LeMay, 1984; Ichihashi K et al., 2002; Kiroglu Y et al., 2008; Annongu et al., 2017; Li Z et al., 2019), while other studies have found larger right ventricle volume (Trimarchi et al., 2013; Honnegowda TM, 2017). The differences in these studies may be a result of the large variation in the ventricular size but may also be due to differences in subject populations, methods (e.g., cadaveric measurement vs. in vivo imaging method), or the presence of comorbidities. In fact, asymmetry between lateral ventricles may be influenced by factors such as sex (male vs. female), handedness, and age, or the interaction thereof. Tied to the above, estimates of the incidence of asymmetry of the lateral ventricles has been postulated to be seen in 5.3% of cases in 1900 (Grosman, 1900), in 6.1% of cases in 2008 (Kiroglu Y et al., 2008), and in 5-12% of cases in 2013 (Mortazavi et al., 2014).

Sex Differences and Ventricular Asymmetry

While men typically have larger brain volumes than women (Ruigrok et al., 2014), the question of whether ventricular volume differs on the basis of sex is still an open question. Some studies have identified that the male lateral ventricles are larger than females in general (Gyldensted, 1977; Allen, Damasio, Grabowski, 2002; Vinoo Jacob, 2013; Singh et al., 2014; M. Gameraddin, 2015; Honnegowda TM, 2017; Kolsur et al. 2018; Li Z et al., 2019; Agarwal S et al., 2023), whereas others have found that the encephalic ventricle volume is larger in females than in males (Cramer et al., 1990). Still other studies have identified no sex difference (Brassow F, Baumann F, 1978; Antar et al., 1984; Erdogan, 2004; Jacob and Kumar, 2013; A Hori et al., 2019; Polat et al., 2019). When comparing the ventricles within males and females, asymmetry is noted in females, but not in males (Gyldensted, 1977). Thus, it is an open question whether ventricular volume or asymmetry differs in males and females.

Handedness and Ventricular Asymmetry

In most right handers, the left cerebral hemisphere is larger than the left LV and such asymmetry might be expected to relate to the morphology of the lateral ventricles. Some studies have shown that ventricular asymmetry did not differ significantly between right-handed males and right-handed females (Cramer et al., 1990; Erdogan, 2004), while in other studies, the left LV was found to be larger in both right- and left-handed subjects when compared to the right LV (Zipursky, Lim, Pfefferbaum, 1990).

Ventricular Size and Asymmetry in Aging

Age is a consistent factor associated with lateral ventricle size. Many studies have shown that the size (both length and width) of the ventricles increase as individuals age (Cramer et al., 2013; Singh et al., 2014; Agarwal S et al., 2023) and that ventriculomegaly is positively associated with age (Vino Jacob, 2013).

The ventricle gradually increases in size between the first and seventh decades, with no significant increase observed between the second and third or fourth and fifth decade of life. However, there are statistically significant increases when comparing all other decades (third and fourth, fifth and sixth, sixth and seventh, etc.), and at the eighth and ninth decade there is a dramatic increase in size (Barron and Jacob et al., 1976). Calculations based on ventricular indices also show increases in ventricular size specifically during the sixth and seventh decade (Vino Jacob, 2013), with the maximum ventricular length observed in participants greater than 70 years of age (Agarwal S et al., 2023).

Some studies have suggested that there are no differences between the right and left ventricle size with relation to aging (Trimarchi et al., 2013), but there does appear to be a positive correlation between ventricular indices (Evan's index, Huckman's index, bicaudate index, bifrontal index, cella media index, third ventricular index, and ventricular index) and increasing age (Kolsur et al., 2018).

Morphometric Studies of Lateral Ventricle Subdivisions

Anterior (Frontal) Horn (AH/FH)

Asymmetry is present of the the AH/FH (Trimarchi, 2013) in approximately 10.3% of cases (Shapiro et al., 1986), with some studies showing a larger left AH, and others a larger right AH (Harvey RW, 1911; Shapiro et al., 1986; Annongu et al., 2017). Other studies have identified no difference in the width of the left and right AH/FH (Gyldensted, 1976; Vidal et al., 2008; Annongu et al., 2017).

Studies examining sex differences of the frontal horn have produced contradictory findings, with some studies showing larger frontal horns in males (Karakas P., 2011; Gameraddin et al., 2015; Polat, 2019), while others find no differences based on sex (Gameraddin et al., 2015; Patnaik et al., 2016; Agarwal S et al., 2023). Other studies have found that females possessed a larger Evans' index, while the males had the higher Evans' ratio (FH/TIDS) (Polat et al., 2019). The data on asymmetry of the frontal horn is similarly contradictory with some studies showing asymmetry only in females, other studies have shown asymmetry in males, and still other studies have shown asymmetry in both males and females (Karakas P., 2011; Singh et al., 2014; Gameraddin, 2015; Honnegowda TM, 2017).

Specific lengths (see Table 1) of the AH have been specified in multiple studies and classified based overall (unspecified), right and left side based on demographics: age (Singh et al., 2014; Shahin S et al., 2020), on cadaveric specimen and MRIs (Shahin S et al., 2020), males and females (Last RJ, Tompsett DH, 1953; Singh et al, 2014; Gameraddin et al., 2015; Honnegowda TM, 2017; Shahin S et al., 2020), and unspecified demographics

(Last RJ, Tompsett DH, 1953; Gameraddin et al., 2015; Honnegowda TM, 2017; Annongu et al., 2017; Shahin S et al., 2020).

Table 1: Length of Anterior (Frontal) Horn (AH/FH)

Portion	Defined	Overall (mm)	Right (mm)	Left (mm)	Author	Year	Study Type	Total (N)	Male (n)	Female (n)	Age(s)								
Length of AH of LV	20-29 yrs	30.15	-	-	Shahin S et al.	2020	MRI	127	78	49	10 to 70								
	20-40 yrs	-	23.93 ± 2.34	-	Singh et al.	2014	CT	358	207	151	270 between 20 – 60 88 above 60								
	30-39 yrs	33.64	-	-	Shahin S et al.	2020	MRI	127	78	49	10 to 70								
	Cadaver	30.64 ± 4.63	-	-															
	Female		34.31 ± 5.83	-	-	Last RJ, Tompsett DH	1953	Casts	29	N/A	N/A	29 to 73							
			-	32	33														
			-	26.16 ± 4.209	26.17 ± 4.237								Gameraddin et al.	2015	CT	152	89	63	3 to 81
			-	28.4 ± 4.2	27.4 ± 3.2								Honnegowda TM	2017	CT	250	130	120	12 to 81
			-	25.34 ± 3.50	26.53 ± 3.38								Singh et al.	2014	CT	358	207	151	270 between 20 – 60 88 above 60
			35.1 ± 3.79	-	-								Shahin S et al.	2020	MRI	127	78	49	10 to 70
	Male		-	32	33	Last RJ, Tompsett DH	1953	Casts	29	N/A	N/A	29 to 73							
			-	28.53 ± 3.882	26.16 ± 3.882	Gameraddin et al.	2015	CT	152	89	63	3 to 81							
			-	30.54 ± 3.4	30.14 ± 4.7	Honnegowda TM	2017	CT	250	130	120	12 to 81							
			-	25.00 ± 3.18	26.26 ± 2.94	Singh et al.	2014	CT	358	207	151	270 between 20 – 60 88 above 60							
	Overall	MRI	34.83 ± 4.56	(blank)	(blank)	Shahin S et al.	2020	MRI	127	78	49	10 to 70							
			29.02 ± 3.59	29.02 ± 3.59	30.38 ± 3.68	Annongu et al.	2017	CT	132	90	42	15 to 74							
			34.83 ± 4.56	-	-	Shahin S et al.	2020	MRI	127	78	49	10 to 70							
			-	32	33	Last RJ, Tompsett DH	1953	Casts	29	N/A	N/A	29 to 73							
			-	27.55 ± 4.175	27.55 ± 4.184	Gameraddin et al.	2015	CT	152	89	63	3 to 81							
		-	29.2 ± 3.72	28.7 ± 2.9	Honnegowda TM	2017	CT	250	130	120	12 to 81								

Body (Central Part)

Minimal research has been conducted on the asymmetry surrounding the body or central portion of the lateral ventricle, but similar to previously cited studies, the research completed has yet to reach a consensus. Results of studies evaluating asymmetry according to sex have found no difference, larger in the left in the male, larger in the right in the male, and larger in the right in the female (Gameraddin et al., 2015; Honnegowda TM, 2017; Agarwal S et al., 2023).

Only one study investigated the length of the body, but it was combined with the AH length in CT scans of males and females on both the right and left side (Singh et al., 2014; see Table 2). Other studies of the body length alone (see Table 3) have been

completed looking at: overall (unspecified), right and left side based on demographics: age (Agarawal S et al., 2023), MRIs (Agarawal S et al., 2023), males and females (Last RJ, Tompsett DH, 1953; Gameraddin et al., 2015; Honnegowda TM, 2017; Agarawal S et al., 2023), and unspecified demographics (Last RJ, Tompsett DH, 1953; Gameraddin et al., 2015; Honnegowda TM, 2017; Agarawal S et al., 2023).

Table 2: Length of Anterior (Frontal) Horn (AH/FH) + Body (Central Part)

Portion	Defined	Right (mm)	Left (mm)	Author	Year	Study Type	Total (N)	Male (n)	Female (n)	Age(s)
Length FH + Body of LV	20-40 yrs	52.23 ± 4.80	-	Singh et al.	2014	CT	358	207	151	270 between 20 - 60 88 above 60
	Female	55.10 ± 6.99	56.28 ± 7.59							
	Male	55.78 ± 6.15	56.70 ± 6.61							

Table 3. Length of Body (Central Part) of the Lateral Ventricle

Portion	Defined	Overall (mm)	Right (mm)	Left (mm)	Author	Year	Study Type	Total (N)	Male (n)	Female (n)	Age(s)	
Length of Body of LV	20-29 yrs	54.88	-	-	Agarwal S et al.	2023	MRI	127	78	49	10 to 70	
	30-39 yrs	52.14	-	-								
	Cadaver	35.49 ± 2.43	-	-								
	Female		53.6 ± 1.92	-	-	Last RJ, Tompsett DH	1953	Casts	29	N/A	N/A	29 to 73 (adult)
			-	41	39							
			-	70.06 ± 8.832	69.56 ± 11.420	Gameraddin et al.	2015	CT	152	89	63	3 to 81
			-	71.36 ± 9.4	71.09 ± 9.4	Honnegowda, TM	2017	CT	250	130	120	12 to 81
			54.78 ± 2.66	-	-	Agarwal S et al.	2020	MRI	127	78	49	10 to 70
			-	41	41	Last RJ, Tompsett DH	1953	Casts	29	N/A	N/A	29 to 73 (adult)
	Male		-	74.89 ± 9.860	74.89 ± 9.860	Gameraddin et al.	2015	CT	152	89	63	3 to 81
			-	77.45 ± 8.6	76.6 ± 8.4	Honnegowda, TM	2017	CT	250	130	120	12 to 81
		MRI	54.37 ± 2.48	-	-	Agarwal S et al.	2023	MRI	127	78	49	10 to 70
		54.37 ± 2.48	-	-								
	Overall		-	40	41	Last RJ, Tompsett DH	1953	Casts	29	N/A	N/A	29 to 73 (adult)
			-	72.89 ± 9.714	72.68 ± 10.823	Gameraddin et al.	2015	CT	152	89	63	3 to 81
		-	76.23 ± 9.4	72.43 ± 8.78	Honnegowda, TM	2017	CT	250	130	120	12 to 81	

Posterior (Occipital) Horn (PH/OH)

Posterior asymmetry is dubbed the rule in the lateral ventricles (Last RJ, Tompsett DH, 1953). In the late 60's, a study was conducted that proved that in 30% of cases, there was no difference between the right and the left PH/OH of the LV (McRae, 1968), meaning that 70% of the PH/OH is asymmetrical. Two separate studies have concluded that the left

PH/OH was larger (McRae, 1968; Strauss and Fitz, 1980), while a more recent study concluded that the right PH/OH was larger (Srijit D, Sherpa P, 2007). When taking into account handedness, left-handed subjects possessed a longer right PH/OH, while the right-handed subjects had a longer left PH/OH (McRae, 1968). The influence of sex on PH/OH asymmetry has not been well characterized. One study in 2020 proved that although the male PH/OH appeared larger, the difference between male and female was not statistically significant (Agarwal S et al., 2023).

Previous studies have assessed the volume or ratios of the lateral ventricle (LV) and its posterior horn (PH) subdivision, but limited research has focused on LV length and the effect of demographic data. The study by Agarwal et al. (2023) stands out as one of the few to provide specific PH lengths across various age groups and sexes, analyzing both cadaveric specimens and MRI data (refer to Table 4). Similarly, Karakas P. (2019) examined the longitudinal dimensions from the frontal to occipital pole in both males and females using MRI (see Table 5), whereas Annongu et al. (2017) determined the right and left LV length using CT imaging (see Table 6). While these studies offer insight into the lengths of the LV and its subdivisions, they suffer from limited demographic variability and a scarcity of comparable data.

Table 4: Length of Posterior (Occipital) Horn (PH/OH)

Portion	Defined	Overall (mm)	Author	Year	Study Type	Total (N)	Male (n)	Female (n)	Age(s)
Length of PH of LV	20-29 yrs	22.02	Agarwal S et al.	2023	MRI	127	78	49	10 to 70
	30-39 yrs	22.35							
	Cadaver	42.29 ± 5.91							
	Female	22.49 ± 2.9							
	Male	23.43 ± 2.24							
	MRI	23.10 ± 2.55							
	Overall	23.10 ± 2.55							

Table 5: Length of Frontal to Occipital Pole (Longitudinal Dimension)

Portion	Defined	Overall (mm)	Author	Year	Study Type	Total (N)	Male (n)	Female (n)	Age(s)
Frontal to Occipital Pole (longitudinal dimension)	Female	150.12 ± 5.04	Karakas P.	2011	MRI	52	23	29	20 to 50
	Male	152.53 ± 5.43							

Table 6: Length of Lateral Ventricle

Portion	Defined	Right (mm)	Left (mm)	Author	Year	Study Type	Total (N)	Male (n)	Female (n)	Age(s)
Length of LV	Overall	78.14 ± 7.61	79.64 ± 6.84	Annongu et al.	2017	CT	132	90	42	15 to 74

Summary of Existing Studies

Overall, in spite of the fact that the lateral ventricles have been carefully studied for over a century, there is surprisingly little consensus on fundamental morphological features of the lateral ventricles, and how these features are affected by factors such as asymmetry and sex differences. This is true for the lateral ventricle in general, but also for the specific subdivisions that comprise the lateral ventricle. The reasons for the discrepancies are manifold, but likely are a result of comparing populations that differ based on age, handedness, sex, and comorbidity status. Each of these variables has the potential to have an independent effect on ventricular size and must be carefully controlled for. In addition, it is highly likely that the morphology of the lateral ventricle in vivo differs greatly from that observed in post-mortem specimens.

Variations

The lateral ventricles are conceived as confluent structures, but close evaluation indicates that in many brains, the spaces are not confluent, compressed, or otherwise

obstructed. These alterations in morphology exist in specific locations within the lateral ventricle, and do not appear in association with clinical studies. To date, few studies have investigated the degree of this type of anatomical variation in the normal population, particularly in normal healthy adults. This gap in knowledge is compounded by a lack of clarity in the definitions of these morphological alterations.

Coarctation And Coaptation

Coarctation and coaptation are two terms that have been used synonymously to describe a narrowing, fusion, closure, or obstruction of the lateral ventricles.

Coarctation was first defined in pneumoencephalography, microscopy, and roentgenological studies of cadaveric specimens as the compression, narrowing or constriction of the lateral angles of the cerebral lateral ventricles (Davidoff, 1946). Less than a decade later, a five-year-long study was done on cadaveric specimens that further defined coarctation or coaptation as, “the apposition or fusion of 2 ventricular walls, resulting in partial or complete obliteration of the lumen.” (Bates and Netsky, 1955). Since this 1955 publication, there have been few research studies (Sener, 1997; Dogan, 2015; Scelsi, 2020; Morris JA et al., 2022) done to determine the frequency and degree of coaptation of the lateral ventricles among individuals.

Coarctation has been characterized as the microscopic appearance of “elongation of ependymal cells between the corpus callosum and the head of the caudate nucleus” (Davidoff, 1946). Sener defined coarctation in the frontal horn in which the horn walls appeared to be fused and was compared to the irregular loss of ependyma in the FH with

astrocytic gliosis (proliferation of astrocytes that produce a glial scar due to a permanent injury (McKeever, 2021), better known as ependymitis granularis (Sener, 1997). Coarctation of the lateral ventricles was observed in the superolateral (external) angles of the lateral ventricles. Within the LV, coarctation was most common in the frontal horns or within the body, and/or within the anterior portion of the foramen of Monro. These researchers determined coarctation, connatal cysts, and frontal horn cysts are synonymous, and are considered normal morphological variations of the LV (Epelman, 2006; Dogan, 2015). The American Journal of Neuroradiology did a detailed review of the lateral ventricles and defined coarctation as an anatomic variant that refers to the “apposition or fusion of 2 ventricular walls” that leads to complete or partial obstruction of the communication through a lumen. The terms “close apposition” and “fusion” of two ventricular walls were also used by the Neuroimaging Clinics of North America who published, “Anatomy of the Ventricles, Subarachnoid Spaces, and Meninges” (Morris JA et al., 2022). Similar to Dogan, a discussion of small rosettes, ependymal lined cysts, or connatal cysts was described (C.L. Scelsi, 2020). Lastly, coaptation, which has been defined as the fusion of ependymal-lined surfaces, shares the same definition as coarctation (Bates, 1955).

In a 1909 correspondence to the Boston Medical and Surgical Journal, E. J. Curran, MD discussed the underrepresented posterior horn variations seen among the autopsied brains he encountered while working at Harvard University Medical School. It was discovered that 22 out of 64 subjects had varying degrees of constriction among the PH of the LV, that were classified into 3 categories (A: ordinary, normal, dilated, or easily

pushed/drawn in manipulated by internal or external pressure; B: constricted with adhesion; C: complete closure). Between class B and C, 42 out of 64 cases fell under these two categories. It is within this correspondence that the author argues that the calcarine fissure and cerebellum play a role regarding the shape of the LV PH/OH. This article adds to the definition of coarctation with specific information regarding the PH. It was found that a large percentage of brains display a cut off of communication with the rest of the ventricle due to this adhesion or constriction. (Curran, 1909).

Coaptation has also been described as an “accessory cerebral ventricle” that can be found in the occipital lobe of the brain. This accessory cerebral ventricle was found in 21.3% (86) of 404 subjects who underwent a CT scan. Of these 86 cases, 34 were seen on the left, 25 on the right, and 27 on both sides. This anomaly was also found in 29.5% of 200 autopsied brains (Hori, 1984).

Despite this knowledge, very little information has been assembled on the incidence of these anatomical variations in healthy adult human brains of both sexes.

Clinical Variations

A number of pathologies lead to changes in the anatomy of the lateral ventricle. Most disorders lead to substantial volumetric increases and reflect global or specific reductions in gray or white matter volumes. These changes are observed in disorders such as Alzheimer's Disease (AD), Autism Spectrum Disorder (ASD), Bipolar Disease (BD), Chronic Traumatic Encephalopathy (CTE), Huntington's Disease (HD), Hydrocephalus, Multiple Sclerosis (MS), Parkinson's Disease (PD), and Schizophrenia

(SCZ). In addition, volumetric changes to specific ventricular subdivisions have been observed in AD, Autism, CTE, and Schizophrenia.

Alzheimer's Disease (AD)

Alzheimer's Disease (AD) is a progressive neurodegenerative disease that has an onset in both middle- and late-age adults. As the most common type of dementia worldwide, leading to an accrual of approximately 156 billion dollars annually in healthcare costs (Apostolova, 2012). AD studies have shown decreases in myelin and axons, leading to an overall volume decrease in the gray and white matter and an increase in cerebrospinal fluid (CSF) filled spaces. Many structures are affected by AD such as the corpus callosum, amygdala, hippocampus, thalamus, caudate nucleus, and deep white matter. AD is associated with increases in the size of the lateral ventricles. These increases are especially pronounced in the temporal/inferior horn (Shape differences of the brain ventricles in AD, 2006).

Autism Spectrum Disorder (ASD)

Autism spectrum disorder (ASD) is a complex developmental disability that causes differences in the brain believed to be caused by a combination of genetics, epigenetics, environmental and biological factors (Basics About Autism Spectrum Disorder (ASD) - CDC, 2022). There have been few studies investigating the anatomy of the lateral ventricles in autism. One CT study of 13 participants between the ages of 3 and 8 found a tendency of individuals with autism to have a smaller right to left ventricular ratio (Rosenbloom S

et al., 1984). More recently, a study with 42 participants spanning 6 to 17 years of age showed localized reductions in regional ventricular volumes in both the right and left AH/FH and PH/OH of the ventricles. These diminished ventricular volumes were also seen in the mid portion of the left lateral ventricle (Vidal et al., 2008). Given the difficulty in predicting the incidence of autism, these results suggest that ventricular anatomy may be a potential biomarker of autism.

Chronic Traumatic Encephalopathy (CTE)

Chronic traumatic encephalopathy (CTE) is a neuropathological condition associated with repeated head injury and/or traumatic brain injuries (TBIs) caused by blows to the head and concussions. CTE is common among individuals who participate in contact sports (football, soccer, baseball, boxing, etc.) or veterans that have been exposed to explosions during war (McKee et al., 2015; NHS, 2017; ALZ.org, 2024). Major symptoms of those affected by CTE include memory issues, attention deficit, balance and motor skills, confusion, personality changes, depression, aggressive behaviors, and many more. There has been little consensus among scientists about what symptoms can be seen in the early stages of CTE, as it can take decades after injury to experience symptoms (NHS, 2017; ALZ.org, 2024). CTE has gross changes within the lateral ventricles that can be identified when looking at gross anatomy. In early or mild CTE, the lateral ventricles show specific enlargements in the AH/FH and TH (McKee et al., 2015). Thus, given the difficulty in diagnosis, ventricular anatomy may aid in predicting whether an individual has CTE.

Schizophrenia (SCZ)

Schizophrenia (SCZ) is a chronic and complex mental health disorder characterized by delusions, and hallucinations (McCutcheon, 2020). In an MRI study that contained 30 controls and 39 age- and sex-matched Schizophrenia subjects between the age range of 14 and 45 years old, male individuals with schizophrenia exhibited a greater amount of shape asymmetries, but there were no significant differences among the female subgroups. In the SCZ group, the greatest amount of asymmetry was seen in the main ventricle body and the AH/FH, but in the control group, the largest amount of asymmetry was found in the tip of the TH and AH/FH (Graham J. et al., 2006). In a case study that followed only 1 male who was 57 years old, CT, MRI, and gross anatomy were used to propose that the PH/OH is adjacent to vital functional areas, and any abnormalities in the PH/OH could lead to diagnosing visual disturbances (such as with schizophrenia or other psychiatric disorders) (Srijit and Shipra, 2007).

Purpose of This Study

The background information shows that many aspects of the morphology of the lateral ventricles are not yet definitively established. In the current study, we have evaluated the anatomy of the lateral ventricles of the human brain in both sexes using high-resolution MRI scans from the Human Connectome Project (HCP; Glasser et al., 2013). The high-resolution MRI scans from the HCP allows for the study of a large number of well-characterized individuals of a similar age and without pathology. The HCP subjects are also scored for handedness and are scanned at a high spatial resolution (0.7mm isotropic), thus ventricular analysis can be performed in the context of variables that

otherwise would impair strong conclusions to be made. In addition, the high resolution allows for evaluation of coaptation or coarctation events as well as precise subregional analysis. This study aims to advance our basic and clinical understanding of lateral ventricle morphology.

METHODS

Experimental Subjects

As previously described by Glasser et al. (2013), three-hundred and two high-resolution T1w MRI images were obtained from the HCP Young Adult dataset (n = 172 female, n = 130 male) with the corresponding demographic characteristics: 55.30% Black or African American, 22.19% White, 20.53% Asian/Native Hawaiian/Other Pacific Islander, 0.66% American Indian/Alaskan Native, 0.99% More than one, and 0.33% Unknown or Not Reported. The mean age of the participants was 28.7 years (standard deviation = 3.9, min = 22, max = 36). Subjects were randomly selected such that only one individual per family was included in the study. The resulting participant pool was unequal in terms of sex distribution, and as a result, randomly selected individuals were swapped within a family to create an even sex distribution within and across demographics. The final population had a grand total of 174 participants (n = 87 female, n = 87 male).

Data Collection

3D Slicer

3D Slicer (<https://www.slicer.org/>) is a free, open-source software used for multiple applications including visualization, processing, segmentation, and much more. Upon download, 3D Slicer was used to visualize the high-resolution MRI scans obtained by the HCP, and to calculate the length of the lateral ventricles and their subdivisions.

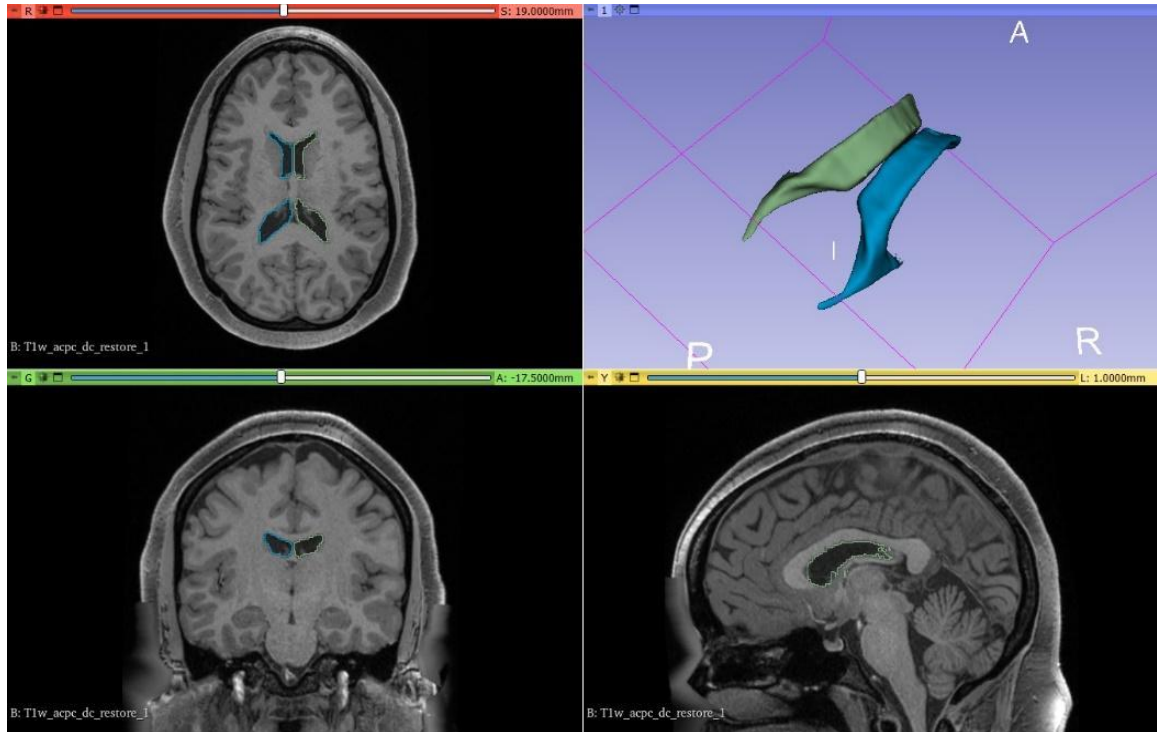


Figure 3. Visualization of MRI dataset in 3D Slicer. Three different views of the same volume are shown: axial (red window, upper left), sagittal (yellow window, lower right), coronal (green window, lower level), and a 3D visualization window of any segmentation. For this study, the green (Coronal) view was primarily utilized for visualization and measurement.

Magnetic Resonance Imaging (MRI) Analysis

Anatomical Definitions

The anterior aspect of the anterior horn was identified by a disruption in the white matter posterior to the start of the corpus callosum for the left and right ventricles (see Figure 4). The posterior aspect was set at the foramen of Monro (see Figure 6), and the distance of the anterior horn was determined. The presence of anatomical variations such as coarctation and compressions were noted, along with the severity of compressions.

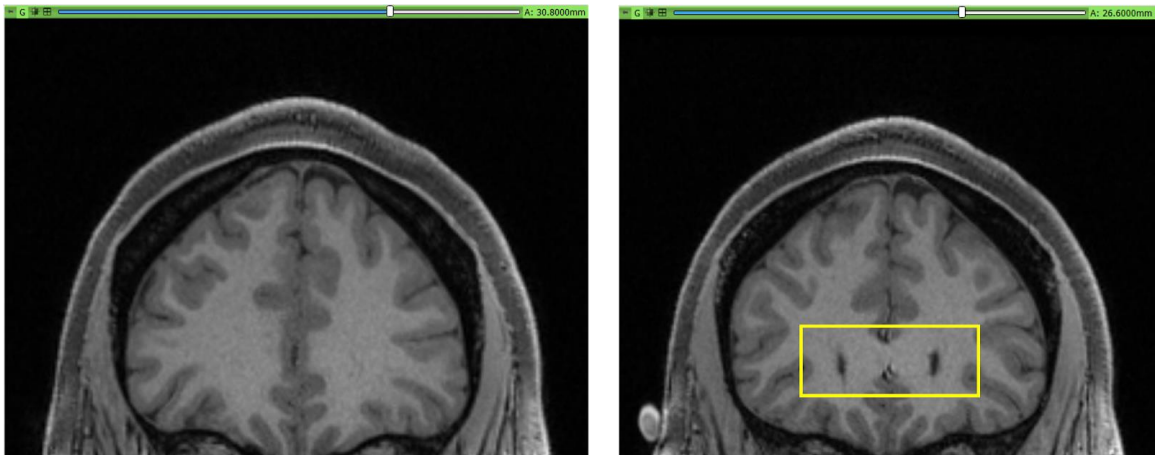


Figure 4. MRI Displaying Opening of Anterior Horn. Moving posteriorly, the anterior horn is marked by a break in the white matter (yellow box) just after the merging of the right and left hemisphere's white matter, which is the corpus callosum.

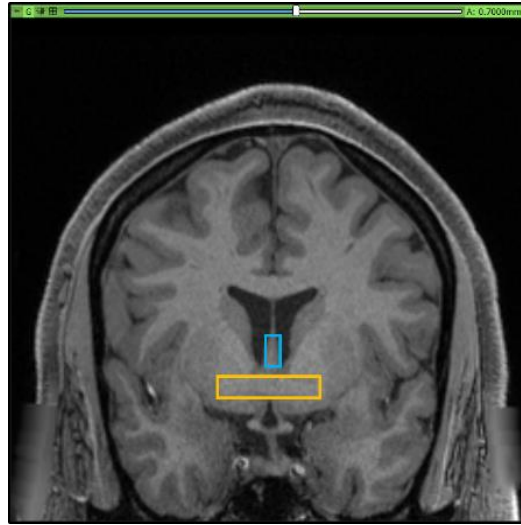


Figure 5. The coronal section immediately prior to the border between the frontal horn and the body. The fornix (blue box) can be identified on the midline, and the anterior commissure (orange box) is notable at this level. Subsequent sections will display the foramen of Monro (Figure 6).

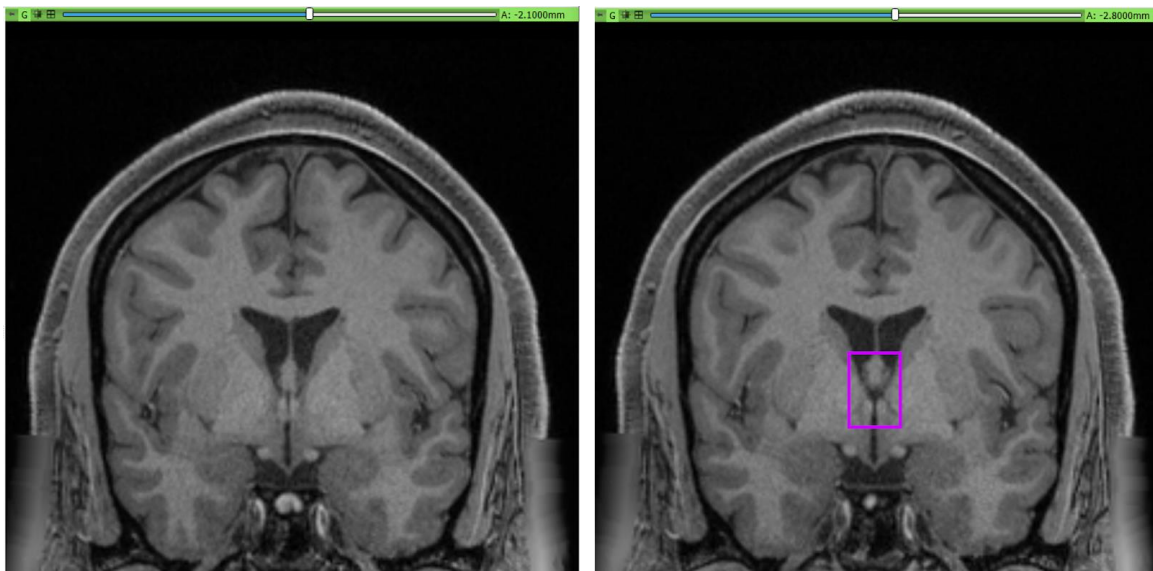


Figure 6. MRI image of the foramen of Monro in two sequential sections. At this level, the anterior commissure has disappeared and the fornix is divided into superior and inferior segments. The space between the two fornical segments is known as the foramen of Monro (purple box) and serves as the border between the anterior horn and the body of the lateral ventricle.

Compression Incidence

Compression of the AH was defined based on severity. Severity of the AH ranged from No Compression (NC), Mild Compression (MC), and Severe Compression (SC). Each side of the LV severity was noted and combined into two large umbrellas: (1) Symmetrical Compression of the AH and (2) Asymmetrical Compression of the AH. Under these two umbrellas are subcategories with combinations of (A) NC and NC, (B) MC and MC, (C) SC and SC, (D) NC and MC, (E) NC and SC, and (F) MC and SC (see Figure 7). Both the left and the right side are noted.

Compression Severity

Compression severity was determined by evaluating the degree to which the walls of the lateral ventricle were close to each other at any point along the anterior-posterior extent. No compression (NC) indicated that the walls of the AH were clearly separated. Mild compression (MC) was classified by a noticeable reduction in the distance between the lateral, inferior, or superior walls, including a pinching or partial occlusion of the lateral or inferior angles of the AH. Severe compression (SC) was characterized by almost complete or complete occlusion of the AH cavity, with minimal or absent CSF.

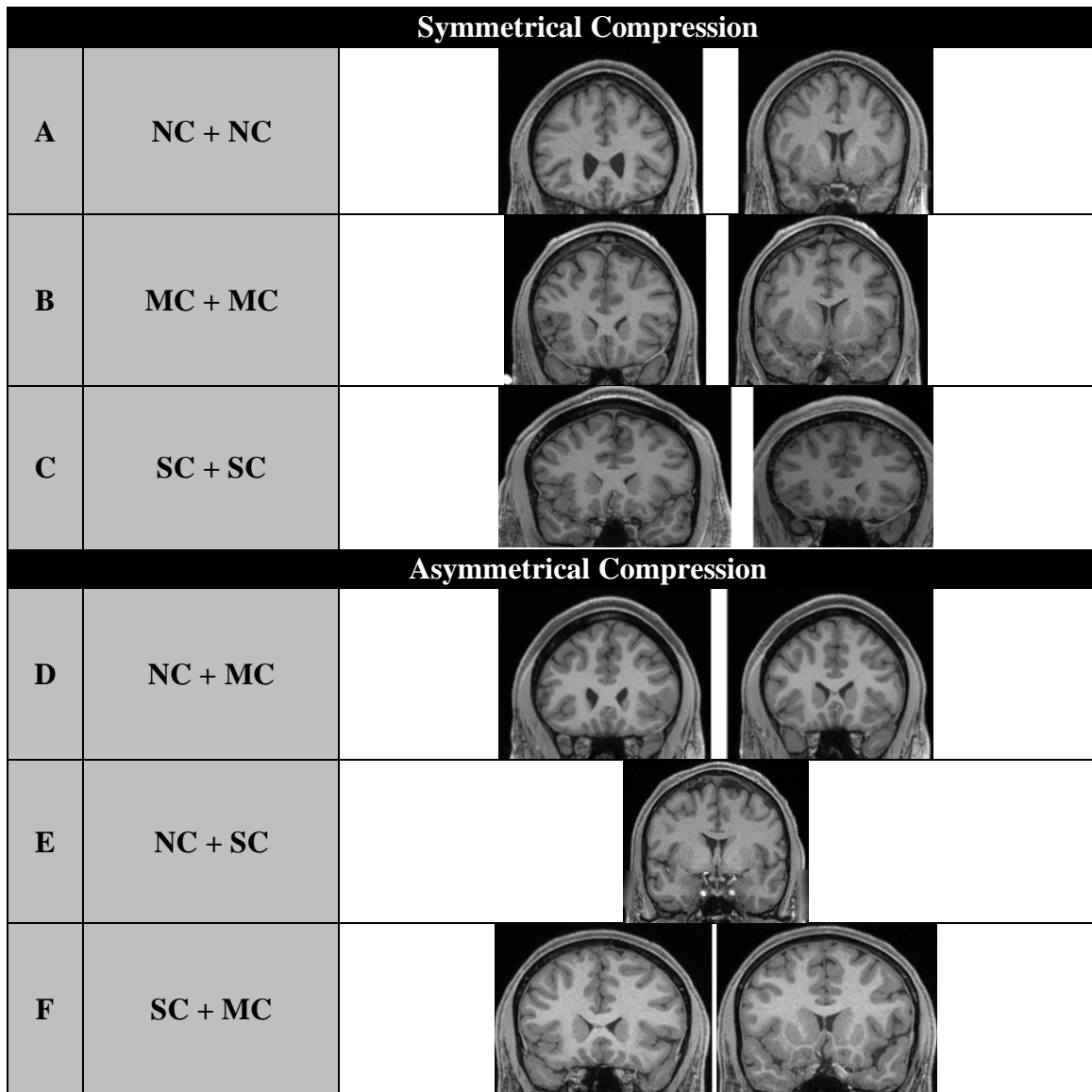


Figure 7. Example of Anterior Horn Compression Severity. The side-by-side images above depict a single case. Symmetrical Compression: (A) No Compression (NC) + No Compression (NC), (B) Mild Compression (MC) + Mild Compression (MC), (C) Severe Compression (SC) + Severe Compression (SC). Asymmetrical Compression: (D) No Compression (NC) + Mild Compression (MC), (E) No Compression (NC) + Severe Compression (SC), (F) Severe Compression (SC) + Mild Compression (MC).

For the body, the distance was calculated between the foramen of Monro and the atrial opening. The atrial opening is identified when the body first extends inferolaterally, with the fornix as its medial margin (Figure 8) continuity with an inferior small space (see Figure 8). Also noted was the onset of continuity on either the right or left side and the occurrence of narrowing on either the right or left side.

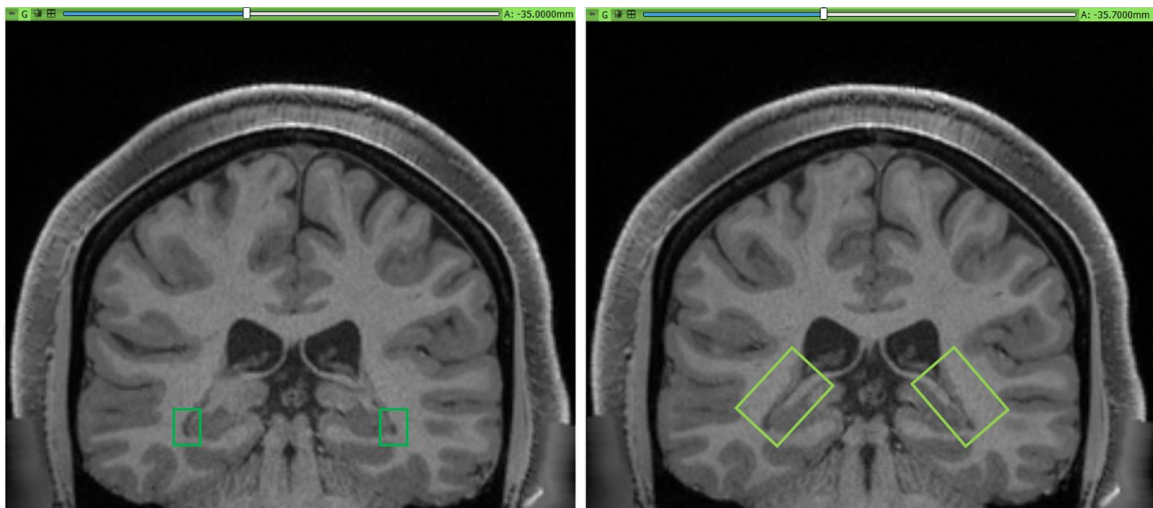


Figure 8. MRI imaging showing the transition from the body (left) to the atrium (right). Notice that in the left image, the superior body of the lateral ventricle does not extend inferolaterally to reach the space in the dark green box, whereas in the subsequent section on the right this extension is observed (light green box).

The atrium is a large cavity that reduces in size in the anterior to posterior direction. At a certain point, the atrium gives rise to the small posterior horn. However, there is no reliable anatomical border between the atrium and posterior horn, a problem noted by several previous investigators (Bates and Netsky, 1995; Mortazavi et al., 2014; Chaddad-Neto, 2022; Morris JA et al., 2022). As a result, the atrium and posterior horn are combined in the present study for the purposes of length. However, the posterior horn takes on a variety of different shapes and will be described as such. In general, the posterior horn

diminishes in diameter before ending completely in the occipital lobe, surrounded by white matter (see Figure 9).



Figure 9. End of the Posterior Horn. Coronal MRI showing the disappearance of the PH (red boxes) leaving only white matter visible (pink box).

While the canonical view of the posterior horn is as a tapered and blind ending subdivision, in many cases, the posterior horn ends in the occipital white matter only to reappear more posteriorly. The posterior horn was thus defined as continuous or discontinuous. This was noted on both the right and the left side of the lateral ventricle. Once the end was determined, the distance of the combined atrium and PH was calculated between the atrial opening and the disappearance of the PH. The presence of anatomical variations such as PH shape and continuity were noted.

Shapes were categorized into four categories defined as (1) 2-pronged, (2) C-shaped, (3) pin, and (4) oblong (see Figure 10). The oblong umbrella contains any shapes that do not fall under the specified umbrella categories (1) 2-pronged, (2) C-shaped, or (3) pin. Notable shapes that fall under the (4) oblong umbrella consist of shapes such as the (4a) crescent moon, (4b) half-moon, (4c) flattened, (4d) oblong (irregular), (4e) teardrop, or (4f) triangle. The progression through multiple shapes on the right and left sides were noted.


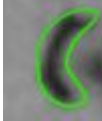
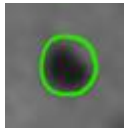
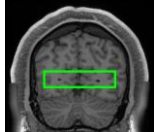
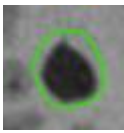
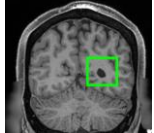
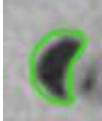
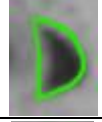

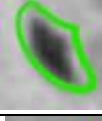
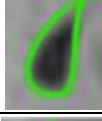
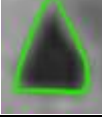
Shape Groups			Photo Example	
1.	2-pronged shaped			
2.	C-shaped			
3.	Pin shaped	A.	Small Pin	 
		B.	Large Pin	 
4.	Oblong shaped	A.	Crescent Moon	
		B.	Half-Moon	
		C.	Flattened	
		D.	Oblong	
		E.	Teardrop	
		F.	Triangle	

Figure 10. Posterior Horn Shapes. Examples of the posterior horn shape classifications: (1) 2-pronged shaped, (2) C-shaped, (3) Pin shaped: (3A) Small Pin and (3B) Large Pin, (4) Oblong shaped: (4A) Crescent Moon, (4B) Half-Moon, (4C) Flattened, (4D) Oblong, (4E) Teardrop, and (4E) Triangle.

The continuity of both the right and left side of the PH were noted. If the PH closed off and then reappeared more caudally, it was classified as discontinuous. If it disappeared and did not reappear, it was classified as continuous.

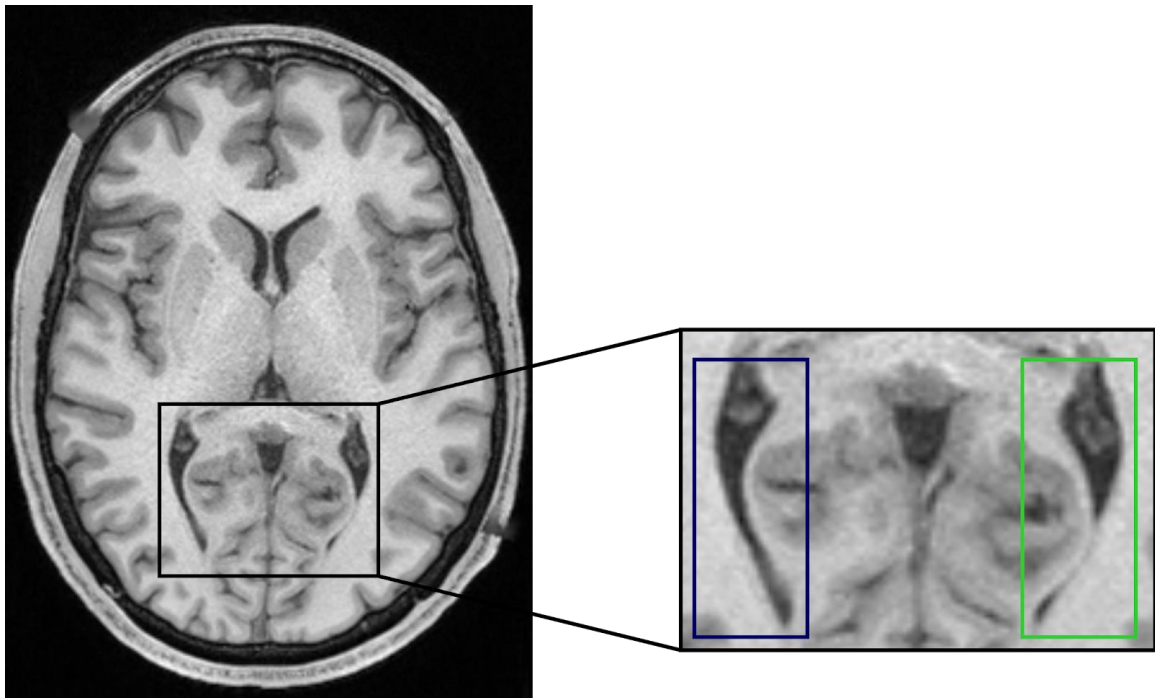


Figure 11. MRI Visualization of Posterior Horn Continuity. Axial MRI exhibiting a case Continuous (C) (dark blue box) and Discontinuous (D) PH (green boxes).

The complete length of the lateral ventricle was determined by calculating the distance between the opening of the anterior horn and the disappearance of the PH.

Statistical Analysis

Using RStudio, a comprehensive analysis was conducted on various anatomical measurements and regions to explore potential influencing factors. Paired t-tests were employed to compare the lengths of the lateral ventricles, as well as specific subdivisions such as the AH subdivision, the body subdivision, and atrium to the end of the posterior horn (PH), between the right and left sides. Analysis of variance (ANOVA) tests were utilized to evaluate the impact of compression and compression severity on these measurements, including the complete length of the lateral ventricles and subdivisions including the AH subdivision, body subdivision, and atrium to the end of PH. ANOVA analyses were conducted to examine the relationships between age, sex, handedness, and length measurements, encompassing the entire LV length, as well as the lengths of the AH subdivision, and body subdivision, and the atrium to the end of the PH of the lateral ventricles. Pearson correlation analyses and linear regression models were applied to investigate the associations between age and the entire LV length, as well as the lengths of the AH subdivision, and body subdivision, and the atrium to the end of the PH of the lateral ventricles. Additionally, chi-square tests were used to explore the relationships between handedness and compression and compression severity. Evaluation of bi or multi-peak characteristics of the distributions of each lateral ventricle was assessed with the bimodality coefficient. Charts were produced using Microsoft Excel and Statistics Kingdom. Overall, these analyses aimed to provide insights into the intricate interplay between lateral ventricle morphology, demographic factors, and anatomical variations.

RESULTS

In the present study, 174 high-resolution T1W MRI scans were analyzed. Unlike previous studies that derived metrics predominantly from White participants, the current study incorporated a more diverse and representative dataset.

Table 7. Demographic Characteristics of Participants

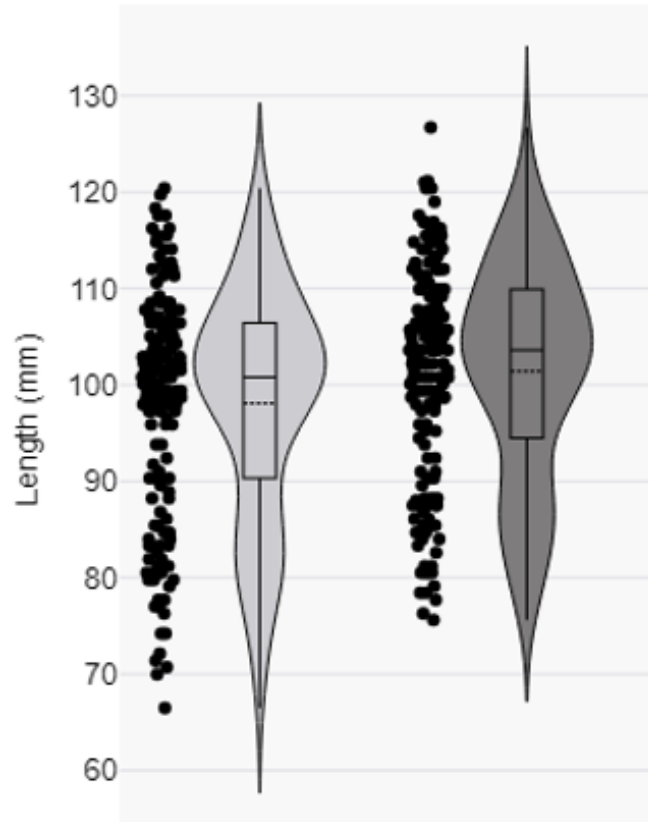
Demographic Information	Am. Indian / Alaskan Nat.		Asian / Nat. Hawaiian / Other Pacific Is.		Black or African Am.		White		More than One		Total Sample	
	<i>n</i>	%	<i>n</i>	%	<i>n</i>	%	<i>n</i>	%	<i>n</i>	%	<i>n</i>	%
Sex												
Female	1	50	18	48.65	33	50	33	50	2	66.67	87	50
Male	1	50	19	51.35	33	50	33	50	1	33.33	87	50
Total	2	1.15	37	21.26	66	37.93	66	37.93	3	1.72	174	100

Ventricle: Overall / General

Length

The anteroposterior length of each LV was calculated for each brain. The average length of the left LV was 101.39 mm, with a standard deviation of 11.18 mm and a median length of 103.6 mm (95% CI = [99.72 - 103.06]; Figure 12). In comparison, the average length of the right LV was 98.10 mm, with a standard deviation of 11.71 mm and a median length of 100.8 mm (95% CI = [96.35-99.86]; Figure 12). The left LV was significantly larger than the right (Student's t-test, unpaired, $p = 0.0078$; Figure 13). Since left and right were measured in the same individual, we also conducted a paired t-test. This showed that when a paired t-test was used to examine the subject-specific effects, a significant difference ($p = 3.29e-06$) between left and right ventricle lengths was identified that the

left LV was larger than the right, with the left side estimated to be approximately 3.29 mm longer on average. Additionally, the bi-modality coefficient was calculated to determine whether there were more than one embedded populations for left and right LVs. For both ventricles, the bimodality coefficients were both <0.55 , indicating insufficient evidence for more than one peak. Moreover, a one-way analysis of the total intracranial volume (eTIV) was performed to confirm that the LV size difference between the left hemisphere ($p < 0.0001$) and right hemisphere ($p = 0.0002$) persisted when the head size was normalized.



	Right	Left	Total
Minimum	66.5	75.6	71.7
Maximum	120.4	126.7	123.6
Average	101.4	98.1	99.7
SD	11.7	11.2	11.4

Figure 12. Length of the Right and Left Lateral Ventricles. Violin plots represent the distribution of anteroposterior length in millimeters (mm) for the right (light gray) and left (dark gray) lateral ventricles, with individual cases shown as black circles. The accompanying table provides the minimum, maximum, average, and standard deviation (SD) lengths for the right (light gray), left (dark gray), and combined total (black).

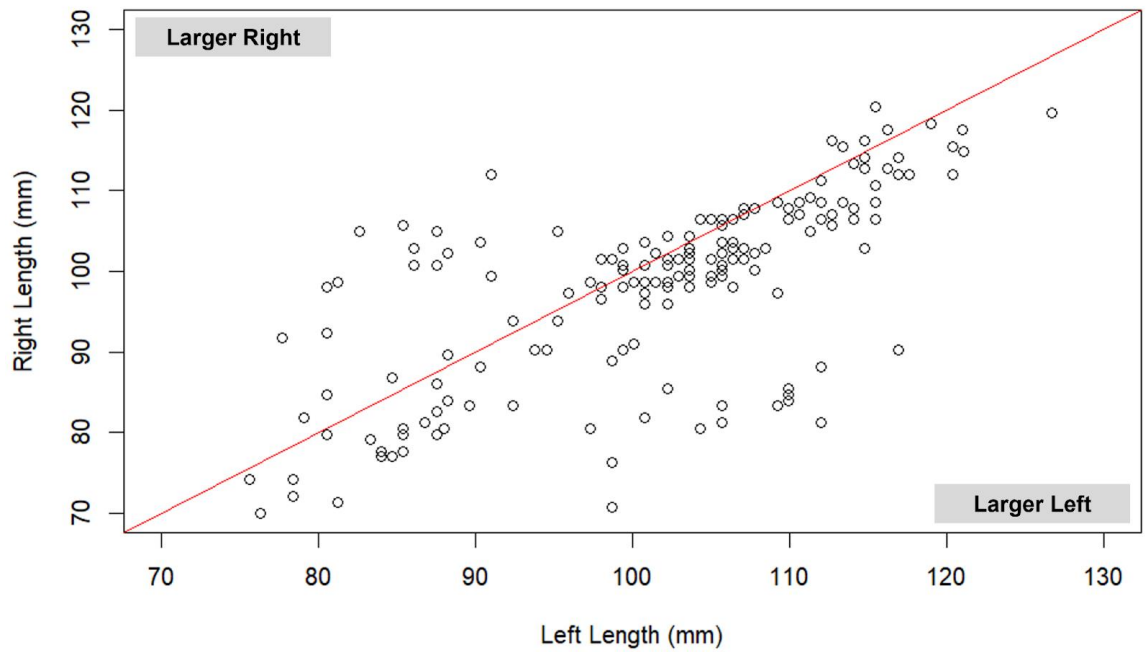
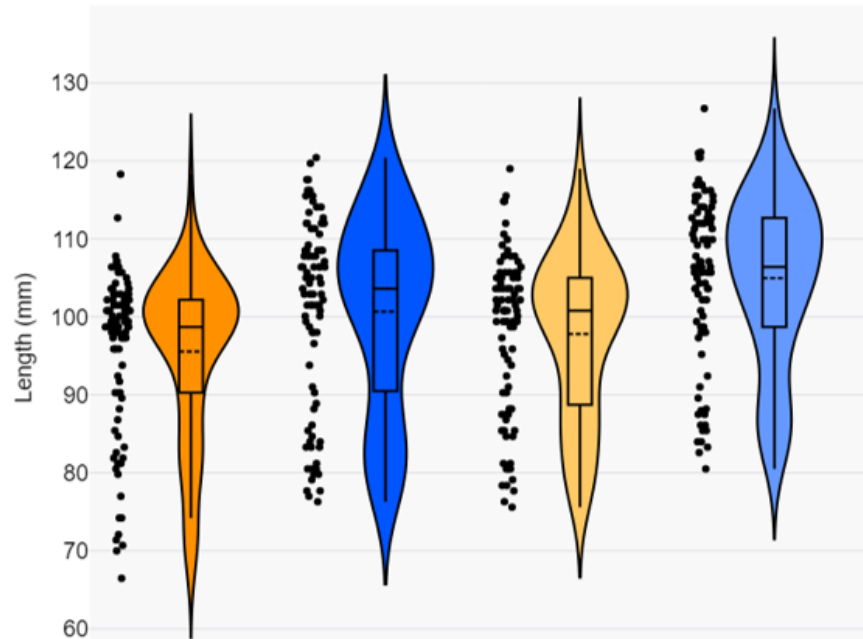


Figure 13. Comparison of Right and Left LV of Size by Case. Scatter plot illustrating the relationship between left and right lateral ventricle lengths (mm) of complete objects. The red line represents the line of equality ($y = x$), indicating perfect symmetry between left and right lengths. Points above the red line indicate a larger right ventricle in individual cases (depicted as open circles), while those below the line indicate a larger left ventricle.

Sex Differences

In males, the average length of the right ventricle was 100.66 ± 12.20 mm with a median length of 103.3 mm. The left ventricle was 104.98 ± 10.86 mm with a median length of 106.4 mm. Females, on the other hand, have an average right ventricle length of 95.55 ± 10.67 mm with a median length of 98.7 mm and a left ventricle length of 97.81 ± 10.36 mm with a median length of 100.8 mm (Figure 14).

The length of the LV was larger on the left than right for both male and female participants. In addition, the male left LV was observed to be larger than the female. An analysis of variance (ANOVA) was conducted to assess whether there was a statistically significant difference in the left and right LV length in males and in females. The results revealed a significant main effect of sex on LV length on the right side ($F(172) = 8.671$, $p < 0.01$) and the left side ($F(1, 172) = 19.89$, $p < 0.01$), indicating that the left LV length was larger than the right in both males and females. Tukey's Honest Significant Difference (HSD) test revealed that males have a significantly longer mean length of the right LV (5.12 mm larger, 95% CI: [1.69 - 8.55]) compared to females ($p = 0.0037$), and that males have a significantly longer mean length of the left LV (7.17 mm larger, 95% CI: [3.99 - 10.35]) compared to females ($p = 1.48e-05$).



	Right		Left	
	Female	Male	Female	Male
Minimum	66.5	76.3	75.6	80.5
Maximum	118.3	120.4	119.0	126.7
Average	95.5	100.7	97.8	105.0
SD	10.7	12.2	10.4	10.8

Figure 14. Length of the Right and Left Lateral Ventricle by Sex. Violin plots represent the distribution of anteroposterior length in millimeters (mm) for the female right (dark orange), male right (dark blue), female left (light orange), and male left (light blue) lateral ventricles, with individual cases shown as black circles. The accompanying table provides the minimum, maximum, average, and standard deviation (SD) lengths for each ventricle category.

Age

In the 22 to 26 age group, the average length of the right LV was 98.5 ± 12.3 mm, and for the left LV, it was 100.8 ± 11.4 mm. In the 27 to 31 age group, the average length of the right LV is 97.2 ± 12.0 mm, and the left LV was 101.4 ± 11.4 mm. In the 32 to 36 age group, the average length of the right LV is 98.9 ± 10.7 mm, and for the left LV, it's 102.0 ± 10.8 mm (Figure 15).

A Pearson correlation analysis was conducted to examine the relationship between right and left LV length and age. The results revealed that age was not correlated with the right and left LV length (right: $r = 0.022$, $p = 0.769$; left: $r = 0.050$, $p = 0.515$).

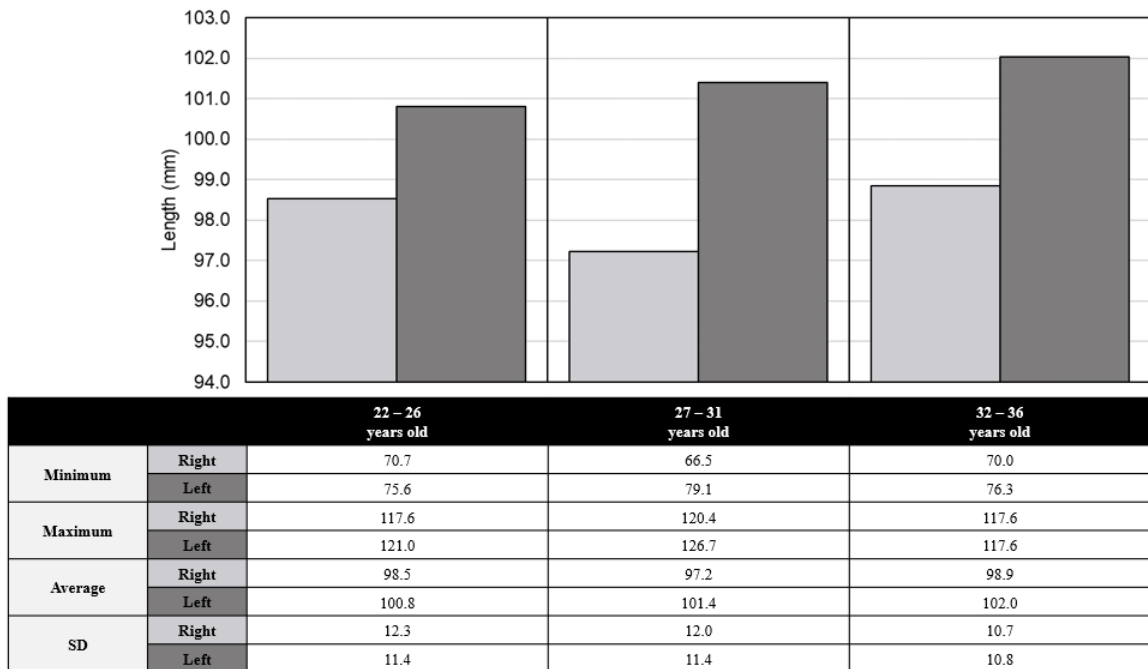


Figure 15. Length of the Right and Left Lateral Ventricles by Age. A bar chart depicting the relationship between the length (in mm) of the right (light gray) and left (dark gray) lateral ventricles across age groups. The accompanying table presents the minimum, maximum, average, and standard deviation (SD) lengths for both ventricles among three age groups (22 - 26, 27 - 31, 32 - 36).

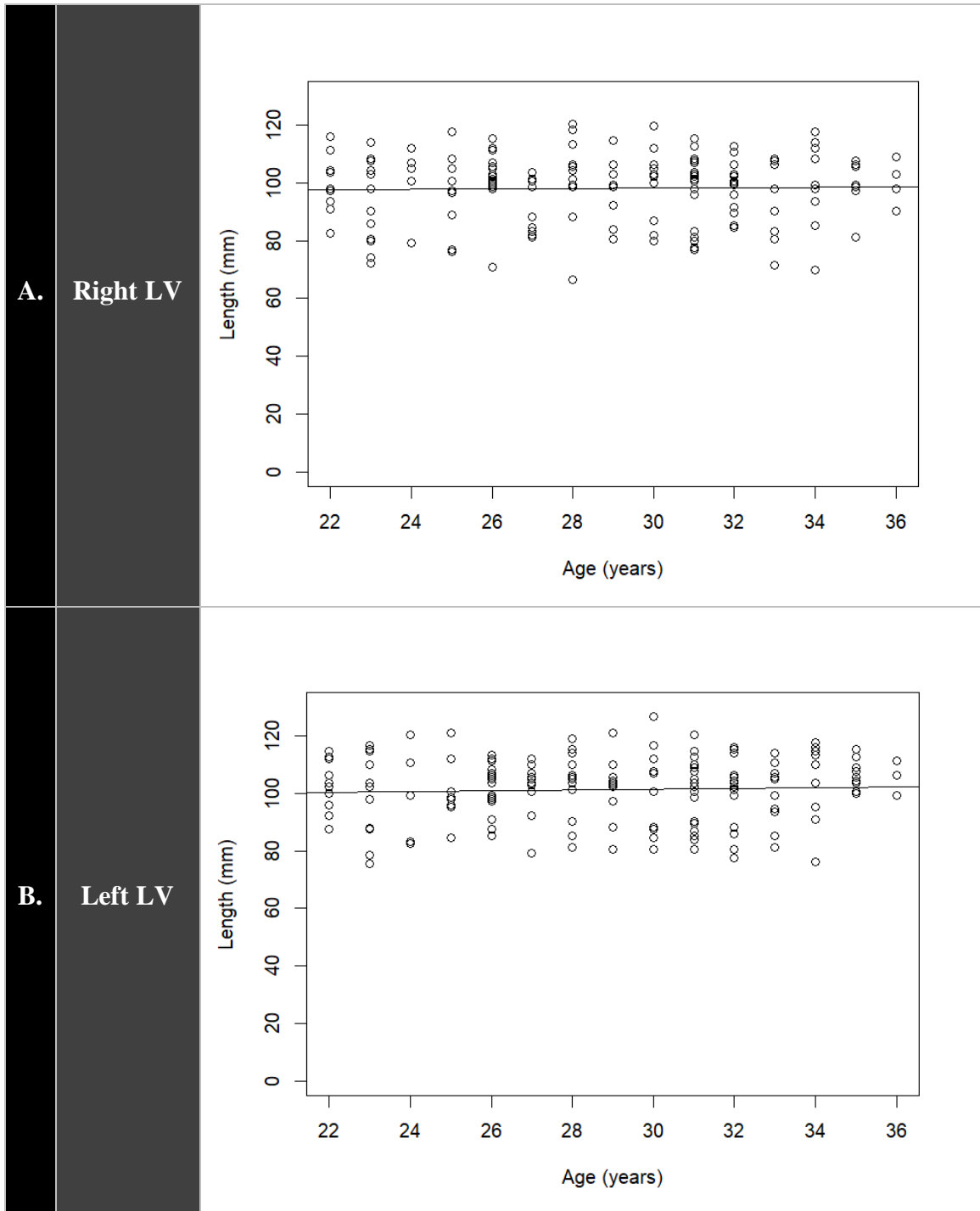


Figure 16. Length of the Right and Left Lateral Ventricles by Age per Case. (A.) Scatter plot depicting the relationship between age (years) and the length (mm) of the right lateral ventricles among individual cases (open circles). The solid line represents the linear regression model fitted to the data. (B.) Similarly, another scatter plot illustrates the relationship between age (years) and the length (mm) of the left lateral ventricles among individual cases (open circles), with the solid line representing the linear regression model fitted to the data.

Handedness

The average length of the left LV was 102.4 ± 10.3 mm for right-handed individuals, 97.41 ± 12.2 mm for ambidextrous individuals, and 98.15 ± 14.9 mm for left-handed individuals. In comparison, the average length of the right LV was 99.22 ± 10.7 mm for right-handed individuals, 92.16 ± 12.8 mm for ambidextrous individuals, and 96.29 ± 15.6 mm for left-handed individuals. Measurements from the anterior horn (AH) to the end of the posterior horn (PH) revealed a consistent trend of longer LV length on the left side for right-handed, ambidextrous, and left-handed individuals (Figure 17).

An analysis of variance (ANOVA) was conducted to assess the LV length differences by handedness and side. The findings indicated unequal ventricle length among right-handed, ambidextrous, and left-handed individuals. A significant main effect of handedness on the right side ($F(2, 171) = 3.512, p < 0.05$) was observed, but not on the left side ($F(2, 171) = 2.644, p = 0.074$).

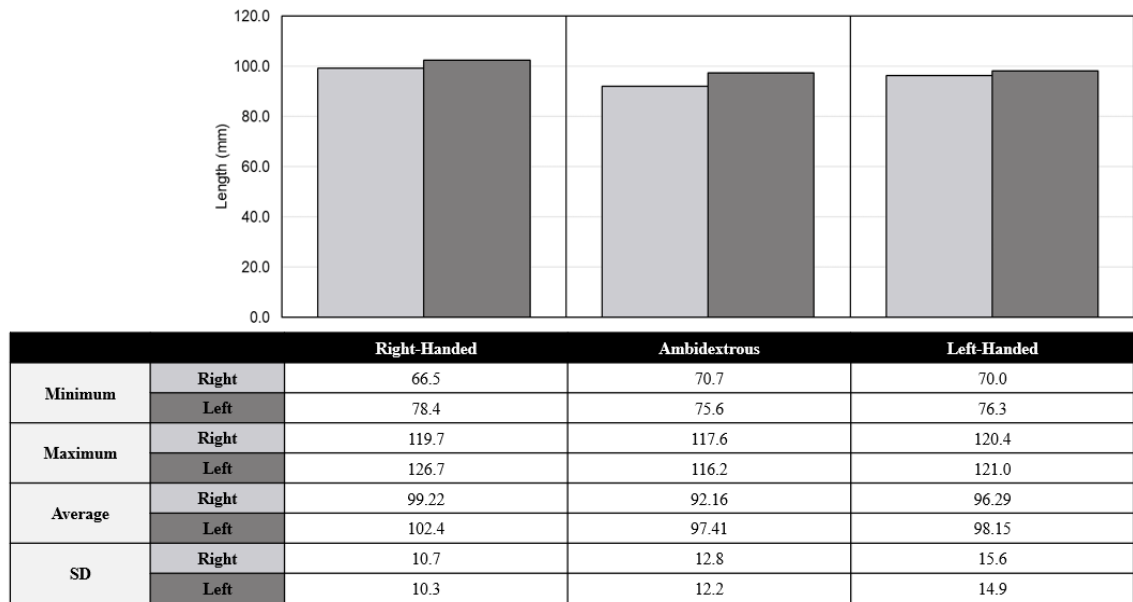


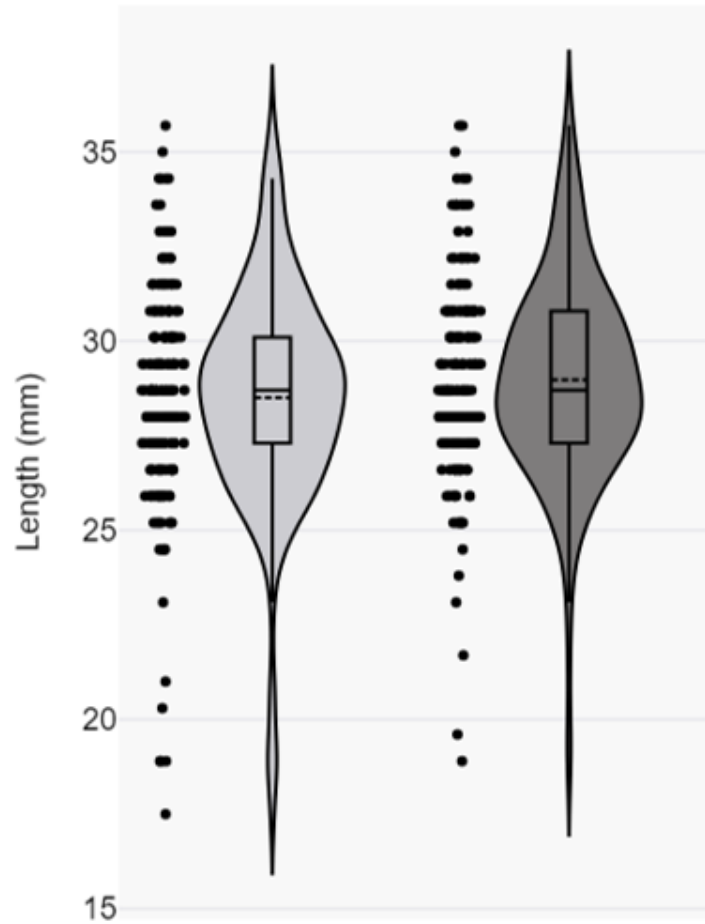
Figure 17. Length of the Right and Left Lateral Ventricles by Handedness. A bar chart depicting the relationship between the length (in mm) of the right (light gray) and left (dark gray) lateral ventricles categorized by handedness. The accompanying table presents the minimum, maximum, average, and standard deviation (SD) lengths for both ventricles among right-handed, left-handed, and ambidextrous individuals.

Anterior (Frontal) Horn

Length

The average length of the right LV AH subdivision was 28.51 mm, with a standard deviation of 2.9 mm and a median length of 28.7 mm (95% CI = [28.07 – 28.94]). In comparison, the average length of the left LV AH subdivision was 28.99 mm, with a standard deviation of 2.6 mm and a median length of 28.7 mm (95% CI = [28.60 – 29.38]) (Figure 18).

The right LV AH subdivision was not significantly larger than the left LV AH subdivision (Student's t-test, unpaired, $p = 0.107$). Since left and right were measured in the same individual, we also conducted a paired t-test. This showed that when a paired t-test was used to examine the subject-specific effects, a significant difference ($p = 0.0001$) between left and right ventricle AH subdivision lengths was identified showing that the left LV AH subdivision was larger than the right, with the left side estimated to be approximately 0.479 mm longer on average.



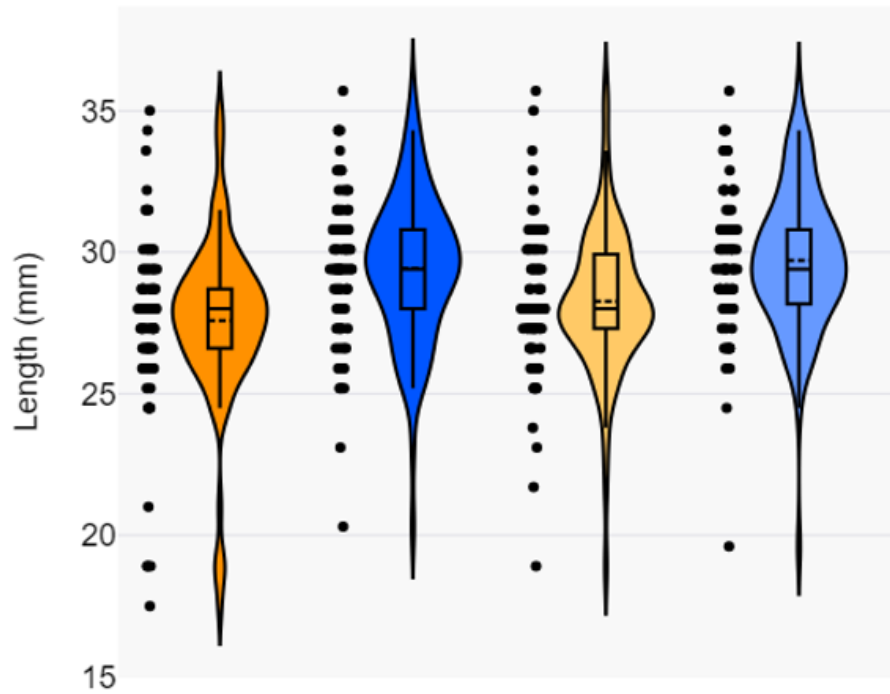
	Right	Left	Total
Minimum	17.5	18.9	18.2
Maximum	35.7	35.7	35.7
Average	28.5	29.0	28.7
SD	2.9	2.6	2.8

Figure 18. Length of the Right and Left Anterior Horn. Violin plots represent the distribution of anteroposterior length in millimeters (mm) for the right (light gray) and left (dark gray) AH subdivision of the lateral ventricles, with individual cases shown as black circles. The accompanying table provides the minimum, maximum, average, and standard deviation (SD) lengths for the right (light gray), left (dark gray), and combined total (black).

Sex Differences

Among males, the left-side AH length averages 34.45 ± 2.10 mm compared to the right side, which averages 33.49 ± 2.04 mm. Similarly, among females, the left-side AH length averages 32.89 ± 1.76 mm, in contrast to the right side, which averages 32.12 ± 1.87 mm (Figure 19).

The male and female AH are longer on the left side than on the right side. The male AH appears to have a longer AH length, with greater variability, than females. The analysis of variance (ANOVA) confirms these findings, showing significant differences in AH length between sexes for both the right ($F(1, 172) = 19.36, p < 0.001$) and left sides ($F(1, 172) = 21.42, p < 0.001$). Tukey's Honest Significant Difference (HSD) test revealed that males have a significantly longer mean length of the right body subdivision (1.85 mm larger, 95% CI: [1.02 - 2.68]) compared to females ($p = 1.89e-05$), and that males have a significantly longer mean length of the left body subdivision (1.44 mm larger, 95% CI: [0.69 - 2.19]) compared to females ($p = 0.0002$).



	Right		Left	
	Female	Male	Female	Male
Minimum	17.5	20.3	18.9	19.6
Maximum	35.0	35.7	35.7	35.7
Average	27.6	29.4	28.3	29.7
SD	3.0	2.6	2.5	2.5

Figure 19. Length of the Right and Left Anterior Horn by Sex. Violin plots represent the distribution of anteroposterior length in millimeters (mm) for the female right (dark orange), male right (dark blue), female left (light orange), and male left (light blue) in the AH subdivision of the lateral ventricles, with individual cases shown as black circles. The accompanying table provides the minimum, maximum, average, and standard deviation (SD) lengths for each ventricle category.

Age

In the 22 to 26 age group, the average length of the right LV was 28.2 ± 2.5 mm, and for the left LV, was 28.5 ± 2.3 mm. In the 27 to 31 age group, the average length of the right LV was 28.7 ± 3.1 mm, and for the left LV, was 29.3 ± 2.7 mm. In the 32 to 36 age group, the average length of the right LV is 28.5 ± 3.1 mm, and for the left LV, it was 29.1 ± 2.7 mm (Figure 20).

Both Pearson correlation analysis and linear regression analysis were conducted to examine the relationship between right and left AH subdivision of the LV length and age. In summary, both Pearson's correlation and linear regression analysis demonstrate that there was no significant relationship between the length of the right-side or left-side AH subdivision of the LVs and age.

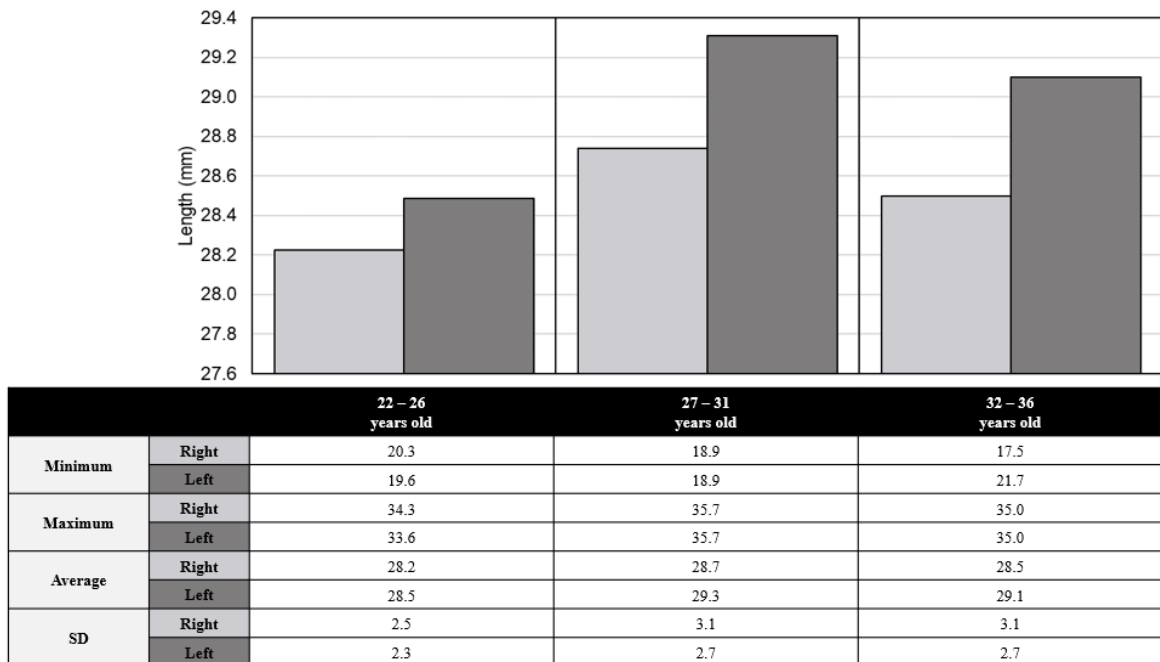
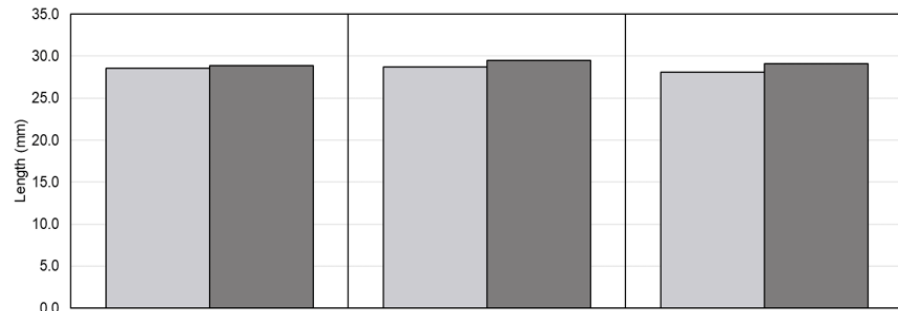


Figure 20. Length of the Right and Left Anterior Horn by Age. A bar chart depicting the relationship between the length (in mm) of the right (light gray) and left (dark gray) lateral ventricles in the AH subdivision across different age groups. The accompanying table presents the minimum, maximum, average, and standard deviation (SD) lengths for both ventricles among three age groups (22 - 26, 27 - 31, 32 - 36).

Handedness

The average length of the right LV was 28.5 ± 2.7 mm for right-handed individuals, 28.7 ± 3.2 mm for ambidextrous individuals, and 28.1 ± 4.3 mm for left-handed individuals. In comparison, the average length of the left LV was 28.9 ± 2.5 mm for right-handed individuals, 29.5 ± 2.6 mm for ambidextrous individuals, and 29.1 ± 3.4 mm for left-handed individuals (Figure 21). Measurements from the anterior horn (AH) to the end of the posterior horn (PH) revealed a longer LV length on the left side for right-handed, ambidextrous, and left-handed individuals.

An analysis of variance (ANOVA) was conducted to explore the potential influence of handedness on the lengths of the right and left sides of the AH subdivision of the LV. The results revealed no significant differences in AH lengths attributed to handedness for either the right or left side. For the right side, the ANOVA showed a sum of squares of 3.8262 attributed to handedness, with an associated F-value of 0.223 and a non-significant p-value ($p = 0.801$). Similarly, for the left side, the sum of squares attributed to handedness was 6.6894, with an F-value of 0.489 and a non-significant p-value ($p = 0.614$). These findings indicate that handedness does not have a statistically significant effect on the lengths of either the right or left side of the AH subdivision of the LVs.



		Right-Handed	Ambidextrous	Left-Handed
Minimum	Right	18.9	24.5	17.5
	Left	18.9	25.9	21.7
Maximum	Right	34.3	35.7	34.3
	Left	34.3	35.7	35.7
Average	Right	28.5	28.7	28.1
	Left	28.9	29.5	29.1
SD	Right	2.7	3.2	4.3
	Left	2.5	2.6	3.4

Figure 21. Length of the Right and Left Anterior Horn by Handedness. A bar chart depicting the relationship between the length (in mm) of the right (light gray) and left (dark gray) lateral ventricles in the AH subdivision categorized by handedness. The accompanying table presents the minimum, maximum, average, and standard deviation (SD) lengths for both ventricles among right-handed, left-handed, and ambidextrous individuals.

AH Variations

Definition

Compression and Compression Severity

Compression refers to the reduction in space or constriction of a cavity, such as the LV in the brain. Compression severity is assessed by observing how close the walls of the LV are to each other along its length. No compression (NC): The walls of the LV are clearly separated. Mild compression (MC): There is a noticeable reduction in the distance between the walls, including partial occlusion of angles. Severe compression (SC): The ventricle is almost or completely occluded, with minimal or no cerebrospinal fluid present.

Left / Right Difference

Compression

A total of 96.6% of cases exhibited AH compression when both the right and left sides were combined (Figure 22). An analysis of variance (ANOVA) was conducted to evaluate the impact of AH compression incidence and whether it affects the right-side and left-side length of the LV and LV subdivisions.

General/Overall

The ANOVA results indicate no significant relationship between the length of the right LV and AH compression ($F(1, 172) = 0.001, p = 0.978$). The ANOVA results for the length of the left LV and AH compression indicate no significant relationship between the two variables ($F(1, 172) = 2.055, p = 0.153$).

AH

The ANOVA results for the length of the right LV AH subdivision and AH compression indicate no significant relationship ($F(1, 172) = 0.926, p = 0.337$). The ANOVA analysis of the length of the left LV AH subdivision concerning AH compression indicates no significant relationship between the two variables ($F(1, 172) = 0.156, p = 0.693$).

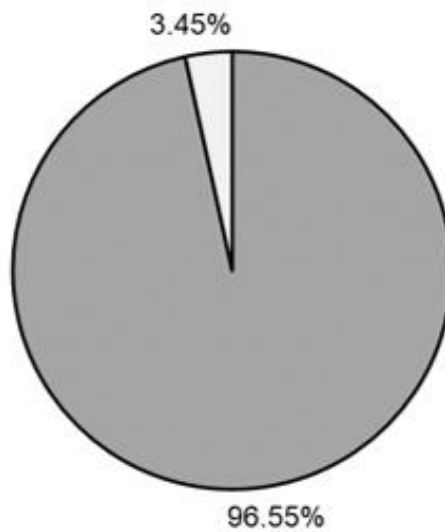
Body

The ANOVA analysis of the length of the right LV body subdivision concerning AH compression indicates no significant relationship ($F(1, 172) = 0.288, p = 0.592$). The ANOVA analysis of the length of the left LV body subdivision concerning AH compression indicates no significant relationship ($F(1, 172) = 0.801, p = 0.372$).

Atrium to the End of the PH

The ANOVA analysis of the length of the right atrium to the end of the PH subdivision concerning AH compression indicates no significant relationship ($F(1, 172) = 0.12, p = 0.73$). The ANOVA analysis of the length of the left atrium to the end of the PH for AH indicates no significant relationship ($F(1, 172) = 1.805, p = 0.181$).

These findings collectively suggest that AH compression does not exert a statistically significant impact on the lengths of various anatomical structures associated with the right or left side of the LV and LVs' subdivisions.



	Count	%
Compressed	168	96.6%
No Compression	6	3.4%
Total	174	100.0%

Figure 22. Anterior Horn Compression Incidence. Pie chart depicting the incidence of compressed AH (dark gray) and no compression in the AH (light gray). The accompanying table presents the counts and percentage of AH that are compressed and exhibit no compression.

Compression Severity

In 77% of cases, there was symmetrical compression severity observed when comparing the left and right ventricles (Figure 23). Breaking this down further: 2.9% of cases had no compression on both sides, 57.5% had mild compression on both sides, and 16.7% had severe compression on both sides (Figure 25).

In 23% of cases, there was asymmetrical compression (Figure 23). Specifically: 0.6% had no compression on the right and severe compression on the left, 1.1% had mild compression on the right and severe compression on the left, 4.0% had mild compression on the right and no compression on the left, 6.9% had no compression on the right and mild compression on the left, and 10.3% had severe compression on the right and mild compression on the left (Figure 24; Figure 25).

An analysis of variance (ANOVA) was conducted to evaluate the impact of AH combined right and left compression severity and whether it affects the right-side and left-side length of the LV and LV subdivisions.

Overall/General

The ANOVA analysis on the length of the right LV and AH combined compression severity indicates significance ($F(7, 166) = 2.31, p = 0.0284$). The ANOVA results for the length of the left LV and AH combined compression severity indicate no significant relationship ($F(7, 166) = 1.452, p = 0.188$).

AH

The ANOVA results for the length of the right LV AH subdivision and AH combined compression severity indicate a significant relationship ($F(7, 166) = 5.591, p < 0.001$). The ANOVA for the length of the left LV AH subdivision and AH combined compression severity shows significance ($F(7, 166) = 5.335, p < 0.001$), indicating that AH combined compression severity significantly explains variability in the length of the left LV AH subdivision.

Body

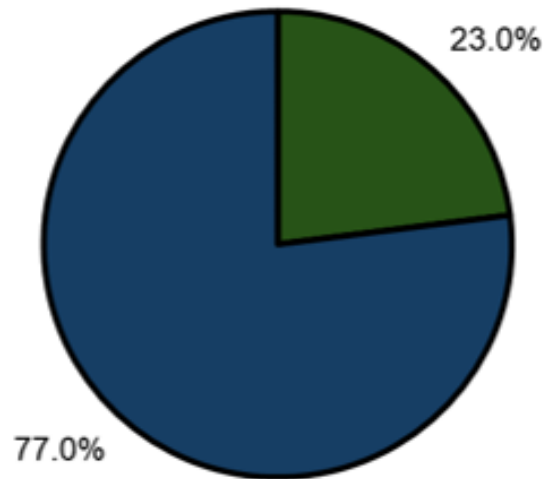
The ANOVA for the length of the right LV body subdivision and AH combined compression severity indicate no significant relationship ($F(7, 166) = 0.381, p = 0.912$). The ANOVA for the length of the left LV body subdivision and AH combined compression severity indicates no significant relationship ($F(7, 166) = 0.819, p = 0.573$).

Atrium to the End of PH

The ANOVA for the length of the right LV atrium to the end of the PH subdivision and AH combined compression severity does not indicate a significant effect ($F(7, 166) = 1.967, p = 0.0624$). The ANOVA for the length of the left LV atrium to the end of the PH subdivision and AH combined compression severity does not indicate a significant effect ($F(7, 166) = 1.167, p = 0.324$).

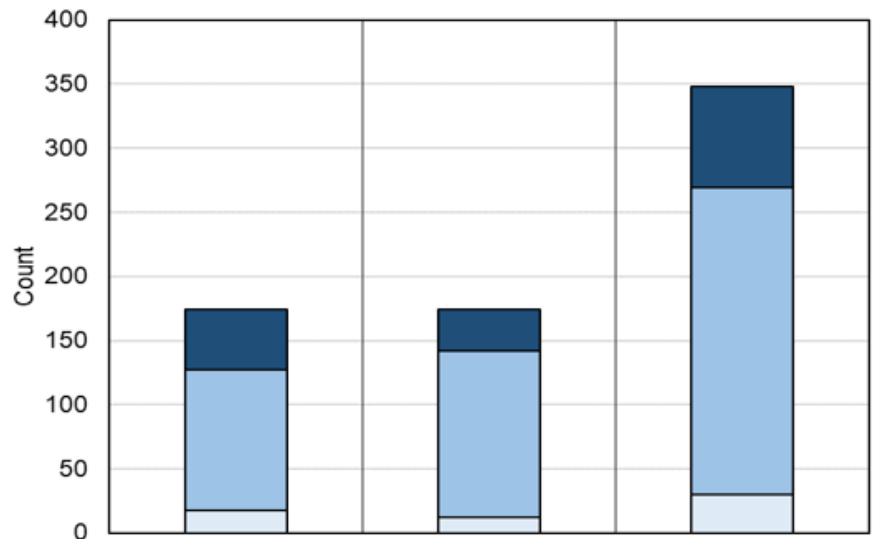
Overall, while AH compression severity significantly affects the length of the AH and the length of the right LV, it does not have a significant impact on left LV length, the

length of the left body subdivision, or the length of the atrium to the end of the PH, as indicated by the non-significant p-values for those measurements.



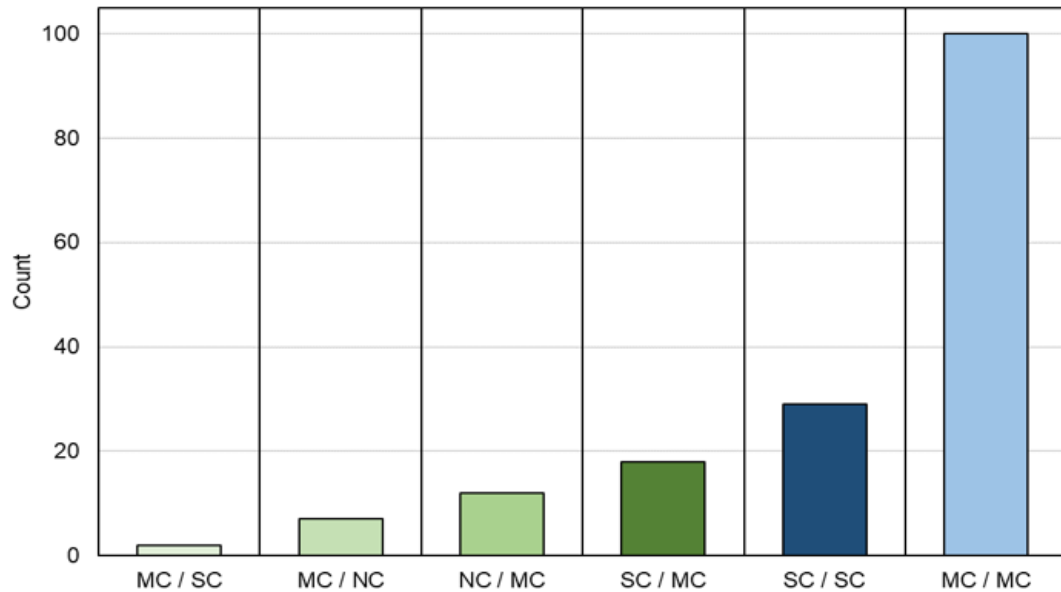
	Count	%
Asymmetrical Compression	40	23.0%
Symmetrical Compression	134	77.0%
Total	174	100.0%

Figure 23. Asymmetrical and Symmetrical Compression Incidence of the Anterior Horn. Pie chart depicting the incidence of asymmetrical compression severity (green) and symmetrical compression severity (blue). The accompanying table presents the counts and percentage of AH that exhibit asymmetrical and symmetrical compression.



	Right	Left	Total
No Compression	18	12	30
Mild Compression	109	130	239
Severe Compression	47	32	79
Total	174	174	348

Figure 24. Right and Left Lateral Anterior Horn Compression Severity. A bar chart depicting the incidence of compression severity in the right hemisphere and left hemisphere, categorized as no compression (off white), mild compression (light blue), and severe compression (dark blue). The accompanying table presents the counts of compression severity among the right (light gray), left (dark gray), and combined (black) hemispheres.



	Right / Left	Count	%	Total Count	Total %
Asymmetrical Compression	NC / SC	1	0.6%	40	23.0%
	MC / SC	2	1.1%		
	MC / NC	7	4.0%		
	NC / MC	12	6.9%		
	SC / MC	18	10.3%		
Symmetrical Compression	NC / NC	5	2.9%	134	77.0%
	SC / SC	29	16.7%		
	MC / MC	100	57.5%		
Total		174	100%	174	100%

Figure 25. Right / Left Combined Compression Severity of the Anterior Horn. A bar chart depicts combined compression severities of the right and left AH as follows: MC/SC (off-white with a green hue), MC/NC (light green), NC/MC (mid-green), SC/MC (dark green), NC/NC (off-white with a blue hue), SC/SC (dark blue), and MC/MC (mid-blue). The bar chart omits NC/SC and NC/NC combinations. The accompanying table presents the counts of each compression severity combination among asymmetrical (green) and symmetrical (blue) AH compressions.

*Sex Difference***Compression**

For the analysis comparing AH compression and sex, Pearson's Chi-squared tests were conducted separately for the right and left sides. For AH compression on the right side, the test yielded an X-squared value of 0.24786 with 1 degree of freedom, resulting in a p-value of 0.6186. This non-significant p-value indicates that there is no significant association between AH compression on the right side and sex. Similarly, for AH compression on the left side, the Chi-squared test resulted in an X-squared value of 1.4321 with 1 degree of freedom, resulting in a p-value of 0.2314. Again, this non-significant p-value suggests that there is no significant association between AH compression on the left side and sex. Therefore, based on these results, there was no evidence to suggest a relationship between AH compression and sex for either the right or left side.

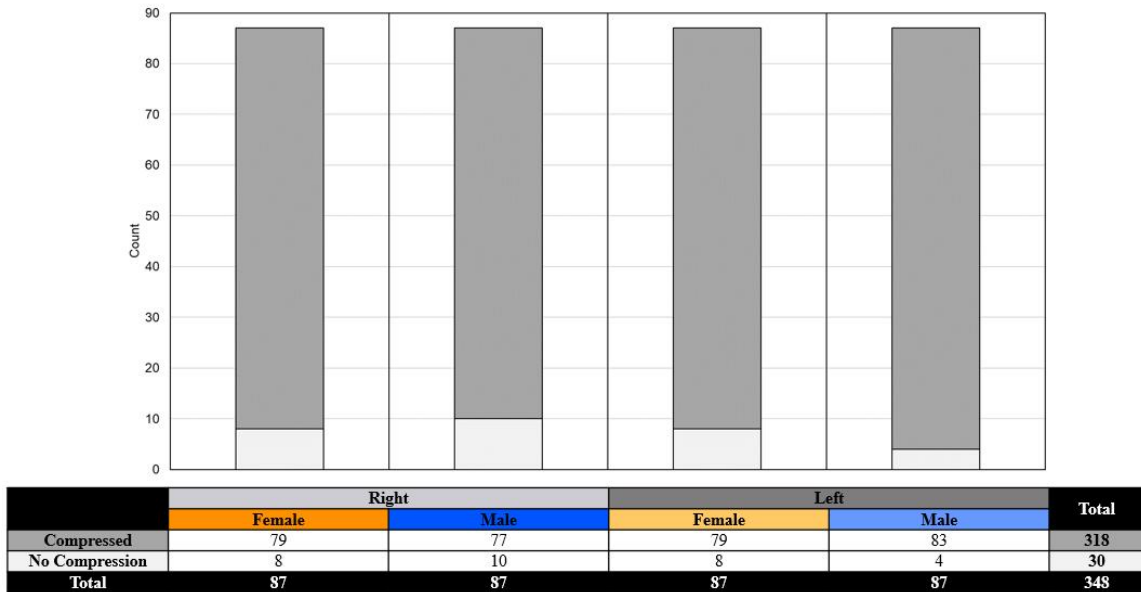
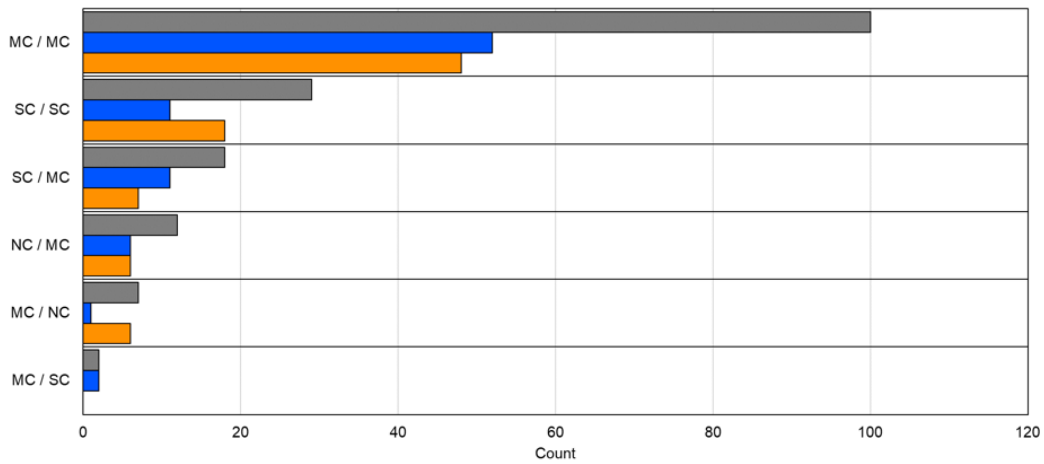


Figure 26. Right and Left Anterior Horn Compression by Sex. A bar chart depicts the incidence of compression in the AH (dark gray) and no compression in the AH (light gray). The accompanying table presents the counts of compressed AH (dark gray) and no compression in the AH (light gray) among females on the right side (dark orange), males on the right side (dark blue), females on the left side (light orange), males on the left side (light blue), and combined totals (black).

Compression Severity

The higher combination of right and left AH compression severity for both males and females are mild compression and mild compression (MC / MC) totaling 57.7% of cases, 29.9% of those cases are male, while 27.6% of those cases are female. Females saw no combination of no compression on the right and severe compression on the left (NC / SC) or mild compression on the right and severe compression on the left (MC / SC). The no compression right and no compression left (NC / NC) is the smallest percentage of female cases (1 out of 78 females or 0.01%), while the no compression right and severe compression left (NC / SC) exhibits the smallest percentage of male cases (1 out of 78 or 0.01%) (Figure 27).

Pearson's Chi-squared test was performed to analyze the relationship between AH compression severity and sex separately for the right and left sides. For AH compression severity on the right side, the test resulted in an X-squared value of 0.42289 with 2 degrees of freedom, yielding a p-value of 0.8094. This non-significant p-value suggests that there is no significant association between AH compression severity on the right side and sex. Similarly, for AH compression severity on the left side, the Chi-squared test yielded an X-squared value of 2.3256 with 2 degrees of freedom, resulting in a p-value of 0.3126. Again, this non-significant p-value indicates that there is no significant association between AH compression severity on the left side and sex. Therefore, based on these results, there is no evidence to suggest a relationship between AH compression severity and sex for either the right or left side.



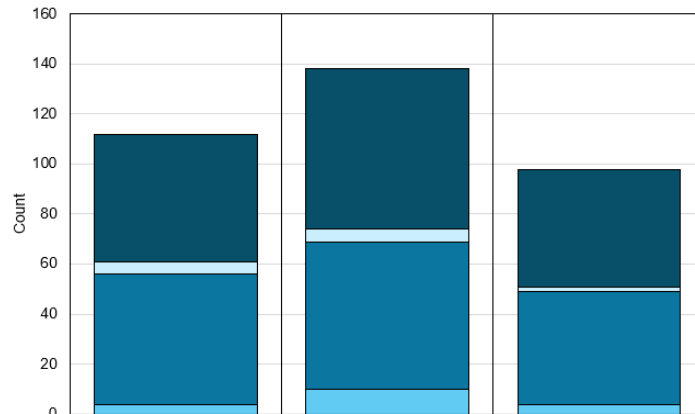
	Right / Left	Female		Male		Total		Overall Count	Overall %
		Count	%	Count	%	Count	%		
Asymmetrical Compression	NC / SC	0		1	0.6%	1	0.6%	40	23.0%
	MC / SC	0		2	1.1%	2	1.1%		
	MC / NC	6	3.4%	1	0.6%	7	4.0%		
	NC / MC	6	3.4%	6	3.4%	12	6.9%		
Symmetrical Compression	SC / MC	7	4.0%	11	6.3%	18	10.3%	134	77.0%
	NC / NC	2	1.1%	3	1.7%	5	2.9%		
	SC / SC	18	10.3%	11	6.3%	29	16.7%		
Total		87		87		174	100%	174	100%

Figure 27. Right and Left Anterior Horn Compression Severity by Sex. A bar chart depicts the incidence of AH compression severity (dark gray) among females (orange), males (blue), and total (gray). The accompanying table presents the counts and percentages of compression severity observed in asymmetrical (green) and symmetrical (blue) AH compression among females (orange), males (blue), and total (gray).

Age

Compression

The ANOVA analysis explored the relationship between age and AH compression as well as AH compression severity. For the impact of AH compression on age, the ANOVA yielded a non-significant F value of 0.378 ($p = 0.539$), suggesting no significant association between AH compression and age.



		22 - 26 years old	27 - 31 years old	32 - 36 years old	Grand Total
Right	No Compression	4	10	4	18
	Compressed	52	59	45	156
Left	No Compression	5	5	2	12
	Compressed	51	64	47	162

Figure 28. Right and Left Anterior Horn Compression by Age. A bar chart depicts the incidence of AH compression across different age groups as follows: no compression on the right side (bright blue), compressed left side (mid blue), no compression on the left side (off white with a blue hue), and compressed left side (dark blue). The accompanying table presents the incidence of compression on the right (light gray) and left (dark gray) sides among three age groups (22 - 26, 27 - 31, 32 - 36).

Compression Severity

Similarly, an ANOVA was performed to investigate the influence of AH compression severity on age also showed a non-significant result with an F value of 1.52 ($p = 0.164$). This indicates that AH compression severity does not significantly correlate with age. Therefore, based on these findings, there is no evidence to suggest a significant relationship between age and AH compression or AH compression severity.

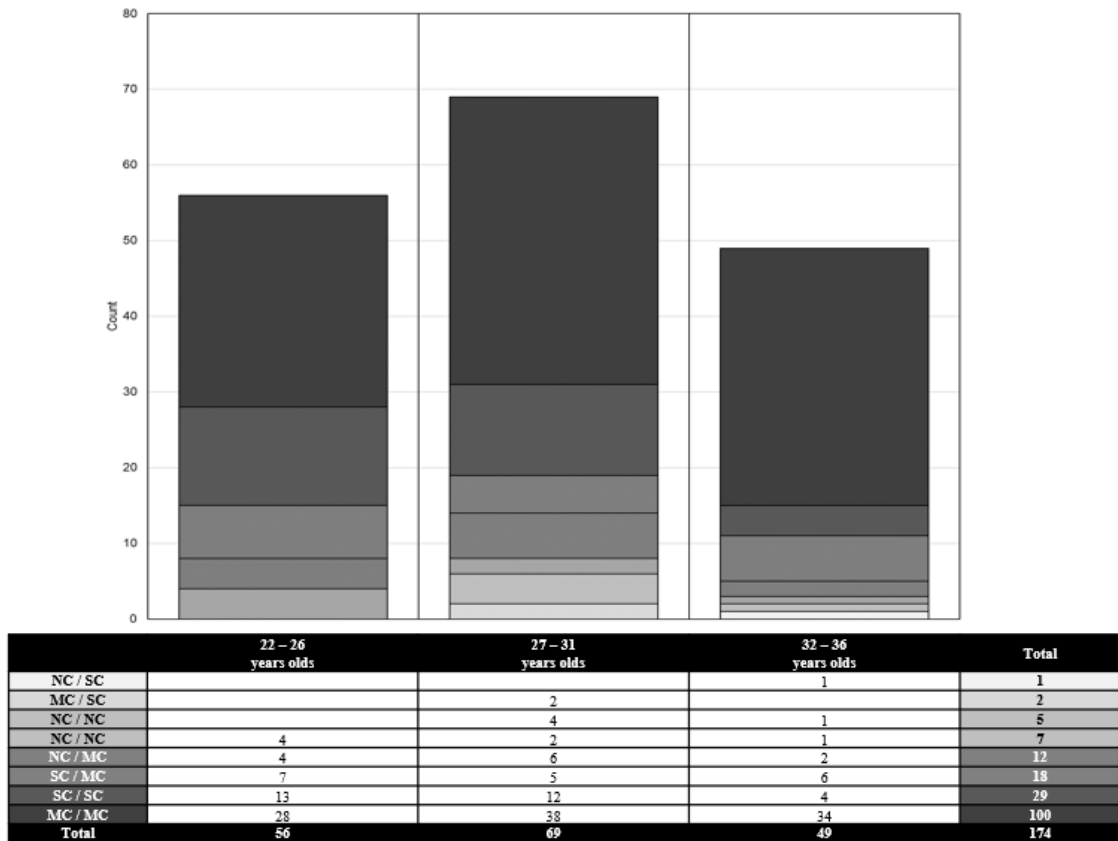


Figure 29. Right and Left Anterior Horn Compression Severity by Age. A bar chart depicts the incidence of AH compression severity across different age groups. The accompanying table presents the incidence of AH compression severity among three age groups (22 - 26, 27 - 31, 32 - 36).

*Handedness***Compression and Compression Severity**

The most common compression severity among right-handed, left-handed, and ambidextrous individuals is mild compression right and mild compression left (MC / MC) which is seen in 100 of 174 cases (57.5%) (Figure 31).

The chi-squared tests were conducted to examine the association between handedness and AH compression as well as handedness and AH compression severity. For the association between handedness and AH compression, the chi-squared test yielded a non-significant result with a chi-squared value of 3.3265 and a p-value of 0.1895, suggesting no significant relationship between these variables. Similarly, the chi-squared test for the association between handedness and AH compression severity also resulted in a non-significant p-value of 0.7035, indicating no significant association between these variables.

Additionally, ANOVA was performed to further investigate the relationship between handedness and AH compression as well as handedness and AH compression severity. For both analyses, the F values were non-significant, with 0.119 ($p = 0.73$) for handedness and AH compression and 0.597 ($p = 0.758$) for handedness and AH compression severity. These results indicate that there is no significant relationship between handedness and either AH compression or AH compression severity. Therefore, based on these findings, handedness does not appear to be associated with AH compression or AH compression severity.

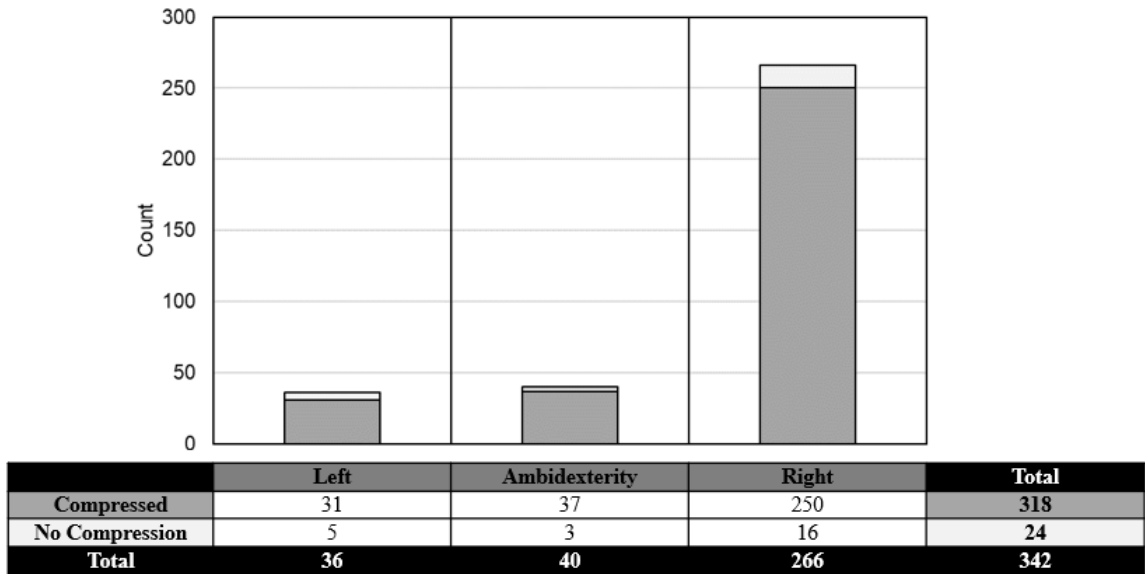


Figure 30. Anterior Horn Compression Incidence by Handedness. A bar chart depicts the incidence of compression in the AH (dark gray) and no compression in the AH (light gray). The accompanying table presents AH compression incidence among right-handed, left-handed, and ambidextrous individuals.

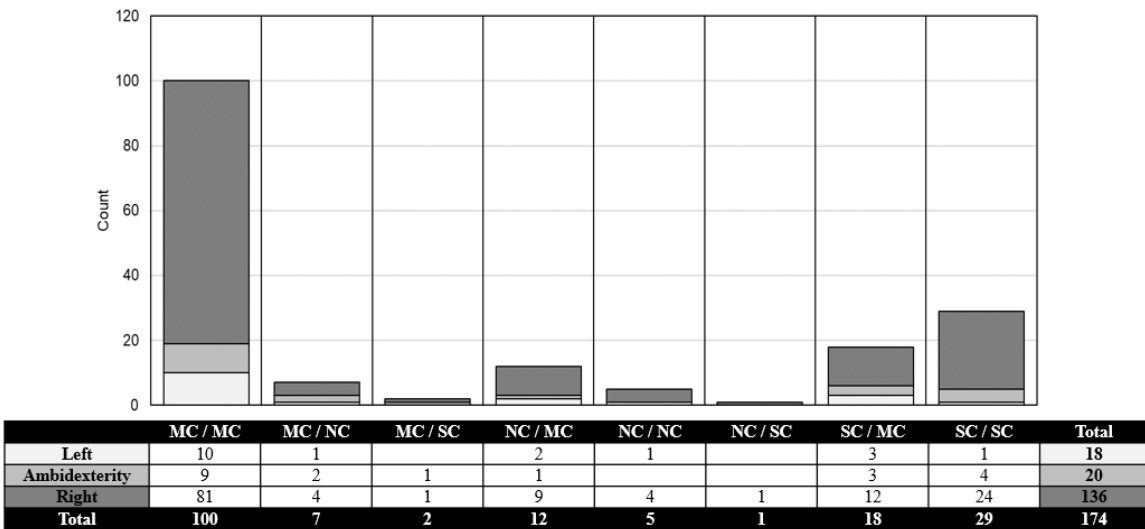


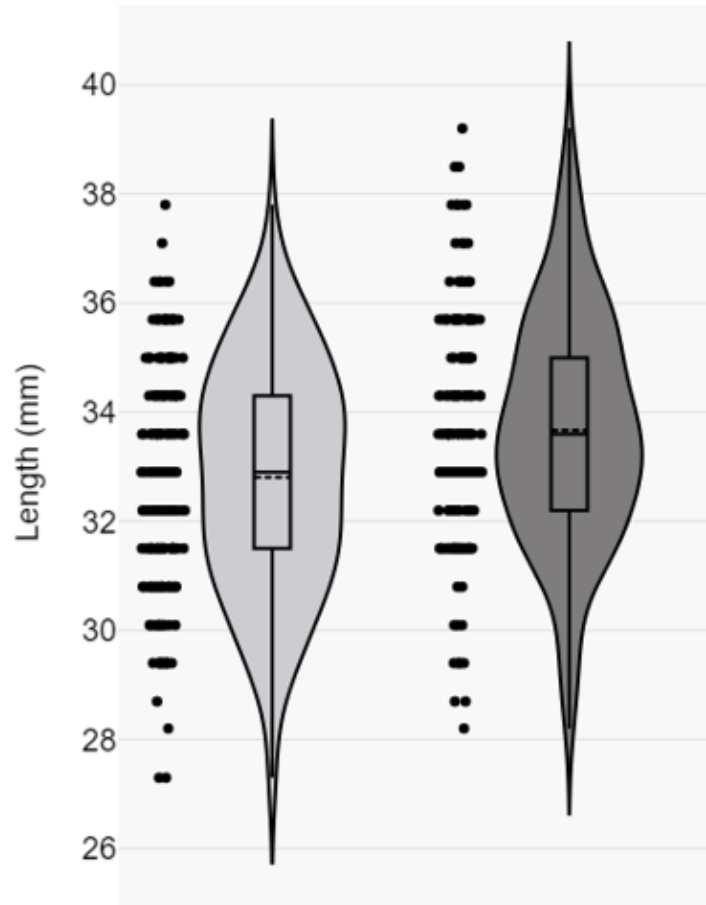
Figure 31. Right / Left Anterior Horn Compression Severity by Handedness. A bar chart depicts the incidence of AH compression severity in right-handed (dark gray), ambidextrous (light gray), and left-handed (off-white with a gray hue) individuals. The accompanying table presents AH compression incidence among right-handed, left-handed, and ambidextrous individuals.

Overall, the study investigated the influence of anterior horn (AH) compression and AH compression severity and the effect of the length of the LV and the LV subdivisions. AH compression did not significantly affect the lengths of the LV and the LV subdivisions. Similarly, while AH compression severity significantly influenced the AH and the right LV length, it did not significantly impact the left LV length, the body subdivision length, or the atrium to the end of the PH length. Additionally, factors such as sex, age, and handedness showed no significant associations with AH compression or its severity. Pearson's Chi-squared tests and ANOVA analyses indicated no significant relationships, suggesting that AH compression and AH compression severity are largely independent of these variables.

Body (Central) Part

Length

The average length of the right LV body subdivision was 32.8 mm, with a standard deviation of 2.1 mm (Figure 32) and a median length of 32.9 mm (95% CI = 32.50 – 33.11]). In comparison, the average length of the left LV body subdivision was 33.7 mm, with a standard deviation of 2.1 mm (Figure 32) and a median length of 33.6 mm (95% CI = [33.36 – 33.98]). The left LV body subdivision was significantly larger than the right LV body subdivision (Student's t-test, unpaired, $p = 0.0001$). Since left and right were measured in the same individual, we also conducted a paired t-test. This showed that when a paired t-test was used to examine the subject-specific effects, a significant difference ($p = 6.104e-09$) between the left and right ventricle body subdivision lengths identified that the left LV body subdivision was larger than the right, with the left side estimated to be approximately 0.865 mm longer on average.



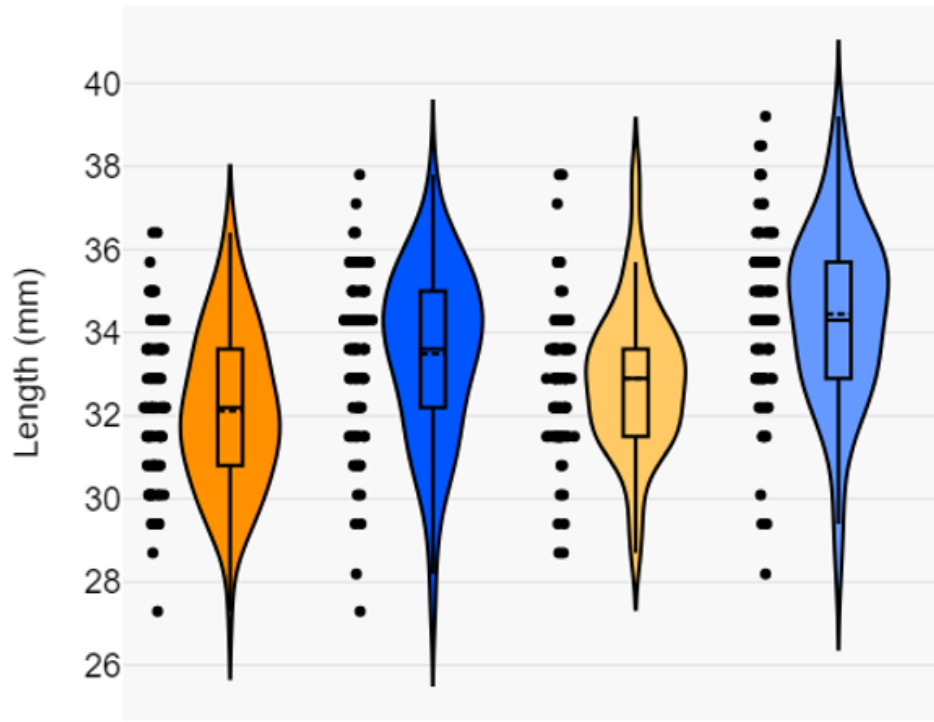
	Right	Left	Total
Minimum	27.3	28.2	27.8
Maximum	37.8	39.2	38.5
Average	32.8	33.7	33.2
SD	2.1	2.1	2.1

Figure 32. Length of the Right and Left Body. Violin plots represent the distribution of anteroposterior length in millimeters (mm) for the right (light gray) and left (dark gray) body subdivision of the lateral ventricles, with individual cases shown as black circles. The accompanying table provides the minimum, maximum, average, and standard deviation (SD) lengths for the right (light gray), left (dark gray), and combined total (black).

Sex Differences

The body length of the male is larger than the female. The body length of the male is larger on the left side (29.71 ± 2.50 mm) than on the right side (29.43 ± 2.58 mm) (Figure 33). The body subdivision length of the female is larger on the left side (28.27 ± 2.52 mm) than on the right side (27.58 ± 2.96 mm) (Figure 33).

The analysis examined the association between sex and the length of the body subdivision of the LV, separately for the right and left sides. Both the length of the right body subdivision and the length of the left body subdivision showed significant effects of sex, with ANOVA results indicating strong evidence ($p < 0.001$). For the length of the right body subdivision, sex had a significant influence ($F(1, 172) = 21.42$), suggesting differences in body subdivision length between males and females on the right side. Tukey's Honest Significant Difference (HSD) test revealed that males have a significantly longer mean length of the right body subdivision (1.37 mm larger, 95% CI: [0.79 - 1.95]) compared to females ($p = 7.2e-06$). Similarly, for the length of the left body subdivision, there was a significant effect of sex ($F(1, 172) = 28.15$), indicating sex-based differences in body subdivision length on the left side. These findings highlight a significant association between sex and the length of the body subdivision of the LV, implying distinct average lengths between males and females on both sides. Tukey's Honest Significant Difference (HSD) test revealed that males have a significantly longer mean length of the left body subdivision (1.56 mm larger, 95% CI: [0.98 - 2.13]) compared to females ($p = 3e-07$).

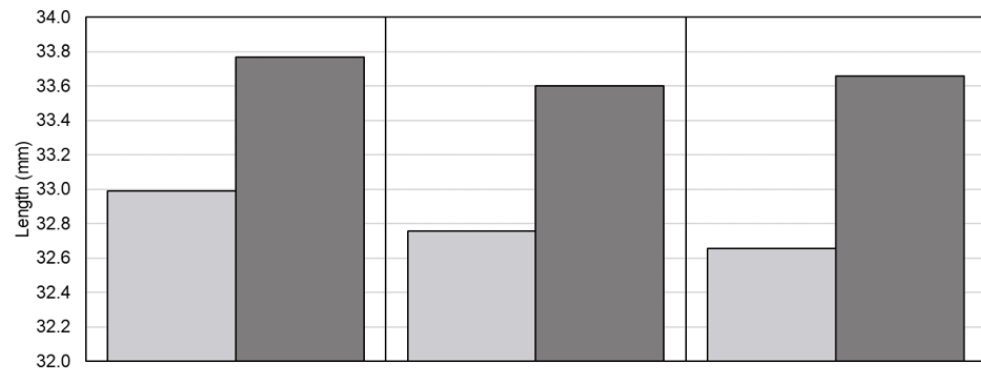


	Right		Left	
	Female	Male	Female	Male
Minimum	36.4	37.8	37.8	39.2
Maximum	27.3	27.3	28.7	28.2
Average	32.1	33.5	32.9	34.4
SD	1.9	2.0	1.8	2.1

Figure 33. Length of the Right and Left Body by Sex. Violin plots represent the distribution of anteroposterior length in millimeters (mm) for the female right (dark orange), male right (dark blue), female left (light orange), and male left (light blue) in the body subdivision of the lateral ventricles, with individual cases shown as black circles. The accompanying table provides the minimum, maximum, average, and standard deviation (SD) lengths for each ventricle category.

Age

For both the length of the right body subdivision and the length of the left body subdivision measurements, the correlation tests with age did not yield significant results. Pearson's correlation coefficients were -0.038 and -0.026, respectively, indicating very weak negative correlations between age and the lengths of the body subdivision of the LV on both sides. Additionally, linear regression analyses were conducted to further explore this relationship, but neither model produced statistically significant results. The coefficients for age were -0.020 and -0.014 for the right and left sides, respectively. This indicates very slight decreases in length with increasing age, but these were not statistically significant. Overall, these findings suggest that there is no substantial correlation or linear relationship between age and the length of the body subdivision of the LV on either the right or left side.



		22 - 26 years old	27 - 31 years old	32 - 36 years old
Minimum	Right	27.3	27.3	29.4
	Left	28.2	28.7	29.4
Maximum	Right	37.1	37.8	36.4
	Left	38.5	38.5	39.2
Average	Right	33.0	32.8	32.7
	Left	33.8	33.6	33.7
SD	Right	2.3	2.0	1.9
	Left	2.2	2.0	2.0

Figure 34. Length of the Right and Left Body by Age. A bar chart depicting the relationship between the length (in mm) of the right (light gray) and left (dark gray) lateral ventricles in the body subdivision across different age groups. The accompanying table presents the minimum, maximum, average, and standard deviation (SD) lengths for both ventricles among three age groups (22 - 26, 27 - 31, 32 - 36).

Handedness

An ANOVA investigated the potential association between handedness and the length of the body subdivision of the LV on both the right and left sides. For the length of the right body subdivision of the LV, the ANOVA did not indicate a significant effect of handedness ($F(2, 171) = 0.663, p = 0.516$), suggesting that handedness does not significantly influence the length of the body subdivision on the right side. Similarly, for the length of the left body subdivision of the LV, the ANOVA also did not reveal a significant effect of handedness ($F(2, 171) = 1.049, p = 0.353$), indicating that handedness does not significantly affect the length of the body subdivision on the left side. Therefore, based on these results, there is no significant association between handedness and the length of the body subdivision of the LV, neither on the right nor left side.

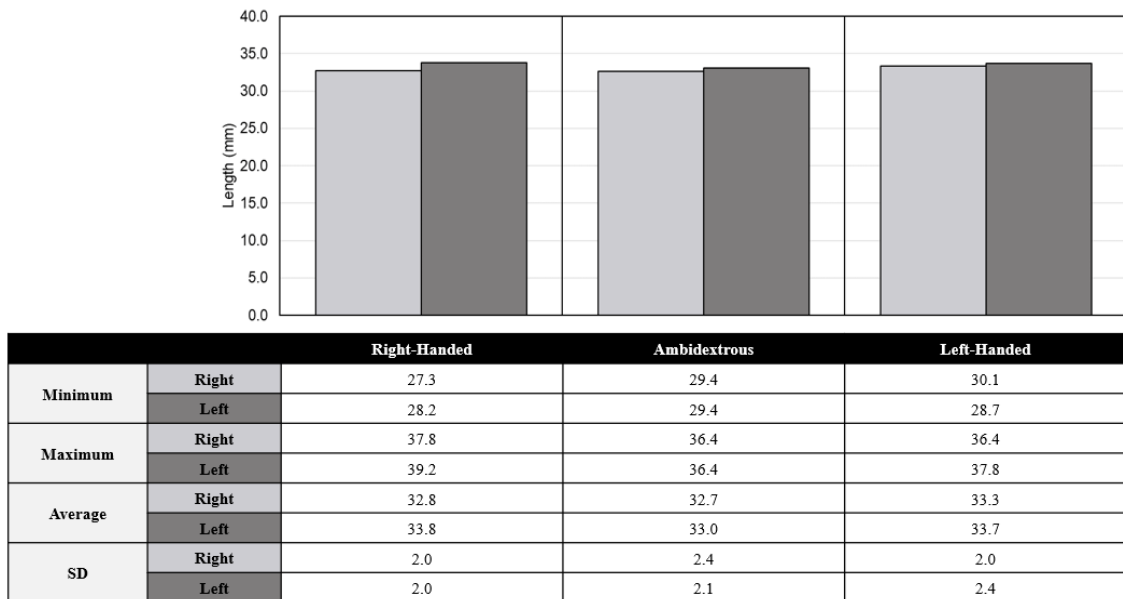
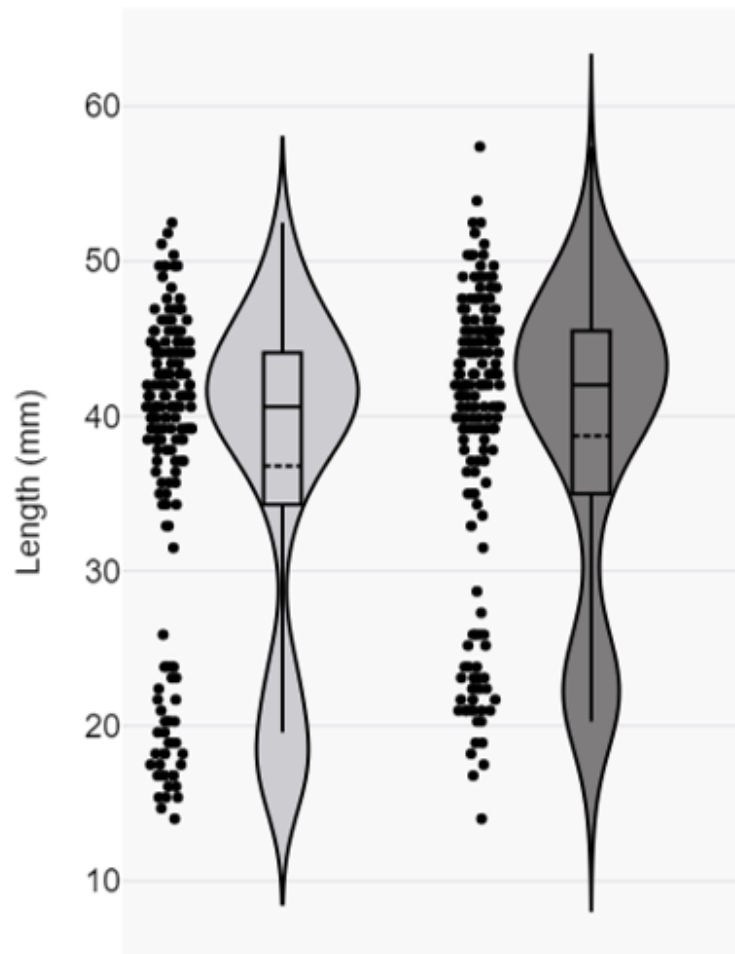


Figure 35. Length of the Right and Left Body by Handedness. A bar chart depicting the relationship between the length (in mm) of the right (light gray) and left (dark gray) lateral ventricles in the body subdivision categorized by handedness. The accompanying table presents the minimum, maximum, average, and standard deviation (SD) lengths for both ventricles among right-handed, left-handed, and ambidextrous individuals.

Atrium + Posterior (Occipital) Horn*Length*

The average length of the right LV atrium to the end of the PH subdivision was 36.8 mm, with a standard deviation of 10.4 mm (Figure 36) and a median length of 40.6 mm (95% CI = 35.24 – 38.34)]. In comparison, the average length of the left LV atrium to the end of the PH subdivision was 38.7 mm, with a standard deviation of 9.8 mm (Figure 36) and a median length of 42.0 mm (95% CI = [37.28 – 40.20]). The right LV atrium to the end of the PH subdivision was not significantly larger than the left LV atrium to the end of the PH subdivision (Student's t-test, unpaired, $p = 0.073$). Since left and right were measured in the same individual, we also conducted a paired t-test. This showed that when a paired t-test was used to examine the subject-specific effects, a significant difference ($p = 0.0035$) between the left and right ventricle atrium to the end of the PH subdivision lengths identified that the left LV atrium to the end of the PH subdivision was larger than the right, with the left side estimated to be approximately 1.94 mm longer on average.



	Right	Left	Total
Minimum	14.0	14.0	14.0
Maximum	52.5	57.4	55.0
Average	36.8	38.7	37.8
SD	10.4	9.8	10.1

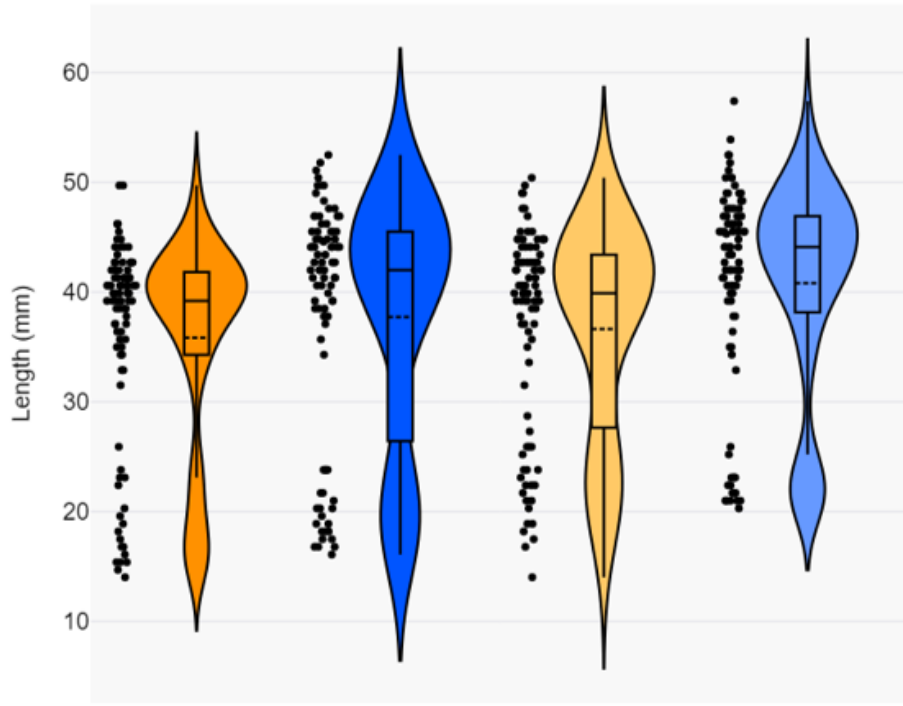
Figure 36. Length of the Right and Left Atrium to the End of the Posterior Horn. Violin plots represent the distribution of anteroposterior length in millimeters (mm) for the right (light gray) and left (dark gray) atrium to the end of the PH subdivision of the lateral ventricles, with individual cases shown as black circles. The accompanying table provides the minimum, maximum, average, and standard deviation (SD) lengths for the right (light gray), left (dark gray), and combined total (black).

Sex Differences

The atrium to the end of the posterior horn (PH) of the male is larger on the left side (40.82 ± 9.58 mm) than on the right side (37.74 ± 11.16 mm) (Figure 37). The atrium to the end of the posterior horn (PH) of the female is larger on the left side (36.65 ± 9.53 mm) than on the right side (35.84 ± 9.49 mm) (Figure 37). The length from the atrium to the end of the PH is larger on both sides in males compared to females.

An ANOVA examined the influence of sex on the lengths of the atrium to the end of the PH for both the right and left sides. For the length of the atrium to the end of the PH on the right, the ANOVA did not reveal a statistically significant effect of sex ($F(1, 172) = 1.459$, $p = 0.229$), suggesting that sex does not significantly influence the length of this structure on the right side.

Conversely, for the length of the atrium to the end of the PH on the left, there was a significant effect of sex ($F(1, 172) = 8.293$, $p = 0.0045$), indicating that sex significantly impacts the length of the atrium to the end of the PH on the left side. Tukey's Honest Significant Difference (HSD) test revealed that males have a significantly longer mean length of the left atrium to the end of the PH (4.17 mm larger, 95% CI: [1.31 - 7.03]) compared to females ($p = 0.0045$).



	Right		Left	
	Female	Male	Female	Male
Minimum	14.0	16.1	14.0	20.3
Maximum	49.7	52.5	50.4	57.4
Average	35.8	37.7	36.6	40.8
SD	9.5	11.2	9.5	9.6

Figure 37. Length of the Right and Left Atrium to the End of the Posterior Horn by Sex. Violin plots represent the distribution of anteroposterior length in millimeters (mm) for the female right (dark orange), male right (dark blue), female left (light orange), and male left (light blue) in the atrium to the end of the PH subdivision of the lateral ventricles, with individual cases shown as black circles. The accompanying table provides the minimum, maximum, average, and standard deviation (SD) lengths for each ventricle category.

Age

Correlation analyses and linear regression models were performed to assess the relationship between age and the lengths of the atrium to the end of the PH for both the right and left sides. For the length of the atrium to the end of the PH on the right, the Pearson correlation coefficient ($r = 0.0224$) and the linear regression model ($p = 0.769$) demonstrated no significant correlation between age and length on the right side. Similarly, for the length of the atrium to the end of the PH on the left, both the correlation coefficient ($r = 0.0315$) and the linear regression model ($p = 0.680$) suggested no significant correlation between age and length on the left side. These findings indicate that age is not a significant predictor of the lengths of the atrium to the end of the PH subdivision of the LV.

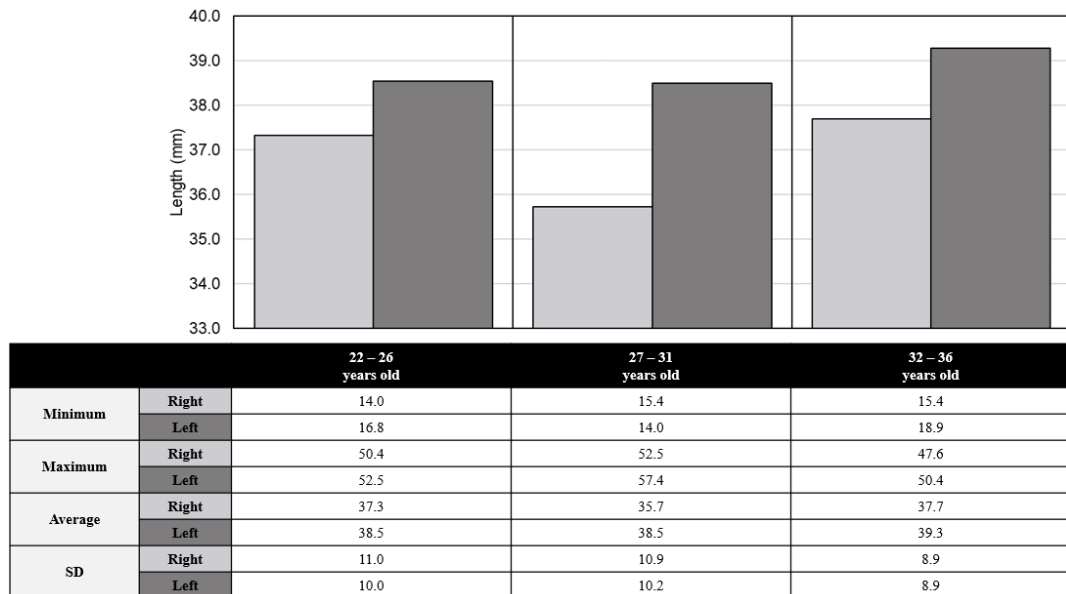


Figure 38. Length of the Right and Left Atrium to the End of the Posterior Horn by Age. A bar chart depicting the relationship between the length (in mm) of the right (light gray) and left (dark gray) lateral ventricles in the atrium to the end of the PH subdivision across different age groups. The accompanying table presents the minimum, maximum, average, and standard deviation (SD) lengths for both ventricles among three age groups (22 - 26, 27 - 31, 32 - 36).

Handedness

The analyses aimed to examine the relationship between handedness and the lengths of the atrium to the end of the PH for both the right and left sides. For the length of the atrium to the end of the PH on the right, the ANOVA revealed a statistically significant effect of handedness ($F(2, 171) = 4.721, p = 0.0101$), suggesting that handedness significantly influences the length of this structure on the right side.

Similarly, for the length of the atrium to the end of the PH on the left, there was a significant effect of handedness ($F(2, 171) = 3.466, p = 0.0335$), indicating that handedness significantly affects the length of the structure on the left side as well. In both cases, the p-values were less than 0.05, indicating significant evidence against the null hypothesis. Therefore, based on these results, there is a significant association between handedness and the lengths of the atrium to the end of the PH, with differences observed among different handedness groups.

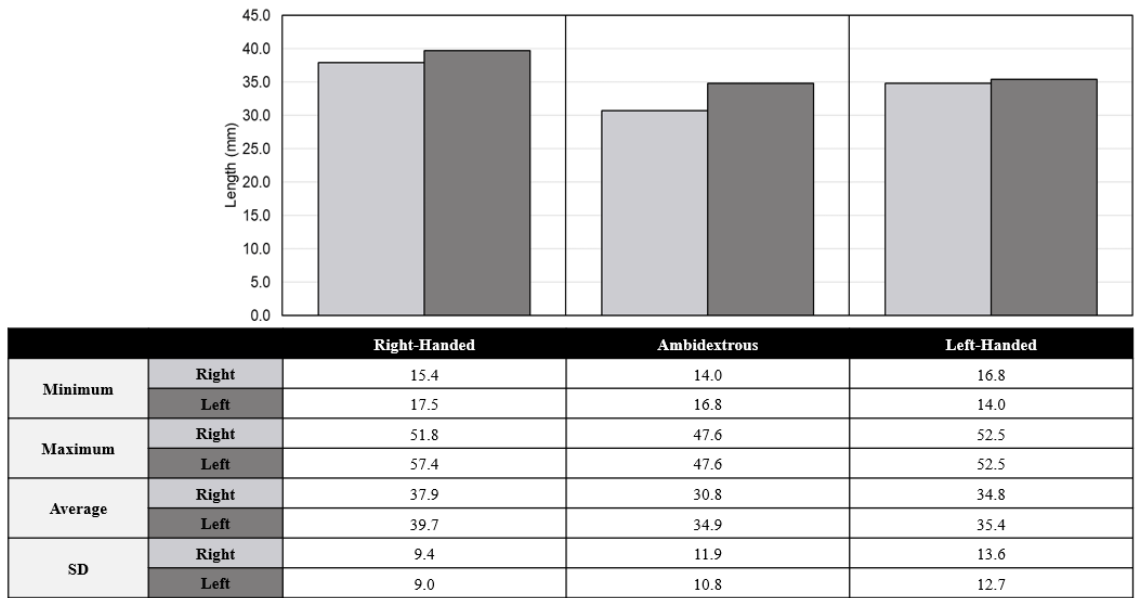


Figure 39. Length of the Right and Left Atrium to the End of the Posterior Horn by Handedness. A bar chart depicting the relationship between the length (in mm) of the right (light gray) and left (dark gray) lateral ventricles in the atrium to the end of the PH subdivision categorized by handedness. The accompanying table presents the minimum, maximum, average, and standard deviation (SD) lengths for both ventricles among right-handed, left-handed, and ambidextrous individuals.

PH Variations

Definition

Shapes

The shapes observed were classified into four main categories: 2-pronged, C-shaped, pin, and oblong. The oblong category encompasses shapes that don't fit into the specific categories mentioned earlier. Notable shapes falling under the oblong category include crescent moon, half-moon, flattened, irregular oblong, teardrop, and triangle. The study also noted the progression of shapes observed on both the right and left sides.

The most common shape progression in the posterior horn (PH) was from oblong to pin shape, observed in 20.69% of cases on the right side (Figure 40) and 25.29% on the left side (Figure 41). Following this, the just pin shape was noted in 18.97% of cases on the right side (Figure 40) and 20.69% on the left side (Figure 41). However, on the right side, the third most common shape progression was 2-pronged (9.77%) (Figure 40), whereas on the left side, it was oblong (11.49%) (Figure 41). The least commonly observed shape progression, occurring once on each side, involved 2-pronged shapes. On the right, it progressed to C-shaped (0.57%) (Figure 40), while on the left, there was no modification (0.57%) (Figure 41).

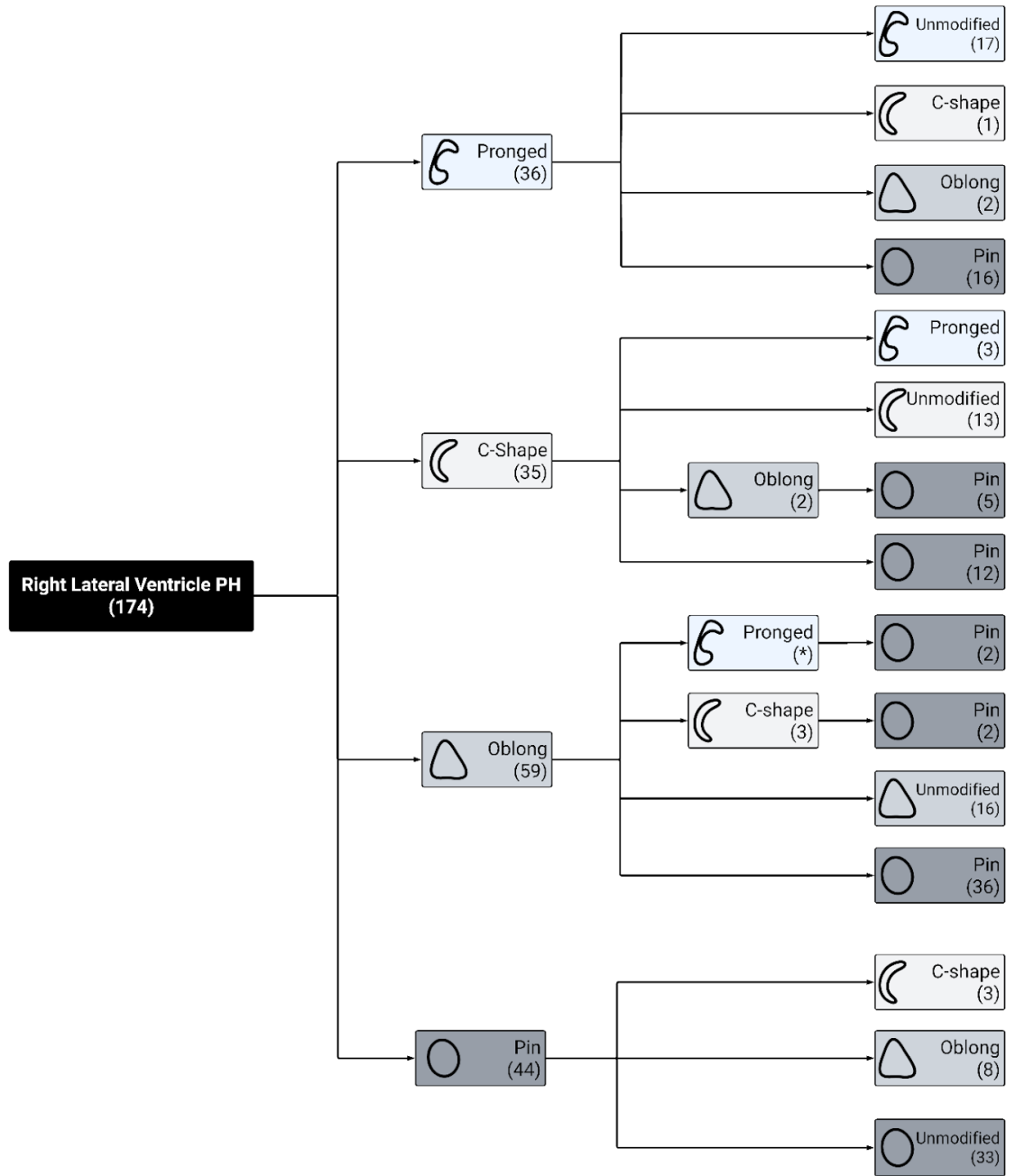


Figure 40. Right Posterior Horn Shape Progression. A flow chart depicting the anteroposterior shape progression observed in the right lateral ventricle PH and the count of observed cases. Pronged (off-white with a blue hue), C-shaped (off-white with a gray hue), Oblong (light gray), and Pin (dark gray).

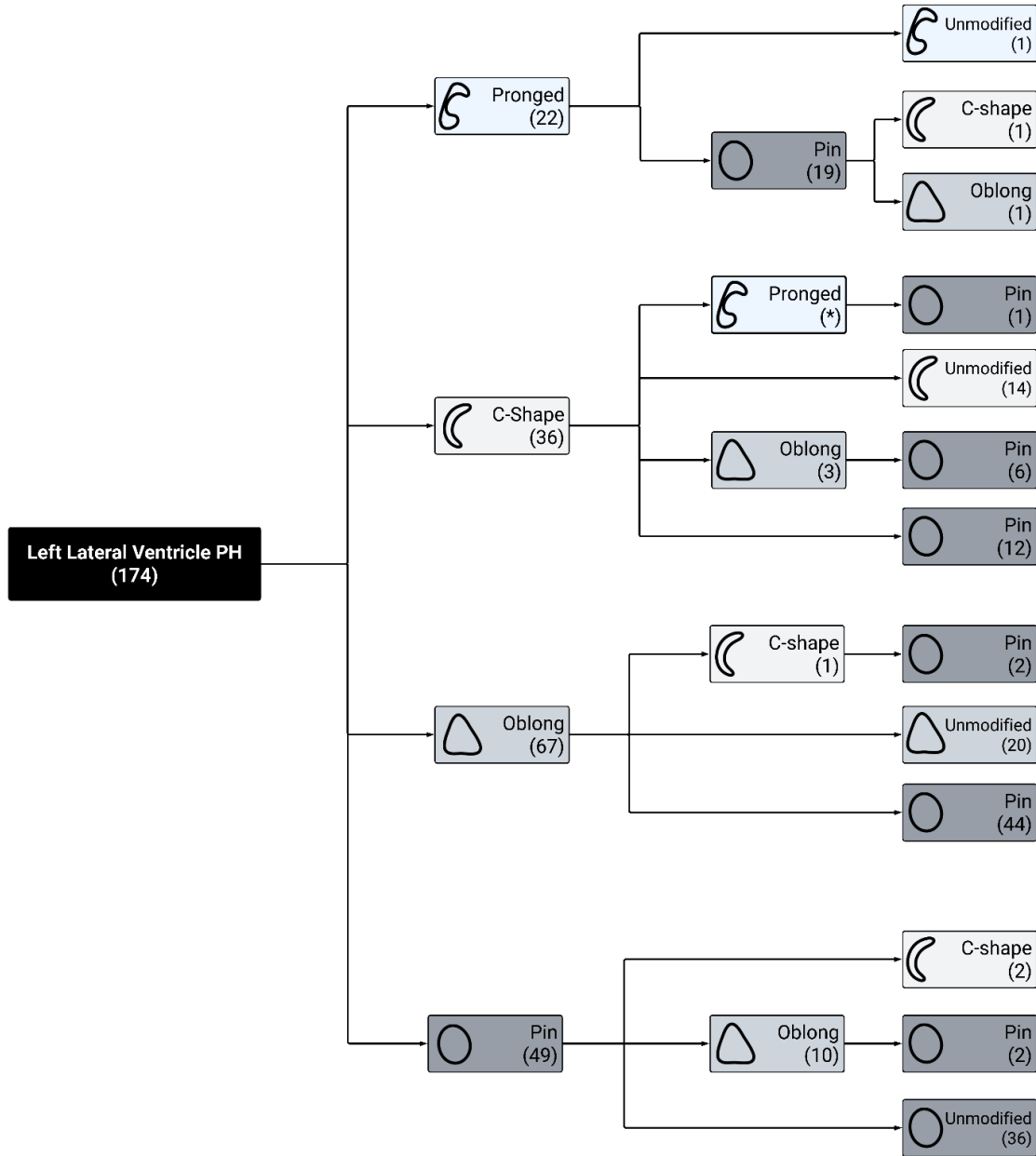


Figure 41. Left Posterior Horn Shape Progression. A flow chart depicting the anteroposterior shape progression observed in the left lateral ventricle PH and the count of observed cases. Pronged (off-white with a blue hue), C-shaped (off-white with a gray hue), Oblong (light gray), and Pin (dark gray).

*Left / Right Difference***Continuity**

Continuity was seen on the right side in 28.2% (98 of 348 hemispheres) of cases and on the left side in 32.2% (112 out of 348 hemispheres) of cases. Consequently, discontinuity was seen on the right side in 21.8% (76 out of 348 hemispheres) of cases and on the left side in 17.8% (62 out of 348 hemispheres) of cases (Figure 42a, Figure 42b, and Figure 42d).

The provided results stem from a series of ANOVA tests aimed at investigating the relationship between the length of the LV and LV subdivisions on the right side and left side, and a right and left combined continuity. These ANOVA tests help in discerning if the variations in the length measurements are associated with different levels of the right and left combined continuity.

General/Overall

The ANOVA revealed a significant effect of right and left combined continuity on the length of the right LV ($F(2, 171) = 13.11, p < 0.001$). The ANOVA revealed a significant effect of right and left combined continuity on the length of the left LV ($F(2, 171) = 13.89, p < 0.001$).

AH

The ANOVA analysis indicates that right and left combined continuity does not significantly affect the length of the right LV AH subdivision ($F(2, 171) = 0.89, p = 0.413$). The ANOVA analysis indicates that right and left combined continuity has no significant effect on the length of the left LV AH subdivision ($F(2, 171) = 0.162, p = 0.851$).

Body

The ANOVA analysis indicates that right and left combined continuity has no significant effect on the length of the right LV body subdivision ($F(2, 171) = 0.346, p = 0.708$). The ANOVA analysis indicates that right and left combined continuity does not significantly impact the length of the left LV body subdivision ($F(1, 172) = 0.261, p = 0.771$).

Atrium to the End of the PH

The ANOVA analysis indicates a significant impact of the right and left combined continuity on the length of the right atrium to the end of the PH subdivision ($F(2, 171) = 17.85, p < 0.001$). The ANOVA analysis indicates a significant relationship between the right and left combined continuity and the length of the left atrium to the end of the PH subdivision ($F(2, 171) = 18.94, p < 0.001$).

In summary, the ANOVA analysis reveals significant effects of right and left combined continuity on the lengths of both the right and left LVs, as well as the atrium to

the end of the PH subdivisions. However, no significant relationships are found for AH subdivision of the LV or the body LV subdivisions.

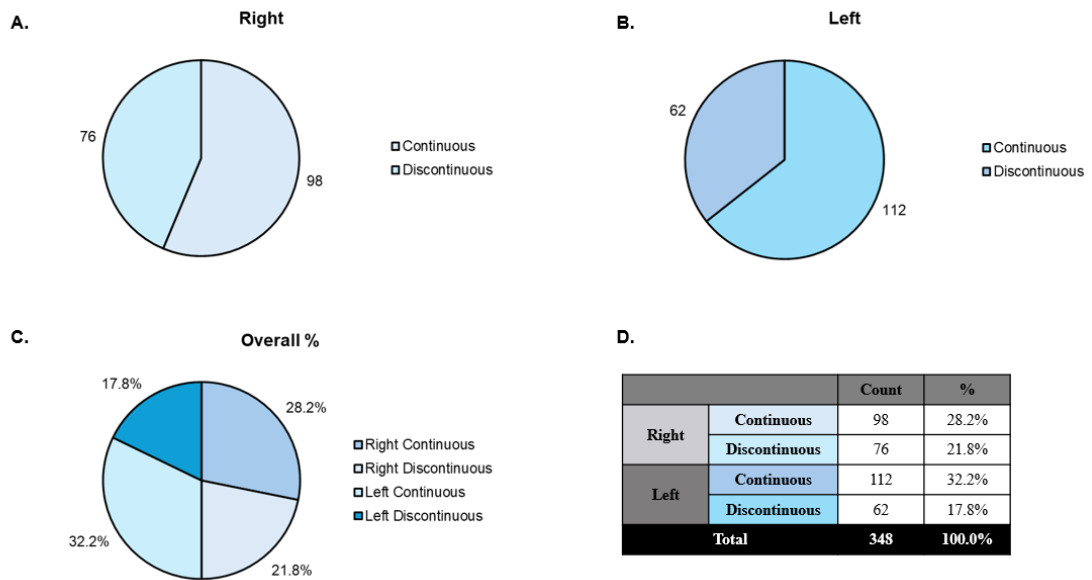


Figure 42. Right and Left Posterior Horn Continuity Incidence. (A) A pie chart depicting the incidence of continuous right PH (light blue) and discontinuous right PH (brighter blue). (B) A pie chart depicting the incidence of continuous left PH (darker blue) and discontinuous left PH (brighter blue). (C) A pie chart depicting the percentage of continuous right PH (mid blue), continuous left PH (light blue), discontinuous right PH (off-white with blue hue), and discontinuous left PH (dark blue). (D) The accompanying table presents counts and percentages of cases exhibiting a continuous right PH (mid blue), a continuous left PH (light blue), a discontinuous right PH (off-white with blue hue), and a discontinuous left PH (dark blue).

Sex Differences

Continuity

The results of the Pearson's Chi-squared test evaluating the association between right and left combined PH continuity and sex indicate a test statistic (X-squared) of 0.63077 with 2 degrees of freedom. The corresponding p-value is 0.7295 indicates there is no significant evidence to suggest that the distribution of sex varies across different levels of right and left continuity.

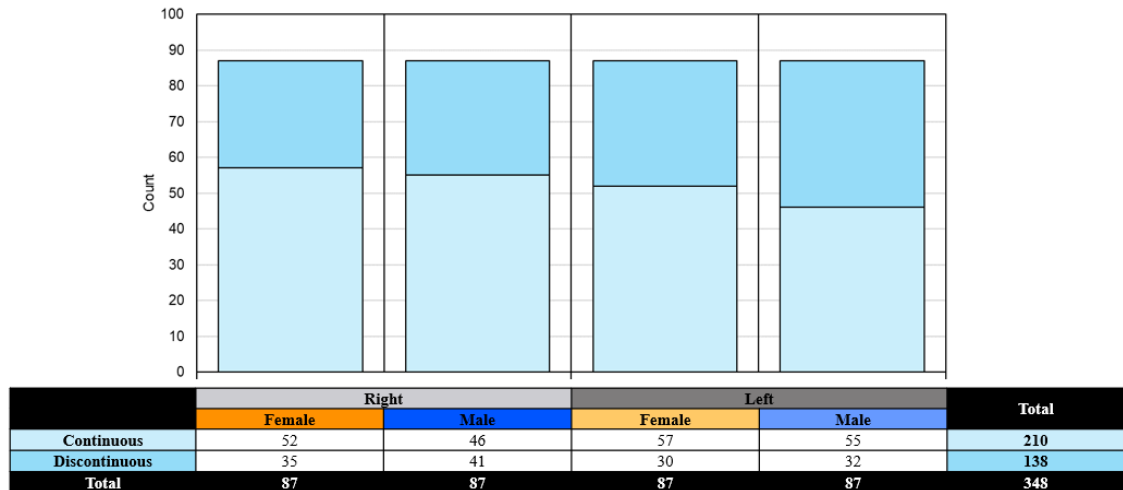
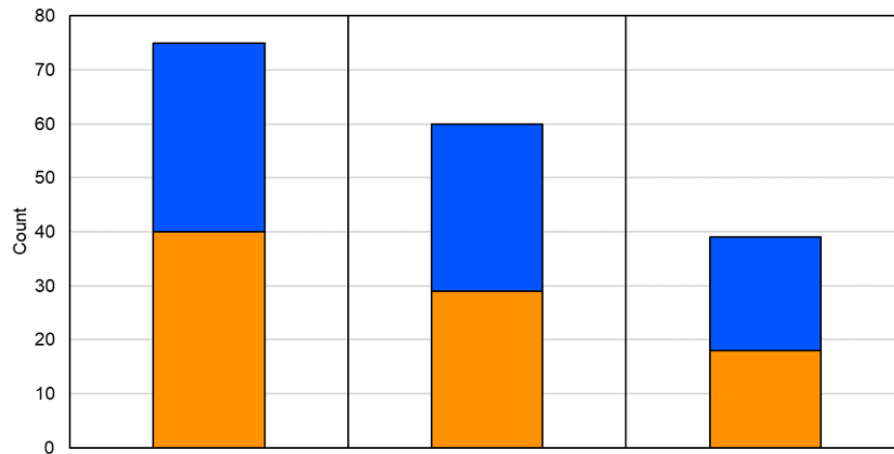
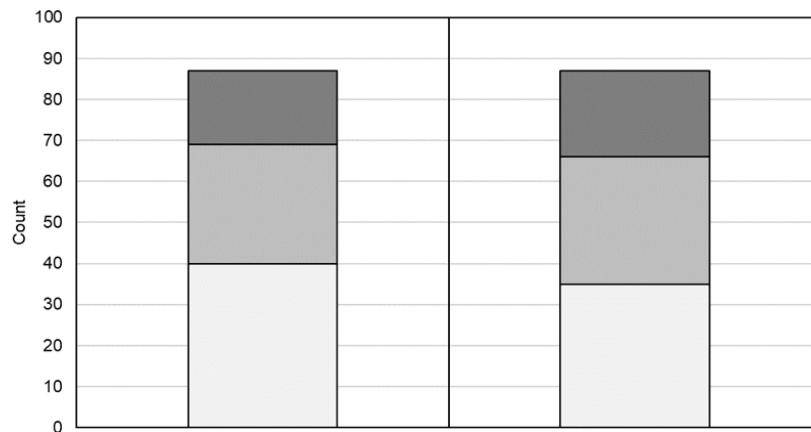


Figure 43. Right and Left Posterior Horn Continuity by Sex. A bar chart depicting the incidence of continuous PH (light blue) and discontinuous PH (dark blue) on the right (light gray) and left (dark gray). The accompanying table presents the incidence of continuous PH and discontinuous PH among females on the right (dark orange), males on the right (dark blue), females on the left (light orange), and males on the left (light blue).



	CC	CD/DC	DD	Total
Female	40	29	18	87
Male	35	31	21	87
Total	75	60	39	174

Figure 44. Right / Left Posterior Horn Continuity by Sex. A bar chart depicting the incidence of combined right and left PH continuity among males (blue) and females (orange). The accompanying table presents the incidence of combined right continuous PH and left continuous PH (CC; off-white with a gray hue), a combination of continuous PH on one side and discontinuous PH on the other side (CD/DC; light gray), and combined right discontinuous PH and left discontinuous PH (DD; dark gray) among females (orange), males (blue), and total (black).



	Female	Male	Total
CC	40	35	75
CD/DC	29	31	60
DD	18	21	39
Total	87	87	174

Figure 45. Right / Left Posterior Horn Continuity by Sex. A bar chart depicts the incidence of combined right continuous PH and left continuous PH (CC; off-white with a gray hue), a combination of continuous PH on one side and discontinuous PH on the other side (CD/DC; light gray) and combined right discontinuous PH and left discontinuous PH (DD; dark gray) among sexes. The accompanying table presents the incidence of combined right continuous PH and left continuous PH (CC; off-white with a gray hue), a combination of continuous PH on one side and discontinuous PH on the other side (CD/DC; light gray) and combined right discontinuous PH and left discontinuous PH (DD; dark gray) among females (orange), males (blue), and total (black).

Age

Continuity

The results of the ANOVA examining the relationship between age and right and left combined continuity indicate a trend towards an association, reflected by a non-zero F-value of 2.973 and a p-value of 0.0538. However, this relationship narrowly misses conventional statistical significance at the 0.05 level. While suggestive of potential influence, the association falls short of definitive confirmation. Further data or a larger sample size may be needed to establish a conclusive link between right and left continuity and age.

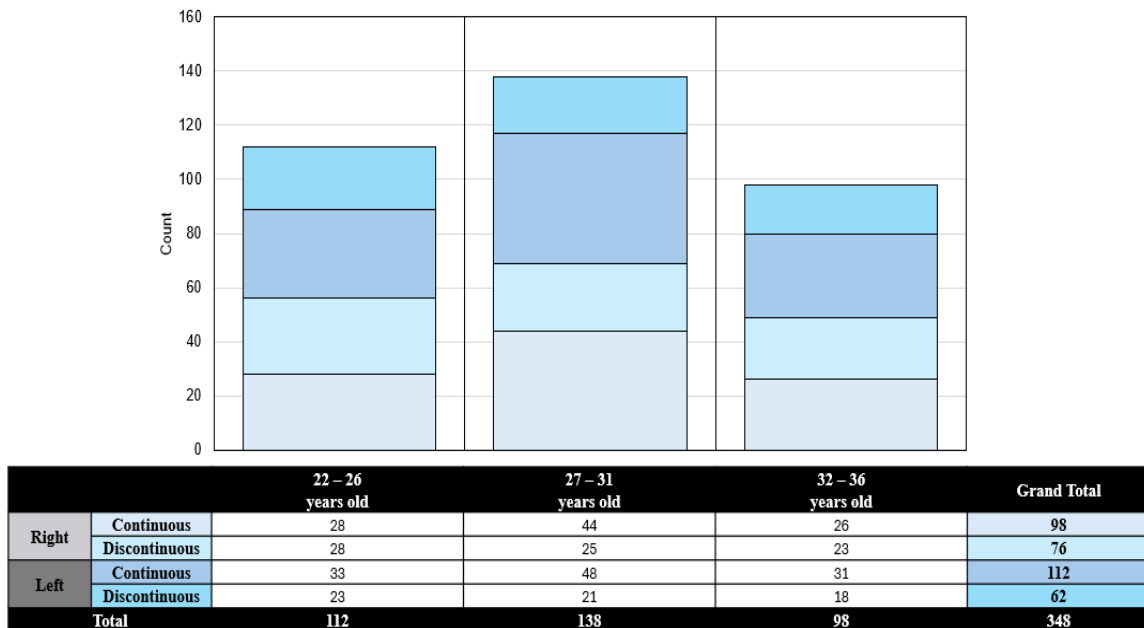
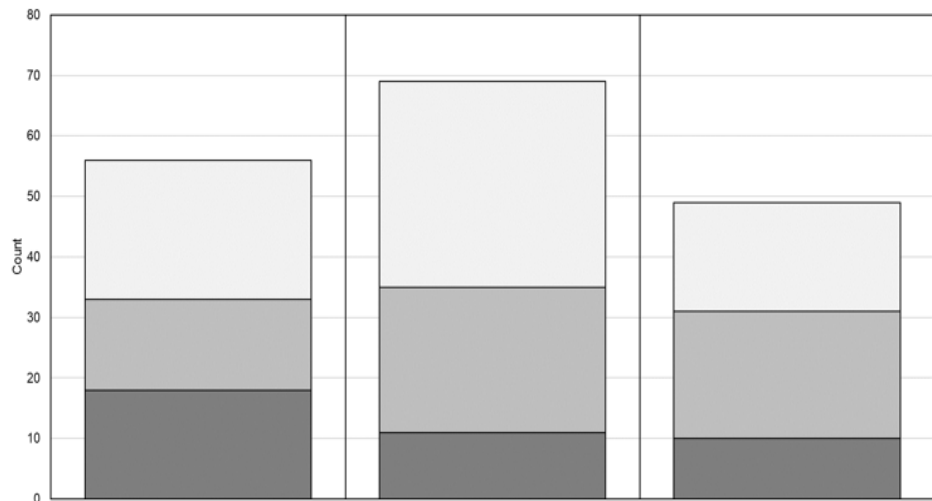


Figure 46. Right and Left Posterior Horn Continuity by Age. A bar chart depicts the incidence of a continuous right PH (mid blue), a continuous left PH (light blue), a discontinuous right PH (off-white with blue hue), and a discontinuous left PH (dark blue) among three age groups (22 - 26, 27 - 31, 32 - 36). The accompanying table presents the incidence of a continuous right PH (mid blue), a continuous left PH (light blue), a discontinuous right PH (off-white with blue hue), and a discontinuous left PH (dark blue) among three age groups (22 - 26, 27 - 31, 32 - 36).



	22 - 26 years old	27 - 31 years old	32 - 36 years old	Grand Total
CC	23	34	18	75
CD/DC	15	24	21	60
DD	18	11	10	39
Total	56	69	49	174

Figure 47. Right / Left Posterior Horn Continuity by Age. A bar chart depicts the incidence of combined right continuous PH and left continuous PH (CC; off-white with a gray hue), a combination of continuous PH on one side and discontinuous PH on the other side (CD/DC; light gray) and combined right discontinuous PH and left discontinuous PH (DD; dark gray) among three age groups (22 - 26, 27 - 31, 32 - 36). The accompanying table presents the incidence of combined right continuous PH and left continuous PH (CC; off-white with a gray hue), a combination of continuous PH on one side and discontinuous PH on the other side (CD/DC; light gray) and combined right discontinuous PH and left discontinuous PH (DD; dark gray) among three age groups (22 - 26, 27 - 31, 32 - 36).

*Handedness***Continuity**

The ANOVA conducted to explore the association between handedness and right and left combined PH continuity revealed that while the right and left combined PH continuity contributes to some variance in handedness, as indicated by a sum of squares of 8560 for the predictor and 450536 for the residuals, the associated F-value of 1.624 was not statistically significant ($p = 0.2$). Consequently, the right and left combined continuity does not significantly influence handedness.

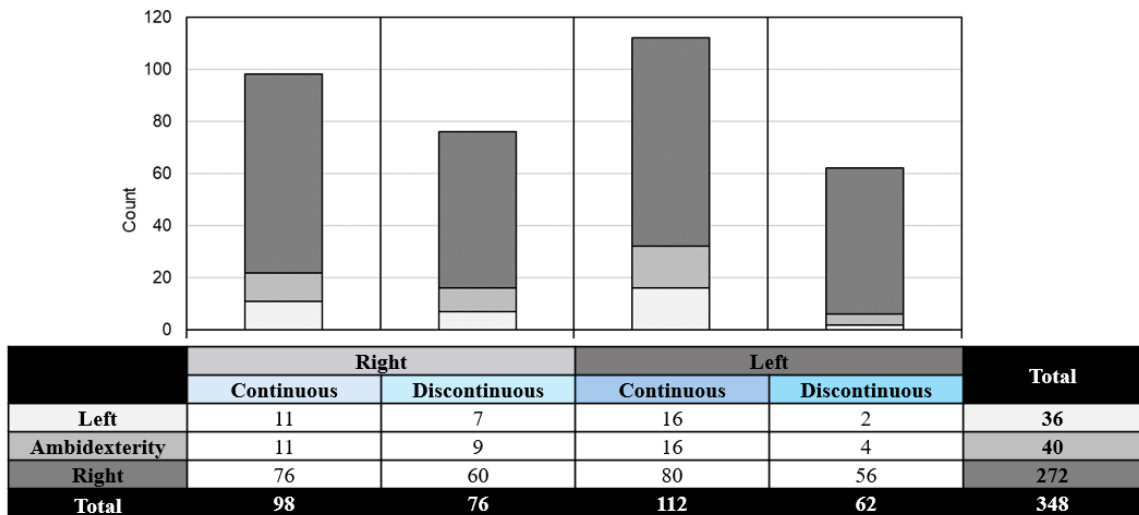


Figure 48. Right and Left Posterior Horn Continuity by Handedness. A bar chart depicts the incidence of right-handed (dark gray), left-handed (light gray), and ambidextrous individuals (off-white with a gray hue) observed among a continuous PH on the right side, a discontinuous PH on the left side, a continuous PH on the left side, and a discontinuous PH on the left side. The accompanying table presents the incidence of right-handed (dark gray), left-handed (light gray), and ambidextrous individuals (off-white with a gray hue) observed among a continuous PH on the right side (off-white with blue hue), a discontinuous PH on the left side (light blue), a continuous PH on the left side (mid blue), a discontinuous PH on the left side (bright blue), and total (black).

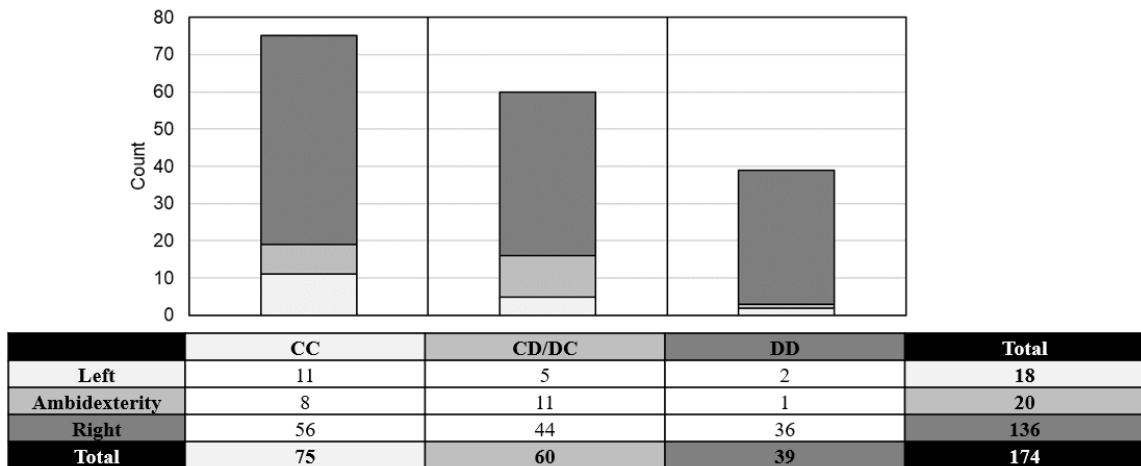


Figure 49. Right / Left Posterior Horn Continuity by Handedness. A bar chart depicts the incidence of combined right continuous PH and left continuous PH (CC; off-white with a gray hue), a combination of continuous PH on one side and discontinuous PH on the other side (CD/DC; light gray) and combined right discontinuous PH and left discontinuous PH (DD; dark gray) among right-handed, left-handed, and ambidextrous individuals. The accompanying table presents the incidence of right-handed (dark gray), left-handed (light gray), and ambidextrous individuals (off-white with a gray hue) observed among combined right continuous PH and left continuous PH (CC; off-white with a gray hue), a combination of continuous PH on one side and discontinuous PH on the other side (CD/DC; light gray), and combined right discontinuous PH and left discontinuous PH (DD; dark gray).

DISCUSSION

Overall Findings

This is the first study that has examined the lateral ventricular morphology using high resolution MRI in a diverse and broadly represented population. This analysis revealed several key findings. First, we identified that the left LV was significantly longer than the right. These differences were reflected in the differential length of the AH, body and atrium to the end of the PH subdivisions. Second, we found that sex had an impact on the length of the LV, with males having a larger LV, and this effect was also observed in the following subdivisions: right and left LV, right and left AH, right and left body, left atrium to the end of the PH. Handedness had an effect on the LV, but it was limited to the right LV, and the right and left atrium to the end of the PH. In addition, we identified several main variants in the lateral ventricle. We found that compression of the wall of the anterior horn to such an extent that it obscured the lumen, was observed in a sizable number of presumably healthy individuals. Finally, we found that the incidence in which the posterior horn of the lateral ventricle was observed as disconnected from the atrium was more frequent than previously observed or noted.

Asymmetry

We confirmed that the ventricles exhibit an asymmetry, with the left lateral ventricle larger than the right. This asymmetry is present at the level of the ventricular subdivisions, both within individual cases and across cases. We found that sex significantly

influences this phenomenon. This is noteworthy as previous research has yielded inconsistent findings regarding the impact of sex on LV asymmetry. We attribute this inconsistency to factors such as imbalanced gender representation in studies, limited imaging resolution, and methodological variations in measurement acquisition.

Our study stands out due to the diverse demographics of our participants, contrasting with previous studies that often focused on specific populations or locations. This broad sample allowed us to observe distinct results between the sexes. However, our investigation revealed mixed findings regarding the influence of handedness on LV asymmetry. Importantly, we determined that the narrow age range of our subjects did not affect symmetry, in contrast to previous studies that emphasized the significant role of age in LV size.

Regarding handedness, our study found varied effects across LV subdivisions, with most showing no significant impact on length. This contrasts with prior research that primarily examined handedness and the entire LV side, potentially explaining the variability in our results. Notably, our study conclusively established that length affects handedness from the atrium to the end of the posterior horn (PH) subdivision, specifically on the right LV.

The variable nature of our data compared to other studies may stem from our comprehensive approach, which included detailed measurements of LV subdivisions. We propose that the atrium to the end of the PH subdivision exerts the most significant influence on handedness and its impact on length. Overall, our findings shed light on the complex interplay of factors influencing LV asymmetry and underscore the importance of

considering diverse demographics and detailed measurement methodologies in future research.

Sex, Age, And Handedness

While the literature detailing the morphology of the lateral ventricle is extensive, it also contains a variety of discrepant findings. These discrepancies may be a result of several unaccounted factors. Subjects may have differences in age, unaccounted comorbidity (e.g., Alzheimer's disease), or other demographic characteristics such as race or ethnicity. These factors have not been sufficiently accounted for, with a minority of studies reporting demographic factors. A second factor that has the potential to confound the results is the means by which the measurements have been carried out, with in vivo methods using MRI or CT likely to produce different results from studies using cadavers. Finally, the detailed morphology may be distorted in cadaveric evaluation, or obscured in suboptimal resolution of imaging modalities. These factors are likely to intersect, which likely underlies the divergent morphological results.

Sex

While acknowledging the ongoing debate surrounding sex-related differences in ventricular volume, previous studies have identified results finding, with some indicating larger ventricles in males, others suggesting larger ventricles in females, and some finding no sex differences (Brassow F, Baumann F, 1978; Cramer et al., 1990; Erdogan, 2004; Jacob and Kumar, 2013; A Hori et al., 2019; Polat et al., 2019). Additionally, these studies

note the presence of ventricular asymmetry in females but not in males, leaving unresolved questions regarding whether ventricular volume or asymmetry differs between sexes (Gyldensted, 1977).

Our study examined sex differences in various parts of the ventricle among males and females and found that males exhibited larger ventricles compared to females, with the left LV consistently larger than the right in both sexes. Additionally, males possessed significantly longer AH than females, and AHs were consistently longer on the left side in both sexes. Furthermore, males had a larger body length compared to females, and there were significant differences in the length of the body subdivision between males and females on both sides. Moreover, the length from the atrium to the end of the PH was larger in males than in females, and there was a significant discrepancy in the length of the left atrium to the end of the PH between males and females, with males having a longer length. However, no significant difference was observed in the length of the atrium to the end of the PH on the right side between males and females. Our study results support previous studies that concluded that the male LV is larger than that of the female (Gyldensted, 1977; Allen, Damasio, Grabowski, 2002; Vinoo Jacob, 2013; Singh et al., 2014; M. Gameraddin, 2015; Honnegowda TM, 2017; Kolsure et al. 2018; Li Z et al., 2019; Shahin S et al., 2020).

Age

Prior studies present a contrasting viewpoint, indicating age as a consistent factor associated with LV size. Numerous cited studies demonstrate that ventricular size tends to

increase with advancing age (Cramer et al., 2013; Singh et al., 2014; Agarwal S et al., 2023; Vinoo Jacob, 2013). While some studies suggest no differences between right and left ventricle sizes concerning aging, there appears to be a positive correlation between various ventricular indices and increasing age (Trimarchi et al., 2013; Kolsur et al., 2018). Previous findings thus underscore age-related changes in ventricular measurements, with significant increases observed across different decades of life, particularly in participants over 70 years old (Barron and Jacob et al., 1976). Our results are derived from a narrow age range, and we were unable to identify any association between age and ventricular morphology in this age range. We conclude that between the ages of 22 and 36, there is now evidence to conclude that the morphology of the lateral ventricle is stable and does not change.

Handedness

Previous studies have provided discrepant results on whether ventricular asymmetry is related to handedness. Some studies have suggested that ventricular asymmetry does not significantly differ between right-handed males and females, others have found the left LV to be larger in both right- and left-handed subjects compared to the right LV (Cramer et al., 1990; Erdogan, 2004; Zipursky, Lim, Pfefferbaum, 1990).

Our study identified that the left LV consistently displayed greater length compared to the right across all handedness categories. While no significant disparities in the lengths of the AH were detected based on handedness, similar non-significant effects were observed for the body subdivision on both sides. However, significant associations emerged between handedness and the lengths of the atrium to the end of the PH, indicating

a nuanced relationship between handedness and specific structures within the ventricular system. These findings underscore the complexity of the interplay between brain anatomy and handedness, suggesting differential influences across ventricular regions.

These varied findings highlight the complexity of the relationship between handedness and ventricular asymmetry, indicating a need for further investigation into the mechanisms underlying structural brain asymmetry in relation to handedness.

Variations in Ventricular Confluence

Our investigation into AH compression incidence and severity, alongside demographic factors, yielded significant findings. We identified three main categories of compression, ranging from no compression to compression severe enough to obscure the lumen of the anterior horn. We unexpectedly found that the incidence of moderate or severe compression was common in a population of healthy adults. The severity of AH compression factors such as sex, age, and handedness has not yet been reported.

We also identified that the posterior horn of the lateral ventricle is frequently disconnected from the atrium in normal adults. The most common conception of the lateral ventricle is that it exists as a confluent structure. In our study, we found that the posterior horn of the lateral ventricle is frequently divided into ventricles that are confluent and those that end and then reappear in the occipital lobe as a ‘bubble’ disconnected from the atrium of the lateral ventricle.

Previous studies defined ventricular coarctation and coaptation as a narrowing, fusion or closure of ventricular walls that potentially relate to luminal obstruction and / or

disease (Davidoff, 1946; Bates & Netsky, 1955). Researchers identified these variations through anatomical dissections, histological examinations, and radiological imaging (Sener, 1997; Dogan, 2015; Morris JA et al., 2022). The prevalence of these variants was rare when evaluated in brains of both sexes (Hori, 1984), and has been unclear about whether these changes were present in the in vivo brain, or principally seen in cadaveric specimens.

In contrast to previous research focusing on anatomical variations, our study assesses the continuity of the lateral ventricle in a large population of normal well characterized adults. Based on our findings, disruptions in the continuity of the PH are a common, normal variation observed in a significant proportion of our cases.

Shape of the Posterior Horn of the Lateral Ventricle

Since the lateral ventricle could be observed at high-resolution, we were able to classify the changes in shape that occur in the posterior horn of the lateral ventricle, which has not been performed before. We identified four main shapes commonly observed in the posterior horn (PH) of the lateral ventricles, likely influenced by external features of the cerebral surface.

While the precise reasons behind the shapes and continuity of these PH structures remain unclear, a combination of embryology, brain development, and our MRI observations could offer insights. It is well-documented that postnatally, the cerebellum undergoes rapid growth and expansion, which alters the cerebral cortex's architecture. Consequently, as the cerebellum enlarges and applies pressure to the brain's posterior

aspect, it likely impacts the PH, potentially causing changes in shape and/or continuity. Similarly, neighboring sulci, such as the calcarine sulcus and parieto-occipital sulcus, are in close proximity to the PH. Considering their proximity and our MRI findings, we propose that deeper folding of these sulci may encroach into the PH, resulting in shape alterations or discontinuities. Our study of healthy young adults suggests that such changes are common and normal.

Moreover, various pathologies affecting the cerebral cortex can contribute to changes in the shape and continuity of the PH. Diseases linked to cortical atrophy, such as Alzheimer's disease (AD), Huntington's disease (HD), Parkinson's disease (PD), and frontotemporal dementia, may induce such alterations. Conversely, conditions causing cortical expansion, such as focal cortical dysplasia, autism spectrum disorder (ASD), hydrocephalus, and vascular malformations, can also impact PH morphology. Additionally, stroke, traumatic brain injury (TBI), brain tumors, and developmental abnormalities like polymicrogyria or lissencephaly are among other potential factors impacting PH shape and continuity.

Limitations and Future Studies

Our study categorized the morphology of the adult lateral ventricle at high resolution and using a broad representation of subjects from different sexes and races. One limitation is that we chose to categorize the ventricular size by length. This decision was made for two reasons: 1) manual volumetric measurement takes around 40 minutes per brain which would represent a large time and effort investment, and 2) automatic methods

that produce estimates of volumes are not always accurate. Future studies could validate our results and provide more information using accurate volume measurements. Such measurements may be generated through the incorporation of AI-based techniques but would require an anatomically accurate training set and considerable quality control and refinement. Nonetheless, such an approach would allow for a more thorough consideration of the lateral ventricle morphology and would allow for additional metrics to be generated.

An additional limitation of the current study is that it contained measures that were subjective in nature. The degree of compression was a qualitative measurement that could be improved by inter-rater reliability in the future.

Finally, a higher resolution imaging technique may provide more information about the discontinuity of the PH. Even at 0.7 μ m resolution, we cannot tell with certainty whether the compression of the PH represents a true disconnection, or whether a small submicron diameter channel exists. Results from cadaveric studies indicate complete fusion of the lateral ventricles in some cases, but it is hard to translate this finding to in vivo results at this time. An important future study is to examine the basis of these morphological alterations and variability. We believe that the compression of the posterior horn or anterior horn is related to the gyrification of the cerebral cortex, but identifying the specific morphological changes that give compression in one individual but not in another will be important in understanding the development of lateral ventricular morphology.

Conclusion

This study offers fresh insights into LV morphology using high-resolution MRI scans in a diverse population. We discovered significant left-right differences in both the overall LV and its subdivisions, consistently finding the left side longer than the right across all LV subdivisions. Sex emerged as a key factor influencing these dimensions, with males generally exhibiting larger ventricles. Identifying the typical degree of compression within the LV is crucial for researchers and clinicians to effectively interpret radiological images and distinguish pathological from normal conditions. Our results show that these variations that may be interpreted as pathology are common and unlikely to be a result of disease. This understanding aids in recognizing deviations indicative of underlying pathologies. By addressing these considerations, future research can deepen our understanding of ventricular morphology and its relationship with demographic factors, which in turn can advance our knowledge of brain structure and function, especially in pathological contexts.

BIBLIOGRAPHY

- Agarwal, S., Choudhury, P., & Biswas, K. (2023). Morphometric Analysis of Lateral Ventricles of the Brain using Magnetic Resonance Imaging and Dissection Method: A Cross-sectional Study. *International Journal of Anatomy Radiology and Surgery*, *12*, 16–19.
- Allen, J. S., Damasio, H., & Grabowski, T. J. (2002). Normal neuroanatomical variation in the human brain: An MRI-volumetric study. *American Journal of Physical Anthropology*, *118*(4), 341–358.
- Annongu, I. T. (n.d.). Morphometric Study Of The Adult Human Brain Ventricular Sized On Computed Tomography Scans In Nigerian. *European Journal of Biomedical and Pharmaceutical Sciences*. Retrieved February 28, 2023, from
- Apostolova, L. G., Green, A. E., Babakchian, S., Hwang, K. S., Chou, Y.-Y., Toga, A. W., & Thompson, P. M. (2012). Hippocampal atrophy and ventricular enlargement in normal aging, mild cognitive impairment and Alzheimer’s disease. *Alzheimer Disease and Associated Disorders*, *26*(1), 17–27.
- Bates, J. I., & Netsky, M. G. (1955). Developmental Anomalies of the Horns of the Lateral Ventricles*. *Journal of Neuropathology & Experimental Neurology*, *14*(3), 316–325.
- Bingxin Zhao, Tengfei Li, Xiaochen Yang, Juan Shu, Xifeng Wang, Tianyou Luo, Yue Yang, Zhenyi Wu, Zirui Fan, Zhiwen Jiang, Jie Chen, Yue Shan, Jiarui Tang, Di Xiong, Ziliang Zhu, Mufeng Gao, Wyliona Guan, Chalmer E. Tomlinson, Qunxi Dong, ... Hongtu Zhu. (2022). Genetic influences on the shape of brain ventricular and subcortical structures. *medRxiv*, 2022.09.26.22279691.
- Brassow, F., & Baumann, K. (1978). Volume of brain ventricles in man determined by computer tomography. *Neuroradiology*, *16*, 187–189.
- Bull, J. W. D. (1961). The Robert Wartenberg Memorial Lecture The volume of the cerebral ventricles. *Neurology*, *11*(1), 1–1.

CDC. (2022, December 9). *Basics About Autism Spectrum Disorder (ASD) | NCBDDD | CDC*. Centers for Disease Control and Prevention.
<https://www.cdc.gov/ncbddd/autism/facts.html>

Celik, H. H., Gürbüz, F., Erilmaz, M., & Sancak, B. (1995). CT measurement of the normal brain ventricular system in 100 adults. *Kaibogaku Zasshi. Journal of Anatomy*, 70(2), 107–115.

Chaddad-Neto, F., & Silva da Costa, M. D. (2022). Surgical Anatomy of the Lateral Ventricles. In F. Chaddad-Neto & M. D. Silva da Costa (Eds.), *Microneuroanatomy and Surgery: A Practical Anatomical Guide* (pp. 121–139). Springer International Publishing.

Chronic traumatic encephalopathy. (2017, October 18). Nhs.Uk.
<https://www.nhs.uk/conditions/chronic-traumatic-encephalopathy/>

Chronic Traumatic Encephalopathy (CTE). (n.d.). Alzheimer's Disease and Dementia.
https://alz.org/alzheimers-dementia/what-is-dementia/related_conditions/chronic-traumatic-encephalopathy

Clarke, E. (1968). *The human brain and spinal cord; a historical study illustrated by writings from antiquity to the twentieth century [by] Edwin Clarke and C. D. O'Malley*. Univ. of California Press.

Cramer, G. D., Allen, D. J., DiDio, L. J., Potvin, W., & Brinker, R. (1990). Evaluation of encephalic ventricular volume from the magnetic resonance imaging scans of thirty-eight human subjects. *Surgical and Radiologic Anatomy: SRA*, 12(4), 287–290.

Curran, E. J. (1909). Variations in the Posterior Horn of the Lateral Ventricle, with Notes on Their Development, and Suggestions as to Their Clinical Significance. *The Boston Medical and Surgical Journal*, 161(22), 777–782.

Davidoff, L. M. (1946). Coarctation of the Walls of the Lateral Angles of the Lateral Cerebral Ventricles. *Journal of Neurosurgery*, 3(3), 250–256.

- De Leon, M. J., DeSanti, S., Zinkowski, R., Mehta, P. D., Pratico, D., Segal, S., Clark, C., Kerkman, D., DeBernardis, J., Li, J., Lair, L., Reisberg, B., Tsui, W., & Rusinek, H. (2004). MRI and CSF studies in the early diagnosis of Alzheimer's disease. *Journal of Internal Medicine*, *256*(3), 205–223.
- Deng, S., Gan, L., Liu, C., Xu, T., Zhou, S., Guo, Y., Zhang, Z., Yang, G.-Y., Tian, H., & Tang, Y. (2023). Roles of Ependymal Cells in the Physiology and Pathology of the Central Nervous System. *Aging and Disease*, *14*(2), 468–483.
- Dogan, M. S., Doganay, S., Koc, G., Gorkem, S. B., & Coskun, A. (n.d.). *Coarctation of lateral ventricles: MRI findings*. Eurorad - Brought to You by the ESR.
- Dwyer, M. G., Silva, D., Bergsland, N., Horakova, D., Ramasamy, D., Durfee, J., Vaneckova, M., Havrdova, E., & Zivadinov, R. (2017). Neurological software tool for reliable atrophy measurement (NeuroSTREAM) of the lateral ventricles on clinical-quality T2-FLAIR MRI scans in multiple sclerosis. *NeuroImage: Clinical*, *15*, 769–779.
- Epelman, M., Daneman, A., Blaser, S. I., Ortiz-Neira, C., Konen, O., Jarrín, J., & Navarro, O. M. (2006). Differential diagnosis of intracranial cystic lesions at head US: Correlation with CT and MR imaging. *Radiographics: A Review Publication of the Radiological Society of North America, Inc*, *26*(1), 173–196.
- Erdogan, A. R., Dane, S., Aydin, M. D., Özdikici, M., & Diyarbakirli, S. (2004). Sex and Handedness Differences in Size of Cerebral Ventricles of Normal Subjects. *International Journal of Neuroscience*, *114*(1), 67–73.
- Ertekin, T., Acer, N., Köseoğlu, E., Zararsız, G., Sönmez, A., Gümüş, K., & Kurtoğlu, E. (2016). Total intracranial and lateral ventricle volumes measurement in Alzheimer's disease: A methodological study. *Journal of Clinical Neuroscience*, *34*, 133–139.
- Fennema-Notestine, C., McEvoy, L. K., Hagler, D. J., Jacobson, M. W., Dale, A. M., Alzheimer's Disease Neuroimaging Initiative, U. (NaN/NaN/NaN). Structural Neuroimaging in the Detection and Prognosis of Pre-Clinical and Early AD. *Behavioural Neurology*, *21*(1–2), 3–12.

- Ferrarini, L., Palm, W. M., Olofsen, H., van Buchem, M. A., Reiber, J. H. C., & Admiraal-Behloul, F. (2006). Shape differences of the brain ventricles in Alzheimer's disease. *NeuroImage*, 32(3), 1060–1069.
- Gameraddin, M., Alsayed, A., Ali, A., & Al-Raddadi, M. (2015). Morphometric Analysis of the Brain Ventricles in Normal Subjects Using Computerized Tomography. *Open Journal of Radiology*, 05(01), Article 01.
- Gawler, J., Bull, J. D., Boulay, G. H. D., & Marshall, J. (1975). Computerized axial tomography: The normal EMI scan. *Journal of Neurology, Neurosurgery & Psychiatry*, 38(10), 935–947.
- Graham, J., Babalola, K. O., Honer, W. G., Lang, D., Kopala, L., & Vandorpe, R. (2006). Lateral asymmetry in the shape of brain ventricles in control and schizophrenia groups. *2006 3rd IEEE International Symposium on Biomedical Imaging: From Nano to Macro - Proceedings/IEEE Int. Symp. Biomed. Imag. Nano Macro Proc.*, 414–417.
- Gross, C. G. *Brain, Vision, Memory*. (1999). MIT Press.
- Grosman, H., Stein, M., Perrin, R. C., Gray, R., & St Louis, E. L. (1990). Computed tomography and lateral ventricular asymmetry: Clinical and brain structural correlates. *Canadian Association of Radiologists Journal = Journal l'Association Canadienne Des Radiologistes*, 41(6), 342–346.
- Guadalupe, T., Mathias, S. R., vanErp, T. G. M., Whelan, C. D., Zwiers, M. P., Abe, Y., Abramovic, L., Agartz, I., Andreassen, O. A., Arias-Vásquez, A., Aribisala, B. S., Armstrong, N. J., Arolt, V., Artiges, E., Ayesa-Arriola, R., Baboyan, V. G., Banaschewski, T., Barker, G., Bastin, M. E., ... Francks, C. (2017). Human subcortical brain asymmetries in 15,847 people worldwide reveal effects of age and sex. *Brain Imaging and Behavior*, 11(5), 1497.
- Gyldensted, C. (1977). Measurements of the normal ventricular system and hemispheric sulci of 100 adults with computed tomography. *Neuroradiology*, 14(4), 183–192.

- Gyldensted, C., & Kosteljanetz, M. (1976). Measurements of the normal ventricular system with computer tomography of the brain. A preliminary study on 44 adults. *Neuroradiology*, *10*(4), 205–213.
- Harvey, I., Persaud, R., Ron, M. A., Baker, G., & Murray, R. M. (1994). Volumetric MRI measurements in bipolars compared with schizophrenics and healthy controls. *Psychological Medicine*, *24*(3), 689–699.
- Harvey, R. W. (1911). The volume of the ventricles of the brain. *The Anatomical Record*, *5*(6), 301–305.
- Honnegowda, T. M. (2017). *A Morphometric Study of Ventricular System of Human Brain by Computerised Tomography in an Indian Population and its Clinical Significance*. <https://www.semanticscholar.org/paper/A-Morphometric-Study-of-Ventricular-System-of-Human-Honnegowda/899b422e9ae8ea6eee08eb0a232a80ca4f917358>
- Horbar, J. D., Leahy, K. A., & Lucey, J. F. (1983). Ultrasound Identification of Lateral Ventricular Asymmetry In The Human Neonate. *Journal of Clinical Ultrasound*, *11*(2), 67–69.
- Hori, A., Bardosi, A., Tsuboi, K., & Maki, Y. (1984). Accessory cerebral ventricle of the occipital lobe: Morphogenesis and clinical and pathological appearance. *Journal of Neurosurgery*, *61*(4), 767–771.
- Ichihashi, K., Iino, M., Eguchi, Y., Uchida, A., Honma, Y., & Momoi, M. (2002). Difference between left and right lateral ventricular sizes in neonates. *Early Human Development*, *68*(1), 55–64.
- Igarashi, H., Tsujita, M., Kwee, I. L., & Nakada, T. (2014). Water influx into cerebrospinal fluid is primarily controlled by aquaporin-4, not by aquaporin-1: 17O JVCPE MRI study in knockout mice. *NeuroReport*, *25*(1), 39–43.

- Jacob, V., & Kumar, A. S. K. (2013). CT assessment of brain ventricular size based on age and sex: A study of 112 cases. *Journal of Evolution of Medical and Dental Sciences*, 2(50), 9842–9856.
- Kempton, M. J., Stahl, D., Williams, S. C. R., & DeLisi, L. E. (2010). Progressive lateral ventricular enlargement in schizophrenia: A meta-analysis of longitudinal MRI studies. *Schizophrenia Research*, 120(1), 54–62.
- Kempton, M. J., Underwood, T. S. A., Brunton, S., Stylios, F., Schmechtig, A., Ettinger, U., Smith, M. S., Lovestone, S., Crum, W. R., Frangou, S., Williams, S. C. R., & Simmons, A. (2011). A comprehensive testing protocol for MRI neuroanatomical segmentation techniques: Evaluation of a novel lateral ventricle segmentation method. *NeuroImage*, 58(4), 1051–1059.
- Kiroğlu, Y., Karabulut, N., Oncel, C., Yagci, B., Sabir, N., & Ozdemir, B. (2008). Cerebral lateral ventricular asymmetry on CT: How much asymmetry is representing pathology? *Surgical and Radiologic Anatomy*, 30(3), 249–255.
- Koeda, T., Ando, Y., Takashima, S., Takeshita, K., & Maeda, K. (1988). Changes in the lateral ventricle with the head position: Ultrasonographic observation. *Neuroradiology*, 30(4), 315–318.
- Kolsur, N., P.M, R., Assistant Professor, Department of Anatomy, Ramaiah Medical College, Bangalore, Karnataka, India, Shetty, S., Professor & HOD, Department of Anatomy, Ramaiah Medical College, Bangalore, Karnataka, India, Kumar, A., & Professor and HOD, Department of Radiology Ramaiah Medical College, Bangalore, Karnataka, India. (2018). Morphometric Study of Ventricular Indices in Human Brain Using Computed Tomography Scans in Indian Population. *International Journal of Anatomy and Research*, 6(3.2), 5574–5580.
- Last, R. J., & Tompsett, D. H. (1953). Casts of the cerebral ventricles. *BJS (British Journal of Surgery)*, 40(164), 525–543.
- LeMay, M. (1984). Radiologic changes of the aging brain and skull. *AJR. American Journal of Roentgenology*, 143(2), 383–389.

- Li, S., An, N., Chen, N., Wang, Y., Yang, L., Wang, Y., Yao, Z., & Hu, B. (2022). The impact of Alzheimer's disease susceptibility loci on lateral ventricular surface morphology in older adults. *Brain Structure and Function*, 227(3), 913–924.
- Li, Z., Xu, F., Zhang, Z., Lin, X., Teng, G., Zang, F., & Liu, S. (2019). Morphologic Evolution and Coordinated Development of the Fetal Lateral Ventricles in the Second and Third Trimesters. *AJNR: American Journal of Neuroradiology*, 40(4), 718–725.
- Lu, Z., He, J., Yu, Y., Li, Z., Li, Z., & Gong, J. (2019). Measurement of lateral ventricle volume of normal infant based on magnetic resonance imaging. *Chinese Neurosurgical Journal*, 5(1), 9.
- McCutcheon, R. A., Reis Marques, T., & Howes, O. D. (2020). Schizophrenia—An Overview. *JAMA Psychiatry*, 77(2), 201–210.
- McKee, A. C., Stein, T. D., Kiernan, P. T., & Alvarez, V. E. (2015). The Neuropathology of Chronic Traumatic Encephalopathy. *Brain Pathology*, 25(3), 350–364.
- Mckeever, P. E., & Venneti, S. (2021). Chapter 20: Immunohistology of the Nervous System. In *Diagnostic Immunohistochemistry* (6th ed., pp. 797–875). Elsevier.
- McLone, D. G. (2004). The anatomy of the ventricular system. *Neurosurgery Clinics*, 15(1), 33–38.
- McRae, D. L., Branch, C. L., & Milner, B. (1968). The occipital horns and cerebral dominance. *Neurology*, 18(1_part_1), 95–98.
- Mirzadeh, Z., Kusne, Y., Duran-Moreno, M., Cabrales, E., Gil-Perotin, S., Ortiz, C., Chen, B., Garcia-Verdugo, J. M., Sanai, N., & Alvarez-Buylla, A. (2017). Bi- and unciliated ependymal cells define continuous floor-plate-derived tanycytic territories. *Nature Communications*, 8(1), 13759.

- Morris, J. A., Gilbert, B. C., Parker, W. T., & Forseen, S. E. (2022). Anatomy of the Ventricles, Subarachnoid Spaces, and Meninges. *Neuroimaging Clinics*, 32(3), 577–601.
- Mortazavi, M. M., Adeeb, N., Griessenauer, C. J., Sheikh, H., Shahidi, S., Tubbs, R. I., & Tubbs, R. S. (2014). The ventricular system of the brain: A comprehensive review of its history, anatomy, histology, embryology, and surgical considerations. *Child's Nervous System*, 30(1), 19–35.
- Patel, K. R., Cherian, J., Gohil, K., & Atkinson, D. (2014). Schizophrenia: Overview and Treatment Options. *Pharmacy and Therapeutics*, 39(9), 638–645.
- Patnaik, P., Singh, V., Singh, D., & Singh, S. (2016). Age and Gender Related Variations in Lateral Ventricle Brain Ratios. *International Journal of Health Sciences and Research*.
- Petty, R. G. (1999). Structural Asymmetries of the Human Brain and Their Disturbance in Schizophrenia. *Schizophrenia Bulletin*, 25(1), 121–140.
- Polat, S., Öksüzler, F. Y., Öksüzler, M., Kabakci, A. G., & Yücel, A. H. (2019). Morphometric MRI Study of the Brain Ventricles in Healthy Turkish Subjects. *International Journal of Morphology*, 37(2), 554–560.
- Prince, Z. L. M. (2013, September 17). Morphometric Study Of Ventricular Sizes On Normal Computed Tomography Scans Of Adult Black Zimbabweans at a Diagnostic Radiology Centre In Harare-A Pilot Study. *Masters thesis, University of Zimbabwe*.
<https://www.semanticscholar.org/paper/MORPHOMETRIC-STUDY-OF-VENTRICULAR-SIZES-ON-NORMAL-A-XXXXX/88a1ebd23b9af23876cb29e64ac546ecb2c85c65>
- Rosenbloom, S., Campbell, M., George, A. E., Kricheff, I. I., Taleporos, E., Anderson, L., Reuben, R. N., & Korein, J. (1984). High resolution CT scanning in infantile autism: A quantitative approach. *Journal of the American Academy of Child Psychiatry*, 23(1), 72–77.

- Ruigrok, A. N. V., Salimi-Khorshidi, G., Lai, M.-C., Baron-Cohen, S., Lombardo, M. V., Tait, R. J., & Suckling, J. (2014). A meta-analysis of sex differences in human brain structure. *Neuroscience and Biobehavioral Reviews*, 39(100), 34–50.
- Rushmore, R. J., Sunderland, K., Carrington, H., Chen, J., Halle, M., Lasso, A., Papadimitriou, G., Prunier, N., Rizzoni, E., Vessey, B., Wilson-Braun, P., Rathi, Y., Kubicki, M., Bouix, S., Yeterian, E., & Makris, N. (2022). Anatomically curated segmentation of human subcortical structures in high resolution magnetic resonance imaging: An open science approach. *Frontiers in Neuroanatomy*, 16.
- Scelsi, C. L., Rahim, T. A., Morris, J. A., Kramer, G. J., Gilbert, B. C., & Forseen, S. E. (2020). The Lateral Ventricles: A Detailed Review of Anatomy, Development, and Anatomic Variations. *AJNR. American Journal of Neuroradiology*, 41(4), 566–572.
- Sener, R. N. (1997). MRI and asymptomatic coarctation of the frontal lateral ventricle horn. *Journal of Neuroradiology = Journal De Neuroradiologie*, 24(2), 163–167.
- Shapiro, R., Galloway, S. J., & Shapiro, M. D. (1986). Minimal asymmetry of the brain: A normal variant. *AJR. American Journal of Roentgenology*, 147(4), 753–756.
- Silverberg, G. D., Heit, G., Huhn, S., Jaffe, R. A., Chang, S. D., Bronte-Stewart, H., Rubenstein, E., Possin, K., & Saul, T. A. (2001). The cerebrospinal fluid production rate is reduced in dementia of the Alzheimer's type. *Neurology*, 57(10), 1763–1766.
- Singh, B. R., Gajbe, U., Agrawal, A., Reddy, Y. A., & Bhartiya, S. (2014). Ventricles of brain: A morphometric study by computerized tomography. *International Journal of Medical Research & Health Sciences*, 3(2), 381.
- Soininen, H., Puranen, M., & Riekkinen, P. J. (1982). Computed tomography findings in senile dementia and normal aging. *Journal of Neurology, Neurosurgery, and Psychiatry*, 45(1), 50–54.
- Srijit, D., & Shipra, P. (2007). Anatomical study of anomalous posterior horn of lateral ventricle of brain and its clinical significance. *Bratislavske Lekarske Listy*, 108(9), 422–424.

- Stratchko, L., Filatova, I., Agarwal, A., & Kanekar, S. (2016). The Ventricular System of the Brain: Anatomy and Normal Variations. *Seminars in Ultrasound, CT and MRI*, 37(2), 72–83.
- Strauss, E., & Fitz, C. (1980). Occipital horn asymmetry in children. *Annals of Neurology*, 8(4), 437–439.
- Styner, M., Lieberman, J. A., McClure, R. K., Weinberger, D. R., Jones, D. W., & Gerig, G. (2005). Morphometric analysis of lateral ventricles in schizophrenia and healthy controls regarding genetic and disease-specific factors. *Proceedings of the National Academy of Sciences*, 102(13), 4872–4877.
- Sylvian fissure* | Radiology Reference Article | Radiopaedia.org. (n.d.). Retrieved February 26, 2024, from <https://radiopaedia.org/articles/sylvian-fissure?lang=us>
- Takeda, S., & Matsuzawa, T. (1985). Age-related change in volumes of the ventricles, cisternae, and sulci: A quantitative study using computed tomography. *Journal of the American Geriatrics Society*, 33(4), 264–268.
- Tan, Z.-Y. J., Naidoo, P., & Kenning, N. (2010). Ultrasound and MRI features of connatal cysts: Clinicoradiological differentiation from other supratentorial periventricular cystic lesions. *The British Journal of Radiology*, 83(986), 180–183.
- Trimarchi, F., Bramanti, P., Marino, S., Milardi, D., Di Mauro, D., Ielitto, G., Valenti, B., Vaccarino, G., Milazzo, C., & Cutroneo, G. (2013). MRI 3D lateral cerebral ventricles in living humans: Morphological and morphometrical age-, gender-related preliminary study. *Anatomical Science International*, 88(2), 61–69.
- van Erp, T. G. M., Hibar, D. P., Rasmussen, J. M., Glahn, D. C., Pearlson, G. D., Andreassen, O. A., Agartz, I., Westlye, L. T., Haukvik, U. K., Dale, A. M., Melle, I., Hartberg, C. B., Gruber, O., Kraemer, B., Zilles, D., Donohoe, G., Kelly, S., McDonald, C., Morris, D. W., ... Turner, J. A. (2016). Subcortical brain volume abnormalities in 2028 individuals with schizophrenia and 2540 healthy controls via the ENIGMA consortium. *Molecular Psychiatry*, 21(4), 547–553.

- Vidal, C. N., Nicolson, R., Boire, J.-Y., Barra, V., DeVito, T. J., Hayashi, K. M., Geaga, J. A., Drost, D. J., Williamson, P. C., Rajakumar, N., Toga, A. W., & Thompson, P. M. (2008). Three-dimensional mapping of the lateral ventricles in autism. *Psychiatry Research*, *163*(2), 106–115.
- Yeo, R. A., Turkheimer, E., Raz, N., & Bigler, E. D. (1987). Volumetric asymmetries of the human brain: Intellectual correlates. *Brain and Cognition*, *6*(1), 15–23.
- Zhao, B., Li, T., Yang, X., Shu, J., Wang, X., Luo, T., Yang, Y., Wu, Z., Fan, Z., Jiang, Z., Chen, J., Shan, Y., Tang, J., Xiong, D., Zhu, Z., Gao, M., Guan, W., Tomlinson, C. E., Dong, Q., ... Zhu, H. (2022). *Genetic influences on the shape of brain ventricular and subcortical structures* (p. 2022.09.26.22279691). medRxiv.
- Zipursky, R. B., Lim, K. C., & Pfefferbaum, A. (1989). MRI study of brain changes with short-term abstinence from alcohol. *Alcoholism, Clinical and Experimental Research*, *13*(5), 664–666.
- Zipursky, R. B., Lim, K. O., & Pfefferbaum, A. (1990). Volumetric assessment of cerebral asymmetry from CT scans. *Psychiatry Research*, *35*(1), 71–89.

CURRICULUM VITAE

